

HELSINKI UNIVERSITY OF TECHNOLOGY

Department of Chemical Technology

Jonas Roininen

**EVALUATION OF SILICA NANOPARTICLE PROCESS CONCEPTS**

Thesis for the degree of Master of Science in Technology.

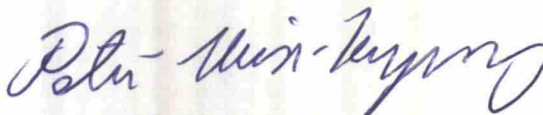
Espoo, September 6, 2007

Supervisor:



Professor Markku Hurme

Instructor:



Petri Uusi-Kyyny, D.Sc. (Tech.)


## Preface

This Master's Thesis was done as part of the TEKES project Silsurf in cooperation with KCL. The research for this thesis was done at Helsinki University of Technology, Laboratory of Chemical Engineering and Plant Design, from March to August, 2007.

I would like to express my gratitude to the following people and organizations who have contributed to this thesis:

- My supervisor Professor Markku Hurme and my instructor Petri Uusi-Kyyny for their assistance and support.
- Thad Maloney and Karita Kinnunen from KCL for providing me this interesting subject and their support during the project.
- Professor Janne Laine and his staff and especially Tiina Nypelö from the Laboratory of Forest Products Chemistry for preparing the AFM images.
- Eero Haimi from the Laboratory of Materials Science for preparing the SEM images.
- The Laboratory of Physical Chemistry for their support with the Zetasizer measurements.

Espoo, September 6, 2007



Jonas Roininen



Author Jonas Roininen	Date September 6, 2007 Pages 105+23
Title of thesis Evaluation of Silica Nanoparticle Process Concepts	
Chair Plant Design	Chair Code Kem-107
Supervisor Professor Markku Hurme	
Instructor Petri Uusi-Kyyny, D.Sc. (Tech.)	
<p>The aim of this thesis was to explore possible methods for the production of silica (silicon dioxide, SiO<sub>2</sub>) nanoparticles. In the literature review part, the polymerization behavior of silica and state-of-the art ion exchange methods for silica nanoparticle production are described. Further, silica nanoparticle aggregation, disaggregation, and production of precipitated and fumed silicas are briefly covered. Judging from the literature survey, ion exchange methods that are currently being used seem unpractical for producing large quantities of silica nanoparticles, and therefore the development of a novel process is required.</p> <p>In the experimental part, three different methods, namely acid neutralization, precipitation, and coagulant processes were tested experimentally. All these methods are based on neutralization of water glass (sodium silicate, Na<sub>2</sub>O·XSiO<sub>2</sub>) with acid. It was found that the Acid Neutralization method, which is characterized by low silica concentration, could only produce small particles in the range of 10 nm in dilute suspensions. Further, the stability of the products was poor. Using the precipitation technique, primary particle sizes of 10-50 nm could be achieved. Silica concentration was the parameter that had the greatest influence on primary particle size. These particles, however, formed always aggregates with sizes up to the millimeter scale. It was not possible to disperse these aggregates using existing equipment. Using the coagulant method, discrete particles up to 100 nm could be produced, but the large amount of coagulant needed in the process proved to be a severe problem. Of these three processes, the precipitation process was chosen as the basis for pilot and industrial process design in the process design part of the thesis.</p> <p>Based on the experiments, a pilot process was designed. The aim was to design a process that can be built using already available equipment. The process consists mainly of a batch stirred tank reactor, where the precipitation reaction is performed, and a bead mill for dispersion of the aggregates. The capital investment cost of the pilot process was estimated at about 170,000 €, the bead mill being by far the most expensive individual item. Scaling up from the pilot process, a preliminary process design for an industrial scale process was conducted. The production cost in the industrial process was estimated at 1.17 €/kg 100 % SiO<sub>2</sub>, which is a competitive price compared to similar commercial silica products.</p> <p>At the end of the thesis, a few innovative reactor concepts described in the literature are explored. The aim of innovative reactor design is to keep aggregation of the particles under control in such a way that no milling is required after the reaction step.</p>	

Tekijä  Jonas Roininen	Päiväys  6.9.2007
	Sivumäärä  105+23
Työn nimi  Piidioksidinanopartikkeliprosessikonseptien evaluointi	
Professuuri  Tehdassuunnittelu	Koodi  Kem-107
Työn valvoja  Professori Markku Hurme	
Työn ohjaaja  TkT Petri Uusi-Kyyny	
<p>Tämän diplomityön tavoitteena oli tutkia menetelmiä piidioksidinanopartikkeleiden valmistukseen. Kirjallisuusosassa luodaan katsaus piidioksidin polymerointikäyttäytymiseen sekä käytössä oleviin, ioninvaihtoon perustuviin valmistusmenetelmiin. Lisäksi sivutaan piidioksidipartikkeleiden aggregoitumista, dispergointia, sekä precipitated silica ja fumed silica -nimisten tuotteiden valmistusta. Kirjallisuuskatsauksen perusteella voidaan päätellä, että käytössä olevat ioninvaihtomenetelmät eivät sovellu sellaisenaan käytettäväksi ja siksi uudenlaisen prosessin suunnittelu on välttämätöntä.</p> <p>Kokeellisessa osassa erilaisia valmistusmenetelmiä kokeiltiin käytännössä. Valitut menetelmät olivat happoneutralointi-, saostus- sekä koagulanttimenetelmät. Kaikki mainitut menetelmät perustuvat vesilasin (natriumsilikaatti, <math>\text{Na}_2\text{O} \cdot \text{XSiO}_2</math>) neutralointiin hapolla. Happoneutralointimenetelmällä saatiin ainoastaan pieniä, halkaisijaltaan noin 10 nm partikkeleita ja tuotteet olivat epästabiileja. Saostusmenetelmällä saatiin 10–50 nm primääripartikkeleita. Tärkein primääripartikkelikokoon vaikuttanut parametri oli piidioksidin konsentraatio. Partikkelit esiintyivät kuitenkin aina aggregaateissa joiden koko ylsi millimetritasolle. Aggregaattien dispergointi käytössä olleella laitteistolla ei ollut mahdollista. Koagulanttimenetelmällä oli mahdollista saada jopa 100 nm partikkeleita, mutta prosessissa vaadittava suuri koagulantin määrä osoittautui ongelmalliseksi. Näistä kolmesta menetelmästä saostusmenetelmä valittiin perustaksi prosessisuunnitteluosassa suunnitelluille pilotti- ja teolliselle prosessille.</p> <p>Kokeellisesta osasta saatujen tulosten pohjalta suunniteltiin pilottiprosessi joka olisi mahdollista rakentaa jo saatavilla olevalla laitteistolla. Prosessi koostuu panostoimisesta sekoitusreaktorista, jossa suoritetaan saostusreaktio sekä helmimyllystä, jossa saostetut aggregaatit dispergoidaan. Prosessin pääomakustannukseksi arvioitiin noin 170 000 €, josta suurin osa on helmimyllyn kustannuksia. Pilottiprosessin pohjalta tehtiin myös alustava suunnitelma teolliselle prosessille. Teollisen prosessin tuotantokustannuksiksi arvioitiin 1,17 €/kg 100 % <math>\text{SiO}_2</math>, mikä on kilpailukykyinen hinta verrattuna vastaaviin kaupallisiin piidioksidituotteisiin.</p> <p>Työn lopussa luodaan katsaus joihinkin kirjallisuudessa esiteltyihin innovatiivisiin reaktorikonsepteihin. Innovatiivisen reaktorisuunnittelun tarkoituksena on kehittää reaktori, jossa partikkeleiden aggregoituminen saataisiin hallittua siten että reaktorin jälkeen ei tarvitsisi enää erillistä jauhusta.</p>	



# Table of Contents

Preface

Abstract

Tiivistelmä

Table of Contents

1	Introduction.....	1
LITERATURE REVIEW PART		
2	Terminology.....	1
3	The Polymerization Behavior of Silica.....	2
3.1	Polymerization of Silicic Acid.....	2
3.2	Sol and Gel Formation.....	3
4	Silica Sols .....	6
4.1	Manufacturing.....	6
4.2	Stability of Silica Sols.....	7
4.3	The Ion Exchange Method.....	8
4.4	The Acid Neutralization Method .....	12
4.5	Methods for Making Large-Particle Sols.....	14
4.5.1	Overview .....	14
4.5.2	Relation of Particle Size and Temperature .....	15
4.5.3	Increasing Particle Size by Adding Active Silica – Buildup Process	16
4.5.4	Limitations of the Buildup Process.....	19
4.6	Experimental Work.....	21
5	Aggregation of Particles .....	22
5.1	Terminology.....	22
5.2	Coagulation Mechanisms.....	23
5.3	Aggregation Models and Experimental Work .....	24
5.4	Break-Up and Dispersion of Aggregates .....	27
5.4.1	High-Shear Mixers.....	27
5.4.2	Bead Mills.....	28
5.4.3	Ultrasonic Dispersing .....	30
6	The Sol-Gel Process.....	31

7	Precipitated Silica .....	33
7.1	Production .....	33
7.2	Chemistry .....	34
7.3	Enhanced Precipitation .....	35
7.3.1	Precipitation from Emulsion Systems .....	35
7.3.2	Precipitation Using Coagulants .....	36
8	Fumed Silica .....	38
9	Continuous Processes .....	39
9.1	Overview .....	39
9.2	Silica Sols .....	40
9.3	Precipitated Silica .....	40
10	Conclusions from the Literature Review .....	42
EXPERIMENTAL PART		
11	Introduction to the Experimental Part .....	44
12	General arrangements .....	44
13	Sample Analysis by Dynamic Light Scattering .....	45
13.1	Theory .....	45
13.2	Measurements of Commercial Silica Sols .....	47
14	Sol via Acid Neutralization .....	48
14.1	Experimental Procedure .....	48
14.2	Neutralization of Water Glass .....	49
14.3	Results .....	50
14.4	Conclusions .....	52
15	Precipitation .....	52
15.1	Experimental Procedure .....	52
15.2	Stirrer Speed and Power Input .....	53
15.3	Measurement of Primary Particle Size .....	54
15.4	Results .....	55
15.5	Microscopic Analysis .....	57
15.6	Conclusions .....	59
16	Coagulant Process .....	61
16.1	Experimental Procedure .....	61
16.2	Results .....	62
16.3	Microscopic analysis .....	63

16.4	Conclusions.....	64
17	Additional Experiments.....	65
18	Conclusions from the Experimental Part.....	66
18.1	General Conclusions.....	66
18.2	Key Variables.....	66
18.3	Product Stability.....	68
18.4	Suggestions for Further Research.....	68
PROCESS DESIGN PART		
19	Evaluation of Process Alternatives.....	70
19.1	Introduction.....	70
19.2	Processes.....	70
19.2.1	Acid Neutralization.....	70
19.2.2	Precipitation.....	71
19.2.3	Coagulant Processes.....	71
19.2.4	Emulsion Process.....	72
19.3	Comparison of the Processes.....	73
19.4	Selection of a Process.....	75
20	Pilot Process Design.....	76
20.1	Introduction.....	76
20.2	Capacity.....	76
20.3	Description of the Process.....	77
20.4	Reactor DC-101 and Heater EB-101.....	78
20.5	Bead Mill KA-101.....	80
20.6	Agitators.....	82
20.6.1	GD-101.....	82
20.6.2	GD-102.....	83
20.7	Pumps.....	83
20.7.1	GA-101.....	83
20.7.2	GA-102.....	83
20.7.3	GA-103.....	84
20.8	Storage Tank FA-101.....	84
20.9	Tubing and Valves.....	84
20.10	On-line Analysis.....	84
20.11	Capital Investment.....	85

20.12	Alternative Pilot Process Design .....	86
21	Scale-up to Industrial Scale .....	87
21.1	Process Design.....	87
21.2	Capital Investment .....	88
21.3	Production Costs.....	89
22	Innovative Reactor Design.....	91
22.1	Introduction.....	91
22.2	Reactor Concepts Presented in Journals .....	91
22.2.1	Taylor-Couette Reactor.....	91
22.2.2	Sliding Surface Reactor .....	92
22.2.3	Ultrasonic Reactor .....	92
22.2.4	Y- and T-mixers.....	94
22.2.5	Cascade Reactor.....	95
22.3	Ideas for Further Research.....	96
23	Conclusions.....	97

References

Appendices



# 1 Introduction

Nanotechnology has been defined by the United States' National Nanotechnology Initiative as "the understanding and control of matter at dimensions of roughly 1 to 100 nanometers, where unique phenomena enable novel applications." Research activity in the field of nanotechnology has exploded in recent years: The ability to engineer materials on the small length scale is opening a broad range of product development opportunities. In paper technology, the use of nanotechnology is seen capable to improve current products and processes to significantly improve the cost structure of current grades of paper or even develop products with improved functionality that can be sold to existing markets and be produced on existing infrastructure. This kind of change is expected to happen in the next five years. (Maloney 2007)

Colloidal retention systems have already been used in the paper industry for two decades. New applications are seen in the field of paper coating, opening the way to mass customization where machines are run like commodity processes but constant changes are made toward the end. (Koeppenick 2001) Although the idea of coating solids with nanoparticles is not new (see for example Iler 1956), only recent developments in imaging have opened the way to evaluating the benefits of nanostructures (Koeppenick 2001).

The aim of this thesis is to study production technologies for silica nanoparticles.

## LITERATURE REVIEW PART

# 2 Terminology

Most nanoparticles appear in colloidal suspensions. A stable dispersion of solid colloidal particles in a liquid is called a *sol*. Silica sols are stable disperse systems in which the dispersion medium (or continuous phase) is a liquid and the dispersed or discontinuous phase is silicon dioxide in the colloidal state. Stable in this case means that the solid particles are yet too small to settle (with diameters less than 1  $\mu\text{m}$ ) but still sufficiently large to show marked deviations from the properties of typical solutions (larger than 1 nm) (Flörke *et al.* 2005, Bergna 2006). Most often, the terms silica sol and colloidal silica are used as synonyms. The term "silica nanoparticles" is normally used for the discrete particles in silica sols.

The term *gel* is applied to systems made of a continuous solid skeleton made of colloidal particles or polymers enclosing a continuous liquid phase (Bergna 2006). The term *aggregation* is used for all forms of colloidal particles linking together, including gels. *Precipitated silicas* and *pyrogenic silicas* or *fumed silicas* are synthetic, white, amorphous forms of silicon dioxide (Flörke *et al.* 2005).

*Water glass* is the trivial name for sodium silicate,  $\text{Na}_2\text{O} \cdot x \text{SiO}_2$ . It is the most important raw material for various silica products and is available in either solid form or as aqueous solutions. (Flörke *et al.* 2005) In this thesis, the term sodium silicate is used when speaking about silica chemistry, while the term water glass is mostly used when speaking about industrial manufacturing processes of silica products.

### 3 The Polymerization Behavior of Silica

#### 3.1 Polymerization of Silicic Acid

Most processes for the preparation of colloidal silica involve the formation of silicic acid which can be considered to be  $\text{Si}(\text{OH})_4$ , a tetrahedral molecule. It can be obtained for example by passing a solution of alkali silicate through a bed of ion exchange resin, a method which will be discussed later.

Monosilicic acid is soluble and stable in water at room temperature for periods of time only at a concentration of less than about 100 ppm as  $\text{SiO}_2$ . When a solution of silicic acid is formed at a higher concentration and in the absence of a solid phase on which the soluble silica might be deposited, then the monomer polymerizes to form dimer and higher molecular weight species of silicic acid. Silicic acid polymerizes by the reaction of the OH-groups to split out a water molecule and form a siloxane (Si-O-Si) bridge between the corners of two tetrahedra. (Iler 1979, Roberts 2006) This process is illustrated in Figure 1.

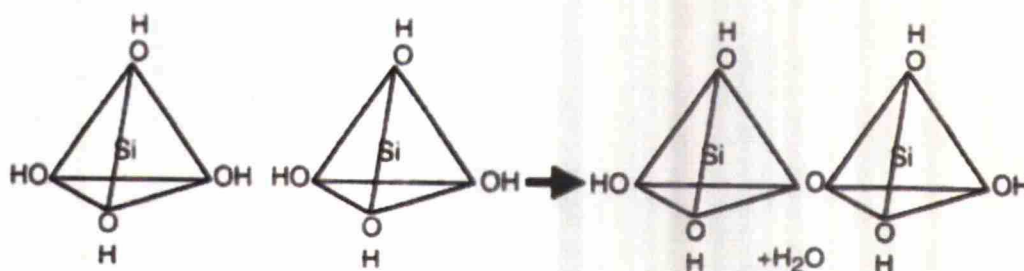


Figure 1. Bonding of  $\text{Si}(\text{OH})_4$  molecules (Roberts 2006)

If alkali, for example sodium, is present in the solution, then the pH of the solution will raise as the result of the polymerization as NaOH that was adsorbed onto the silicic acid is released (Yoshida 1994).

Silicic acid has a strong tendency to polymerize in such a way that in the polymer there is a maximum number of siloxane bonds and a minimum number of uncondensed SiOH groups. Thus polymerization quickly leads to ring structures which link together to larger three-dimensional molecules. These condense internally to the most compact state with SiOH groups remaining on the outside (Figure 2). The resulting spherical units, which are 1-2 nm in diameter, are the nuclei that develop into larger particles. (Iler 1979, Roberts 2006)

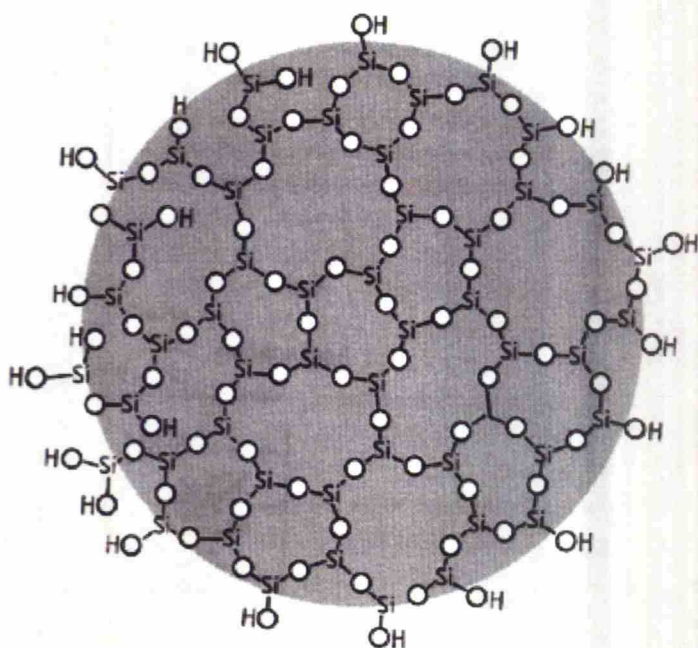


Figure 2. Two-dimensional random network of a dehydrated but hydroxylated colloidal silica particle (Flörke *et al.* 2005)

### 3.2 Sol and Gel Formation

The polymerization of silica goes through three stages (Iler 1979):

- Polymerization of silica to form particles (nucleation).
- Growth of particles.
- Linking of particles together into branched chains, then networks, finally extending throughout the liquid medium, thickening into a gel.



The control over the polymerization reaction is the key to the formation of different silica products.

As discussed before, freshly formed silicic acid tends to agglomerate quite rapidly to small particles of 1-2 nm in diameter. The further polymerization depends mainly on pH, salt concentration, and temperature. The polymerization behavior is summarized in

Figure 3.

- *Sol formation.* At pH 7-10 with no salts present, the silica particles are negatively charged and repel each other. Therefore, they do not collide, so that particle growth continues without aggregation. Since not all the small three-dimensional particles are of the same size, there is a solubility difference between particles of slightly different sizes. Particles grow in average size and diminish in number as the smaller ones dissolve and the silica is deposited on the larger ones. This process is called Ostwald ripening and continues as long as the solubility difference between smaller and larger particles is high enough. The final particle size depends on the temperature. At 100 °C particle growth stops at diameters of 12-15 nm. (Iler 1979, Roberts 2006). This process is illustrated in Figure 4.
- *Gel formation.* At pH below 7, or if salt is present at a concentration higher than 0.2-0.3 N at pH 7-10, the charge repulsion is reduced and aggregation of particles and the formation of a continuous gel are favored. (Iler 1979)

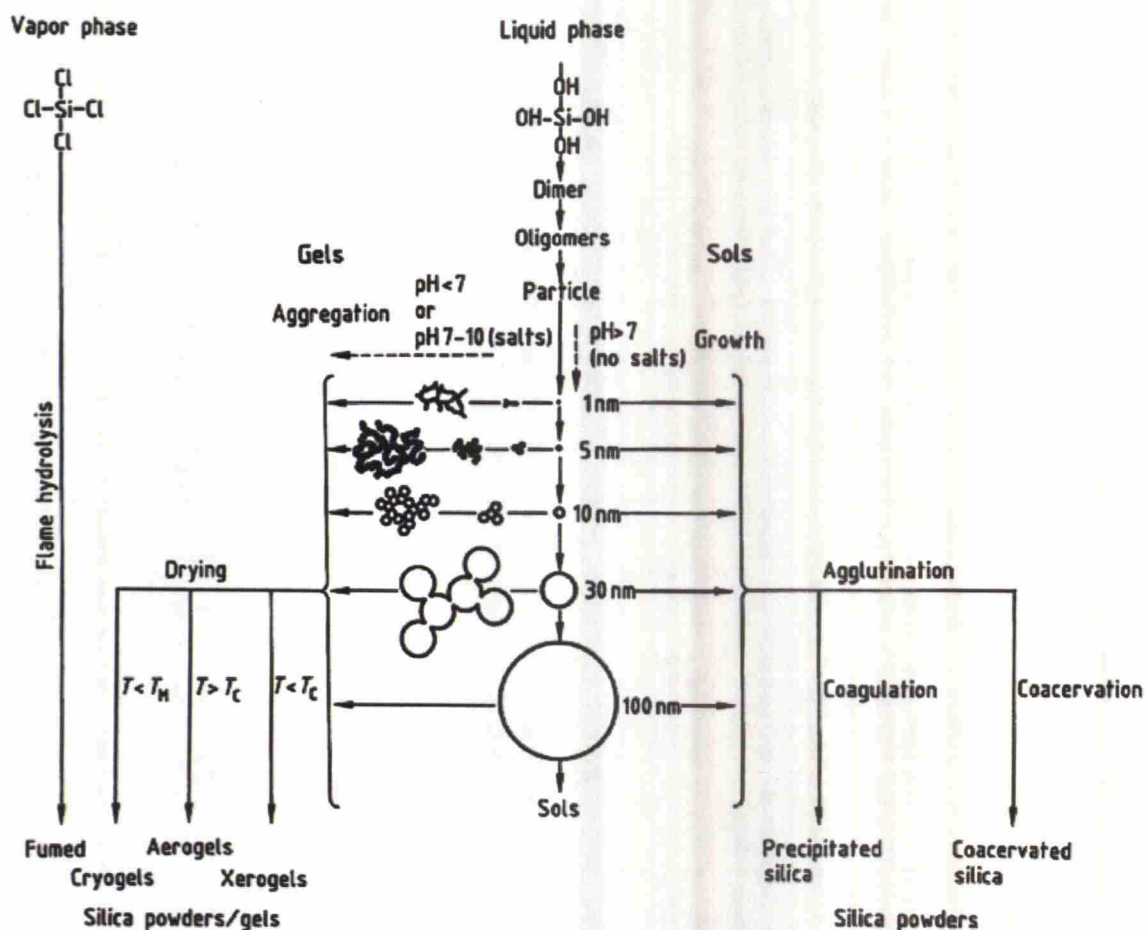


Figure 3. Polymerization behavior of silica and the formation of different silica products (Flörke *et al.* 2005)

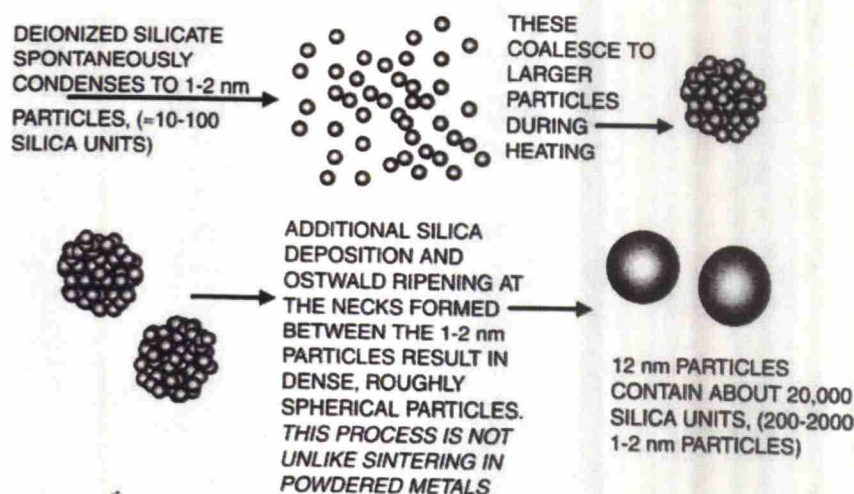


Figure 4. Particle growth (Roberts 2006)

Aggregation and gelling can be prevented to some extent by raising the temperature. In the pH range 7-10.5 a sol of 2-3 % silica with a salt concentration of 0.2-0.3 N gels at room temperature. However, if the sol is first heated to 80-100 °C, the particles grow in size and decrease in number so that aggregation and gelling are greatly retarded or even prevented permanently (Iler 1979). Generally speaking, at low temperatures, the formation of a continuous gel is favored, whereas at high temperatures, the formation of discrete particles is favored (Roberts 2006).

## **4 Silica Sols**

### **4.1 Manufacturing**

Most commercial manufacturing processes use an alkali silicate, such as sodium or potassium silicate, as the source of silica. Because of its low cost, compared to other alkali silicates, sodium silicate is the preferred starting material. Sodium silicates are low melting glasses, which vary in their ratio of  $\text{SiO}_2:\text{Na}_2\text{O}$ , typically in the range from about 1:2 to about 3.25:1. This ratio is used to characterize sodium silicates. It is often given as a weight ratio, but since the molecular weights of  $\text{SiO}_2$  and  $\text{Na}_2\text{O}$  are almost the same (60 and 62 respectively) the weight ratio is very close to the molar ratio. The higher (>3) ratio silicates are usually preferred since a major cost in the process is the removal of sodium from the silicate. (Roberts 2006)

So far, virtually all commercial processes to making silica sols involve methods whereby sodium is removed from the silicate and held apart from the silicic acid units. Most, or all, of the alkali is removed from the solution by ion exchange or electro-dialysis and is replaced by hydrogen ions, thus forming silicic acid, which is then polymerized to give particles as described in Paragraph 3.1 (Roberts 2006, Iler 1979). In general terms, the processes used to make colloidal silica involve the following steps (Roberts 2006):

- The removal of most or all of the sodium hydroxide from a solution of sodium silicate converting it to silicic acid.
- Adjusting the alkali content to give a silica:alkali ratio and pH appropriate to the desired final particle size and stability.
- Polymerization under controlled conditions to give colloidal silica particles.



- Concentration to give normal shipping conditions.

## 4.2 Stability of Silica Sols

Three forms of stability can be distinguished in silica sols, namely stability against particle growth, stability against aggregation, and stability against gelling.

Stability against particle growth means that there is no change in particle size or particle size distribution. Normally, concentrated sols with small particle sizes usually grow to larger sizes while standing, say from 4 nm to 5 nm. (Flörke *et al.* 2005)

Stability against aggregation is the central issue in colloidal silica and colloidal systems in general. In this case colloiddally stable means that the particles do not aggregate at a significant rate. Silica sols are stabilized against aggregation by either (Iler 1979)

- an ionic charge on particles so that particles are kept apart by charge repulsion, or
- an adsorbed, generally monomolecular, layer of inert material which separates the silica surfaces to an extent that prevents direct contact.

Commercial silica sols are stabilized at pH 8.5-10.5 by the use of low concentrations of alkalis, usually sodium hydroxide. High concentrations, however, destabilize the sol. Stability against aggregation becomes critical at high silica concentrations which are required for shipping. Maximum concentration as a function of particle size is given in Figure 5. Silica sols are said to be stable because they do not settle or aggregate for long periods of time. (Flörke *et al.* 2005)

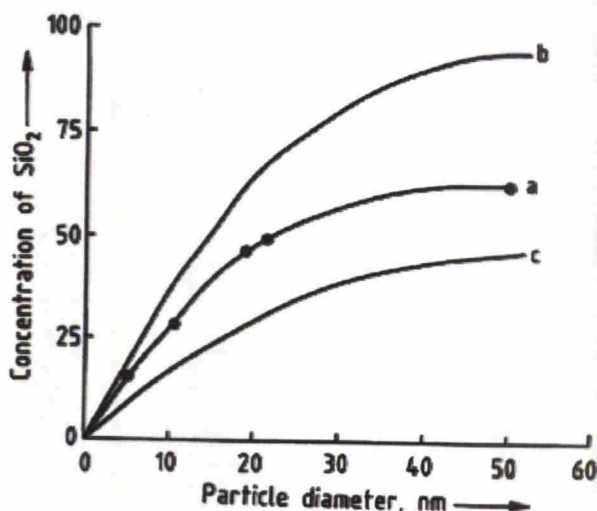


Figure 5. Maximum concentration versus particle size in stable aqueous silica sols at about pH 9.5; a) weight-%; b) g SiO<sub>2</sub>/100 ml, c) volume fraction of SiO<sub>2</sub> (×100) (Iler 1979, p. 325)

Stability against gelling is particularly important during the manufacturing process. Gelling of silica sols is highly dependent on the pH of the solution, as illustrated in Figure 6. The basic step in gel formation is the collision of two silica particles so that siloxane bonds are formed, holding the particles irreversibly together. This requires the catalytic action of hydroxyl ions. Thus gel formation increases with increasing pH in the pH range 3-5 and is proportional to the hydroxyl ion concentration. Above pH 6, scarcity of hydroxyl ions is no longer limiting, but instead, the rate of aggregation decreases because of the increasing charge on the particles. The net result of these two effects is a maximum rate of gelling at around pH 5. In the range of pH 8-10, sols are generally stable in the absence of salts. There is also a region of temporary stability at about pH 1.5. At lower pH, traces of hydrogen fluoride catalyze gel formation. In addition to pH, particle size affects the rate of gelling. Gelling is more rapid in sols with smaller particles than in sols with larger ones because of the larger surface area in sols with small particles. (Iler 1979)

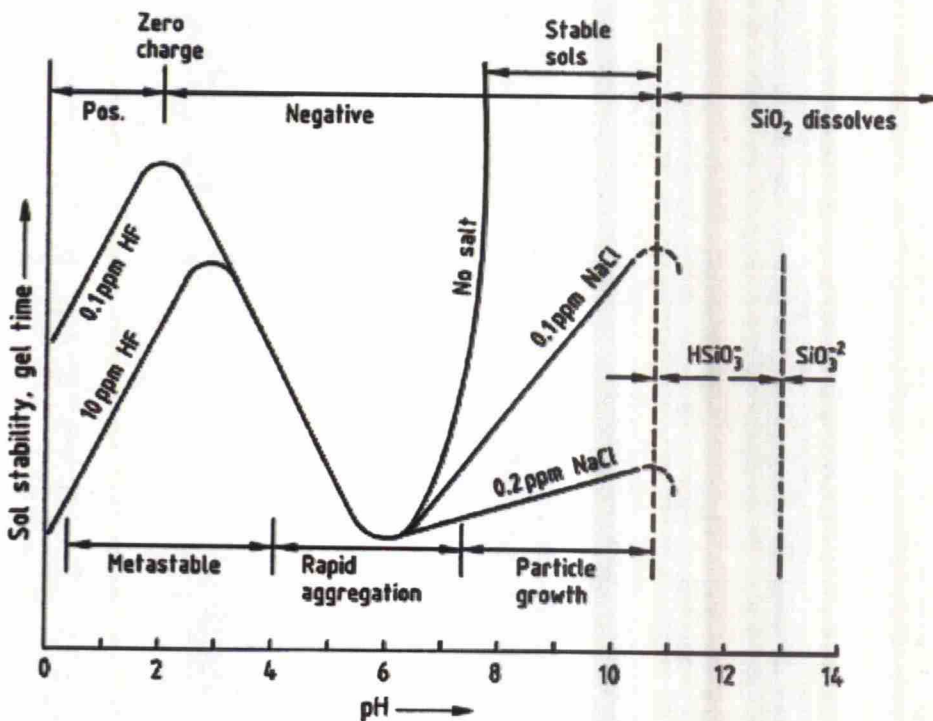


Figure 6. Effect of pH in the colloidal silica–water system (Iler 1979, p. 367)

### 4.3 The Ion Exchange Method

The ion exchange process is currently the primary means of manufacturing silica sols industrially. Various processes for making colloidal silica via the ion exchange

method have been described by Yoshida (1994) and Roberts (2006). Many of the processes involve the following basic steps (Roberts 2006):

- Complete removal of sodium from a dilute solution of sodium silicate. At this stage, the sodium ions are exchanged for hydrogen ions, and silicic acid is formed, which then polymerizes to nuclei.
- Readjustment of the  $\text{SiO}_2\text{:Na}_2\text{O}$  ratio using sodium hydroxide or sodium silicate.
- Heating to produce particles.
- Continued addition of silica to grow the particles. (This step may or may not be part of the process. It is discussed in detail in Paragraph 4.5.3.)
- Concentrating the dilute sol.

Figure 7 shows the basic flow chart for ion exchange processes.

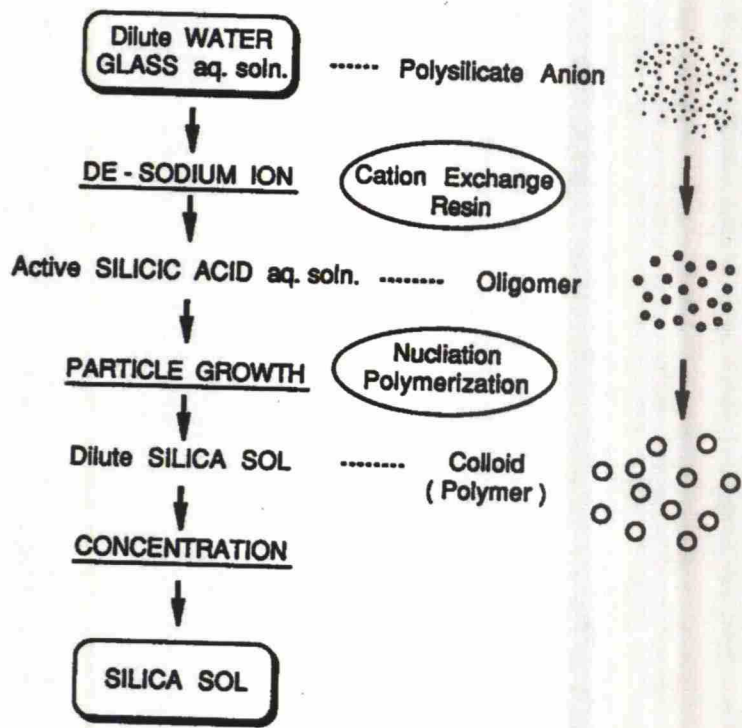


Figure 7. Basic flow chart for ion exchange processes (Yoshida 1994)

Yoshida (1994) classifies ion exchange methods into four categories according to different technical combinations of nucleation, particle growth, and concentration as shown in Figure 8. He also gives a qualitative characterization of the outcomes of those methods with respect to control of particle size and particle size distribution (Table 1). However, this classification is not very useful since the author does not



further specify terms as “slow”, “fast”, “small”, or “large” and it is unclear where the data was obtained from. Figure 9 shows two different industrial processes.

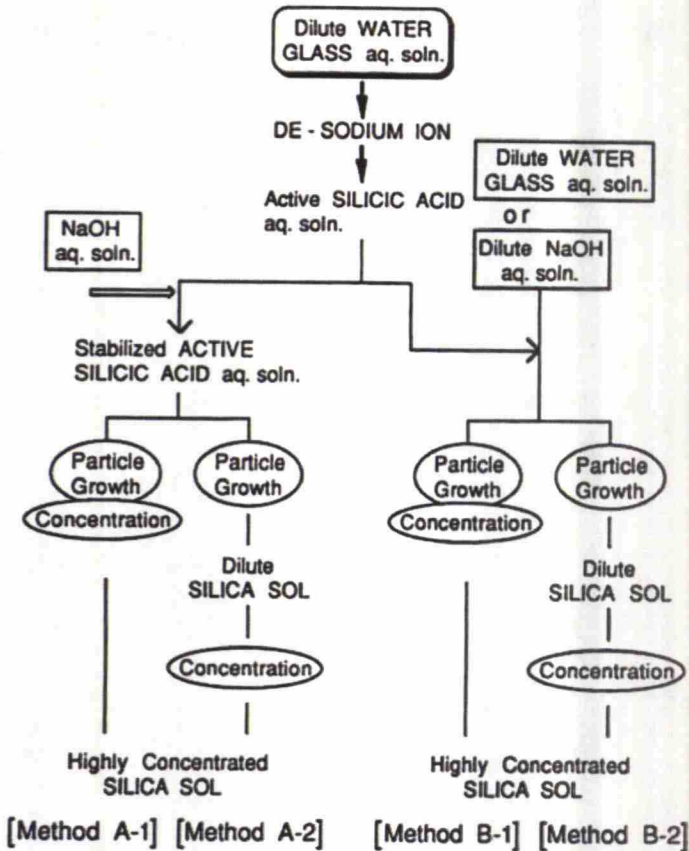


Figure 8. Classification of ion exchange methods by Yoshida (1994)

Table 1. Characteristics of the silica sol manufacturing methods in Figure 8 according to Yoshida (1994)

Characteristics	Method A-1	Method A-2	Method B-1	Method B-2
Intermediate material	dilute silica sol		silicic acid and water glass	
Particle growth and concentration	simultaneous	separate	simultaneous	separate
Change in pH during particle growth	7 → 9- 10.5		11.5 → 9-10.5	
Particle growth rate	slow		fast	
Size of nuclei	small		large	
Nucleation mechanism	Polymerization of particles		initial: hydrolysis of water glass; intermediate to final: polymerization of particles	
Manufacturing of large-particle sols	difficult (normal pressure); possible (with pressurization)		possible	
Ease of buildup	more difficult than in process B		easy	
Control of particle size	possible for microscopic- to medium-sized particles		possible for microscopic- to large-sized particles	
Control of particle size distribution	impossible or difficult	possible	impossible or difficult	possible
Manufacturing time	long (longer than in B-1)	short (longer than in B-2)	long	short

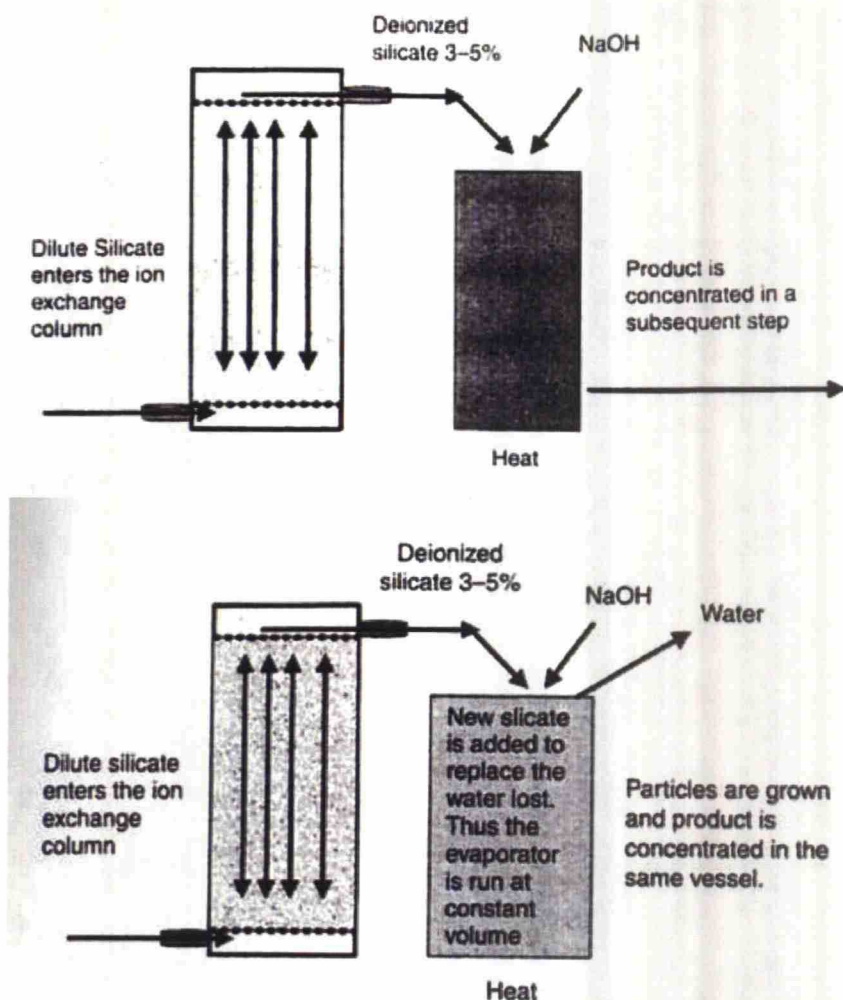


Figure 9. Industrial processes for silica sol production (Roberts 2006)

In the processes shown in Figure 9, the concentration of the product is constrained by the concentration of the silicic acid (deionized silicate in Figure 9). Its maximal concentration seems to be about 6 %, probably based on the fact that this is the maximum concentration at which a sol consisting of particles about 2 nm in diameter is stable, as can be seen in Figure 5. Thus an additional concentration step is required to give appropriate shipping conditions. This is done normally by evaporation, but also some membrane separations could be possible.

In the so-called Consol (Concentrated Sol) process developed and used at DuPont, the sodium silicate and the ion exchange resin are fed simultaneously to a stirred tank reactor containing a heel of water or silica sol (see Figure 10). The flow rates are controlled in order to remove most, but not all of the alkali from the system. This avoids the need for further alkali addition. The sodium silica concentration in the feed can be as high as 25 %, resulting in a final product concentration in the range

12-15 %. Moreover, a more uniform particle size distribution than in the other processes can be obtained. (Roberts 2006)

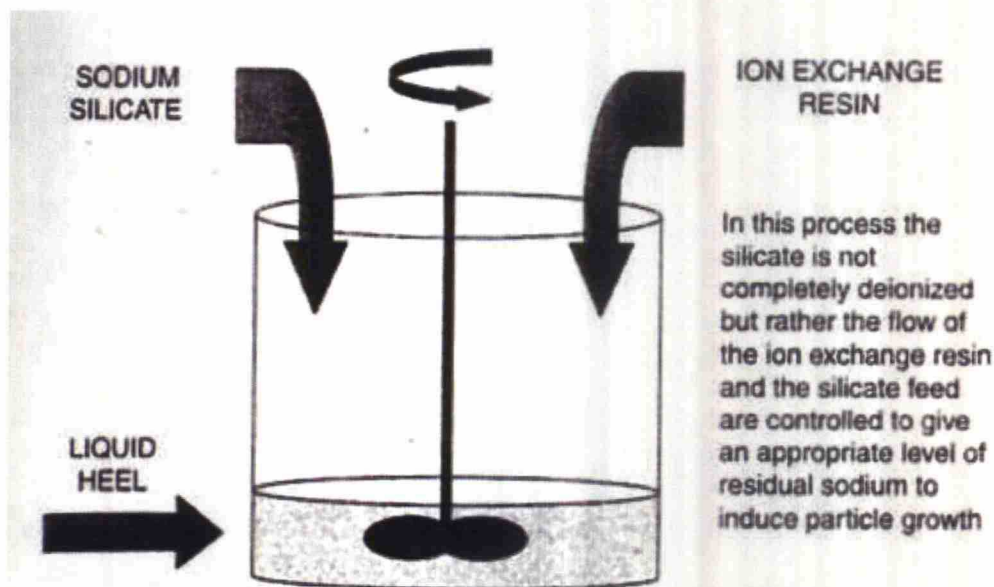


Figure 10. The Consol process (Roberts 2006)

#### 4.4 The Acid Neutralization Method

Sodium silicate reacts with acids, for example sulfuric acid, according to Equation (1). In the reaction silica is set free, which then can polymerize to form particles.



When a dilute solution of sodium silicate is partially neutralized with an acid to a pH of 8-9, a silica sol is obtained if the concentration of the resulting sodium salt is less than about 0.3 N (critical coagulation concentration, c.c.c.), and if the neutralization is carried out at elevated temperature, so that the particles grow to several nanometers as soon as they are formed, as described in Paragraph 3.2. If a sodium silicate solution with a sodium:silica ratio of 3.3 is used, then the maximum stable concentration of the product is about 3 %.

The reaction described above is basically a precipitation reaction. It can be said that the addition of the acid creates a supersaturation of silica in the solution, which then precipitates as silica nanoparticles. The same chemistry is also used to make precipitated silica (see Paragraph 7).



It is essential that the mixing is carried out in such a way that none of the mixture remains in the pH range 5-6 even locally, or otherwise gelling will occur almost instantly. This means that the acid and the silicate must be mixed with intense turbulence in the presence of either excess acid or excess silicate. (Iler 1979) An ultrafiltration or other separation step can be included in the process to wash out the salt and concentrate the solution, if desired (Yoshida 1994). The basic flow chart is presented in Figure 11.

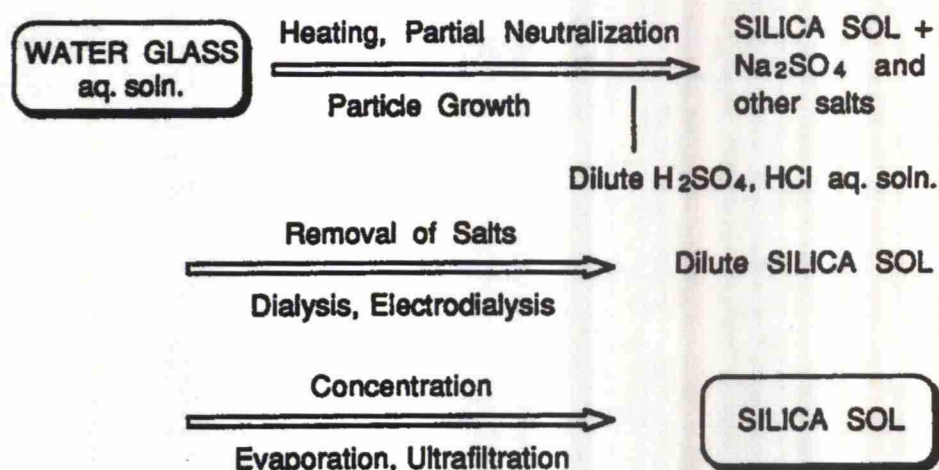


Figure 11. Flow chart of the acid neutralization method (Yoshida 1994)

More control over the reaction can be achieved by first removing sodium ions from the water glass solution and then adding sodium silicate and acid. Alexander *et al.* (1952) patented such a process to make a 3 % silica sol consisting of particles 37 nm in diameter. This process involves the use on an ion exchange resin to form a sodium silicate solution containing 2.2 % SiO<sub>2</sub> with a weight ratio of SiO<sub>2</sub>:Na<sub>2</sub>O of 85:1. This dilute sol is then heated at 100 °C for about 10 min to form nuclei. Then dilute solutions of sodium silicate and sulfuric acid are added simultaneously while the mixture is stirred vigorously at 95 °C for 8 h and the pH is maintained at about 9. The concentration of the sodium ions must not exceed 0.3 N at any time to prevent aggregation.

Iler (1976) patented a process, whereby a hot solution of sodium silicate is partly neutralized with acid at such dilution that the salt concentration does not exceed the critical coagulation concentration. The sol, which contains 2-3 % SiO<sub>2</sub>, is cooled to 50 °C and concentrated by ultrafiltration while salt is simultaneously washed out by adding water.

It is not known whether the acid neutralization method is in commercial use. However, because of its low cost it seems the most promising way to low-cost mass production of silica nanoparticles if stability of the product is not an issue.

## 4.5 Methods for Making Large-Particle Sols

### 4.5.1 Overview

There are two basic ways for making large-particle silica sols in aqueous solutions, both of them shown in Figure 12. In Process A, a silica sol consisting of medium-sized particles is heated in an autoclave at elevated temperature. In Process B, a medium- to large-sized silica sol is added to an alkaline solution. Then a silicic acid solution is added to the mixture to allow buildup of particles. Yoshida (1994) says that particles up to 200 nm in diameter could be produced by this method. However, only particle sizes up to 130 nm have been reported (Flörke *et al.* 2005).

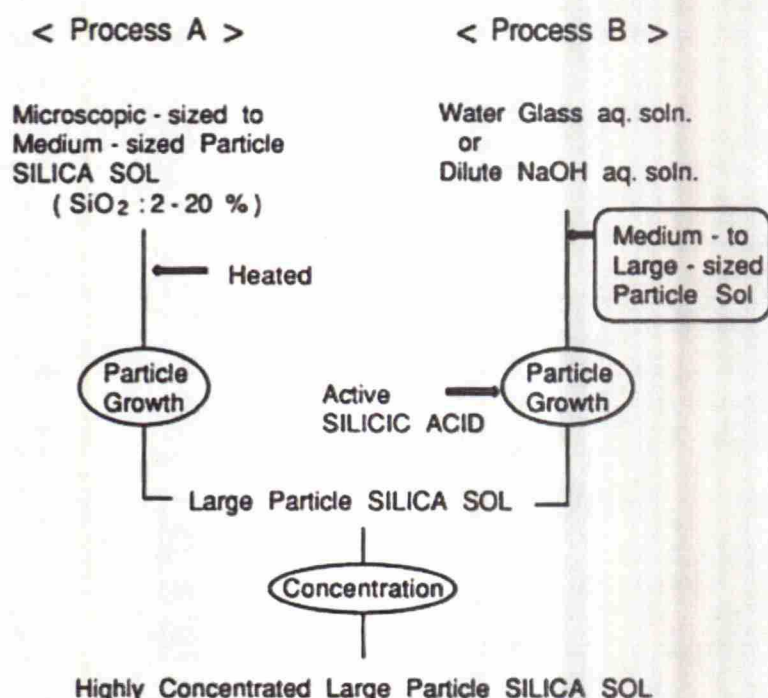


Figure 12. Methods for making large-particle silica sols (Yoshida 1994)

In journals and in patent literature, the terms “active silica” or “active silicic acid” are often used for silicic acid solutions obtained by passing a silicate solution through an ion exchange bed. It has been explained before that freshly deionized silicic acid will form spontaneously small particles of about 2 nm in diameter. These are “ac-

tive” in the sense that they are more soluble and dissolve in the presence of larger particles (Iler 1979).

### 4.5.2 Relation of Particle Size and Temperature

The most straightforward method for making sols which consist of large particles is by autoclaving an existing sol at high temperature. At higher temperatures, larger particles can be dissolved and the number of particles further decreases as the particle size distribution shifts towards larger particles.

In a given sol at a given temperature, particle size appears to approach asymptotically a final value that depends on the temperature. At temperatures higher than 300 °C alkali-stabilized sols tend to form quartz crystals instead of stable colloids. If the starting sol is first almost completely deionized and then autoclaved at 300-350 °C crystallization does not occur (Iler 1979, p. 240). By this method, the particle size range can be extended to at least 300 nm (Iler 1979, Flörke *et al.* 2005). However, the high pressures and long residence times needed make this process impractical for mass production. Table 2 summarizes some experimental results given by Iler (1979).

**Table 2. Growth of silica particles by heating a 4 % sol of silicic acid at pH 8-10 (Iler 1979, p. 241)**

Mole Ratio SiO <sub>2</sub> :Na <sub>2</sub> O	Time	Temperature (°C)	Specific Surface Area (m <sup>2</sup> /g)	Estimated Particle Diameter (nm)
100	1 h	80	600	5
64	6 h	85	510	6
100	5 h	95	420	7
78	6 h	98	406	7
80	30 min	100	350	8
85	3 h	160	200	15
85	3.25 min	270	200	15
85	0.9 min	250	225	15
90	3.1 min	200	271	10
85	10 min	200	228	12
85	10 min	295	78	36
85	30 min	295	N/A	64
Very high	3 h	340	N/A	88
Very high	6 h	340	N/A	105
Very high	3 h	350	20	150



### 4.5.3 Increasing Particle Size by Adding Active Silica – Buildup Process

The most promising approach to exact control over particle size seems to be a method, whereby silicic acid or active silica is continuously added to an existing sol, called a “heel” (Iler 1979, Yoshida 1994, Roberts 2006) or “seed” (Tsai *et al.* 2004, 2005a, 2005b). If the number of particles can be assumed constant, resulting particle size can be predicted from a mass balance equation. In growing particles by this process, the silicic acid must not be added to the system more rapidly than the silica surface can take it up (Iler 1979).

If the newly added small units, which are present in the active silica solution, encounter a larger particle, the very large difference in their solubility will cause the small particles to deposit on the larger ones (Figure 13). However, if the deionized silica units only run into similar size particles, they will form new small particles which will then act as nuclei for a new smaller family of particles. In that case the resulting sol will have a very broad particle size range. This happens if the silica is added faster than the larger particles can absorb it or if the concentration of the larger particles becomes so small as to make it improbable that the incoming silica will encounter one (Figure 14). (Roberts 2006) In order to keep the number concentration of particles constant, water has to be constantly removed from the system as the active silica is added. Tsai *et al.* (2005a, 2005b) showed the results of those effects in their experiments.

This also applies for the acid neutralization process (see Paragraph 4.4). If all the sodium silicate is neutralized at once, a large number of small particles will be the result. The small particles then agglomerate to give larger particles, whereby the final particle size is constrained by the temperature. If, however, the acid is added to the solution slowly, then the freshly formed silica can build up on the already existing particles, allowing larger particles to be formed.

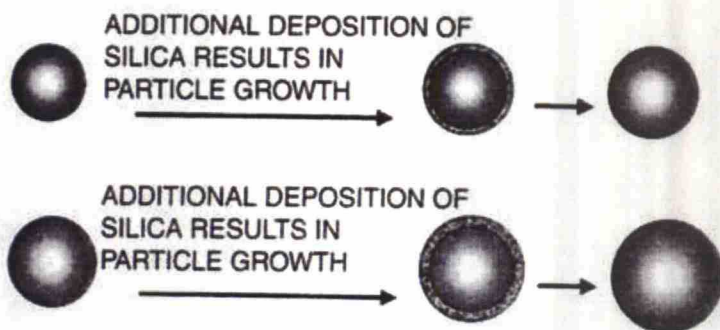


Figure 13. Continued silica deposition to give larger particles (Roberts 2006)

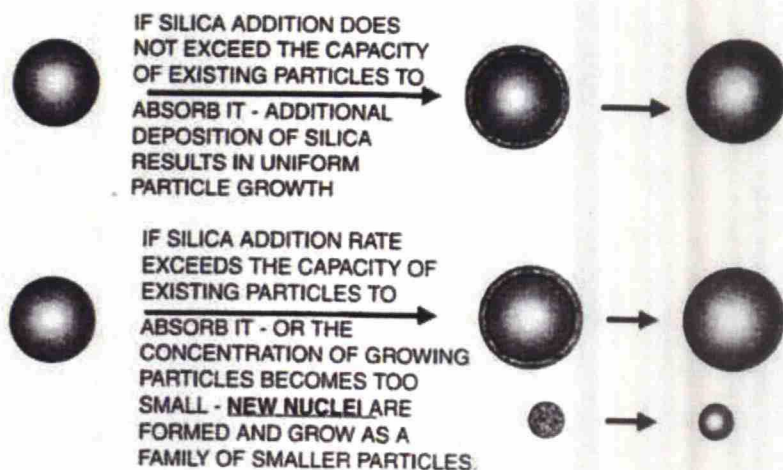


Figure 14. The key to narrow particle size distribution (Roberts 2006)

The maximum rate of addition without nucleation was given by Iler (1979, p. 315) as about 10 g of active  $\text{SiO}_2$  per  $1000 \text{ m}^2 \text{ hr}^{-1}$  area of silica surface. The surface area obviously decreases with increasing particle size, as can be seen in Figure 15. From this information, an estimated maximum addition rate can be calculated for a specific particle size. This is shown in Figure 16

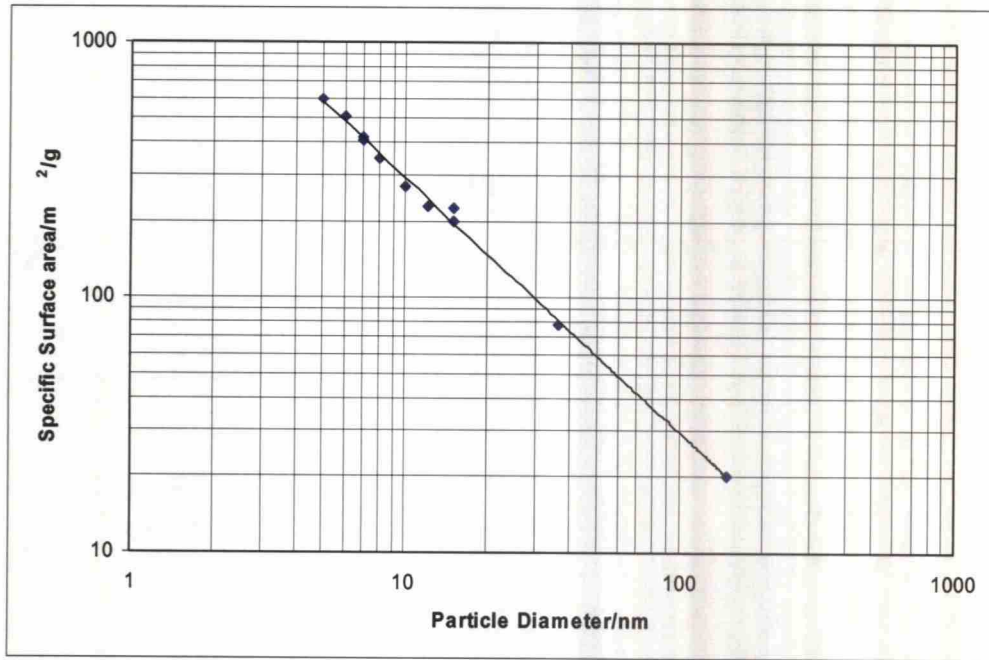


Figure 15. Relation between particle size and specific surface area, with data from Table 2

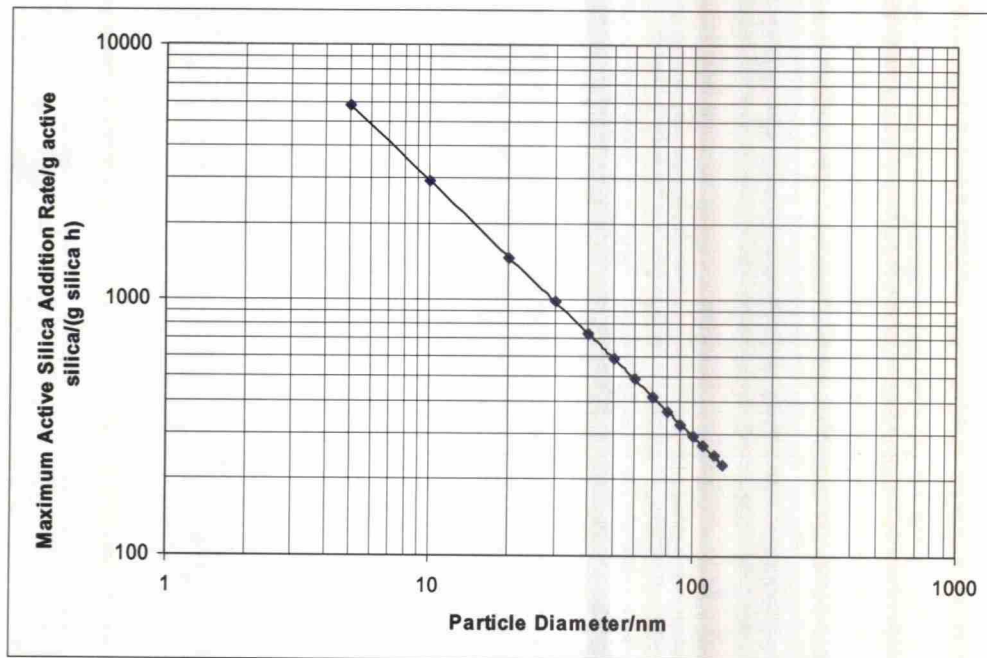


Figure 16. Relation between maximum active silica addition rate and particle size

If the number of particles remains constant, the theoretical increase in particle size can be calculated from the following mass balance equation (Iler 1979, Tsai *et al.* 2005b)

$$\left(\frac{d_f}{d_i}\right)^3 = \frac{W_n + W_a}{W_n}, \quad (2)$$

where



$d_f$  is the final particle size,

$d_i$  is the initial particle size,

$W_n$  is the mass of silica initially present as nuclei, and

$W_a$  is the mass of active silica added to the system.

Equation (2) can be written as

$$\left(\frac{d_f}{d_i}\right)^3 = 1 + B_r, \quad (3)$$

where the buildup ratio  $B_r$  is defined as

$$B_r = \frac{W_a}{W_n}. \quad (4)$$

#### 4.5.4 Limitations of the Buildup Process

Although the buildup process seems to be the most promising way to make large particles, it has some important limitations. The theoretical maximum diameter as a function of the buildup ratio, calculated from Equation (3), is illustrated in Figure 17.

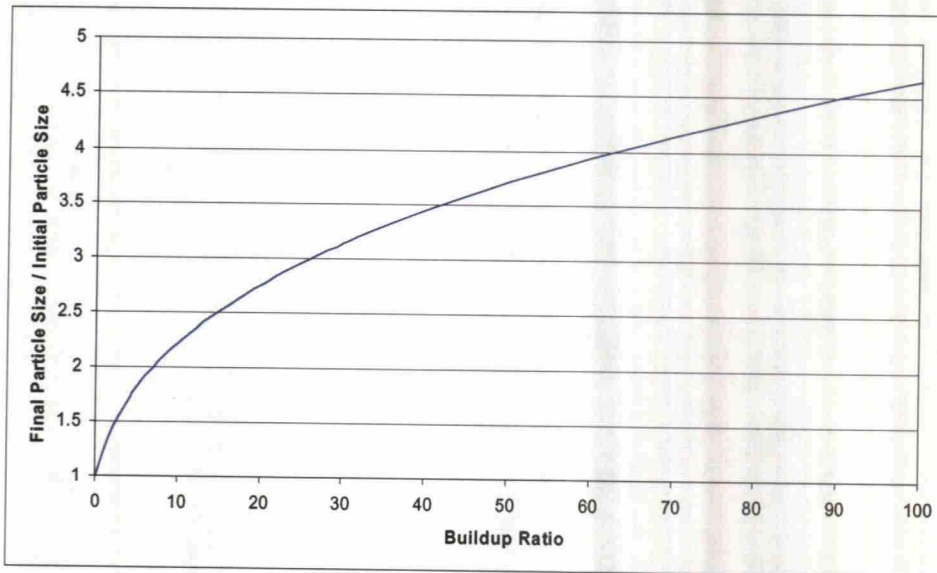
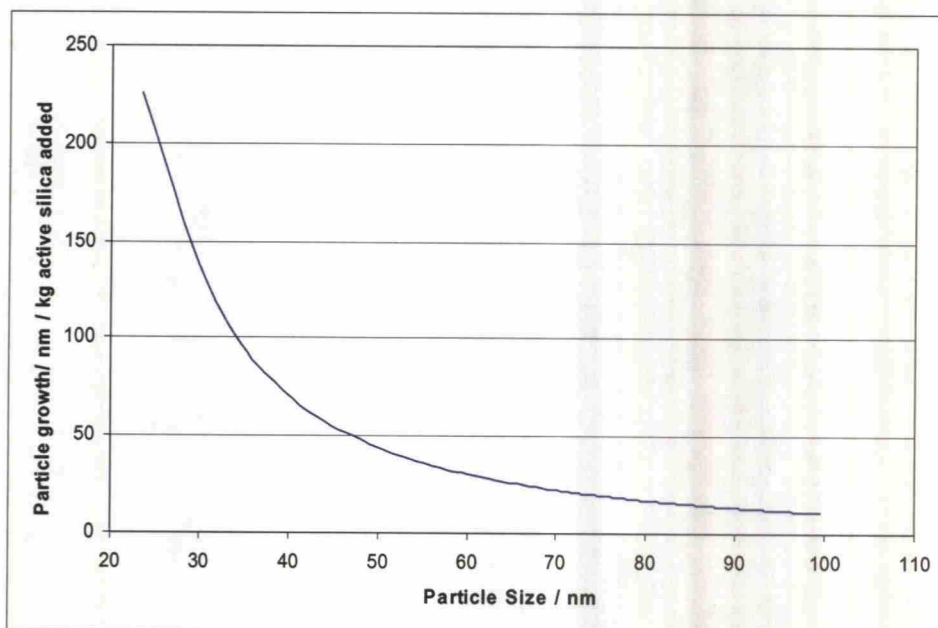
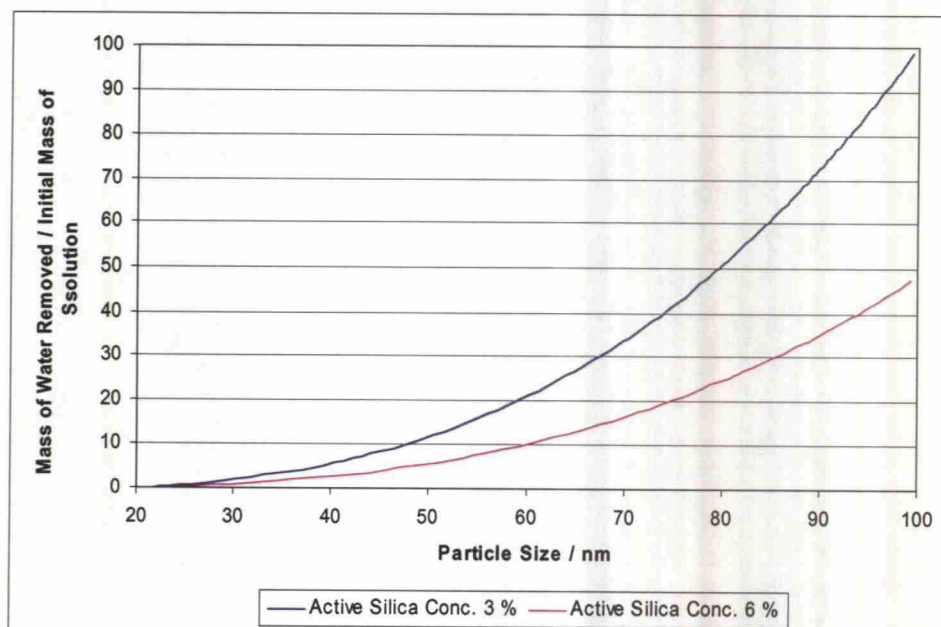


Figure 17. Particle size as a function of buildup ratio calculated from Equation (3)

Obviously particle growth rate decreases quite rapidly with increasing buildup ratio. This is further illustrated in Figure 18, which shows the particle growth rate as a function of particle diameter. Figure 19 shows the amount of water that has to be removed from the system in a constant volume process.



**Figure 18. Theoretical growth rates of particles in the buildup process**



**Figure 19. The amount of Water that has to be removed from the system for a heel concentration of 2.5 % and active silica concentrations of 3 % and 6 % in the titrate**

From these figures it can be clearly seen that the buildup process is not practical for making particles much larger than 100 nm in diameter. If water is removed by evaporation, then alone the energy requirements of the process are tremendous. However, at least one continuous process of this kind has been patented by Brekau *et al.* (1999), where active silica is added into the reactors of a multi-stage cascade reactor containing a colloidal silica solution. The average particle sizes produced by the

process are given as 27 to 72 nm. This and similar processes are discussed in more detail in Paragraph 9.

## 4.6 Experimental Work

Tsai *et al.* have published a series of articles about their experimental work on silica sol formation. The first one (Tsai 2004) deals with a basic ion exchange process, where active silicic acid was titrated to a solution of potassium hydroxide. This is basically Method B-2 in Yoshida's classification (see Figure 8). The influences of temperature, KOH concentration and silicic acid addition rate on mean particle size were studied. The resulting particle sizes were in the range of 10-50 nm. Larger particles were obtained at high temperatures and with low silicic acid addition rates.

The second article (Tsai *et al.* 2005a) basically deals with the buildup process. Active silicic acid was titrated to a heel of silica particles in order to grow larger particles. Two processes, namely the constant concentration process and the constant volume process, were introduced. Both processes were carried out at boiling temperature. In the constant volume process, the reaction volume was kept constant during the titration by evaporation of water. The constant concentration process was a reflux process, in which the reaction volume increased during the reaction. Better results were obtained by the constant volume process, as could be expected.

In the third article (Tsai *et al.* 2005b) the influence of heel concentration on the outcome of the constant volume process was investigated. It was found that at a heel concentration of 2.47 %, measured particle size matched with particle size calculated from Equation (2). At lower concentrations a new family of smaller particles was formed, and at higher concentrations gel formation occurred. Figure 20 shows TEM images of the outcomes. These results, however, can not be generalized, since the outcome of the process depends on the silicic acid addition rate (not given in the article) and the surface area of the colloidal silica in the solution. Despite these shortcomings the work by Tsai *et al.* provides a useful basis for making silica sols in laboratory scale.



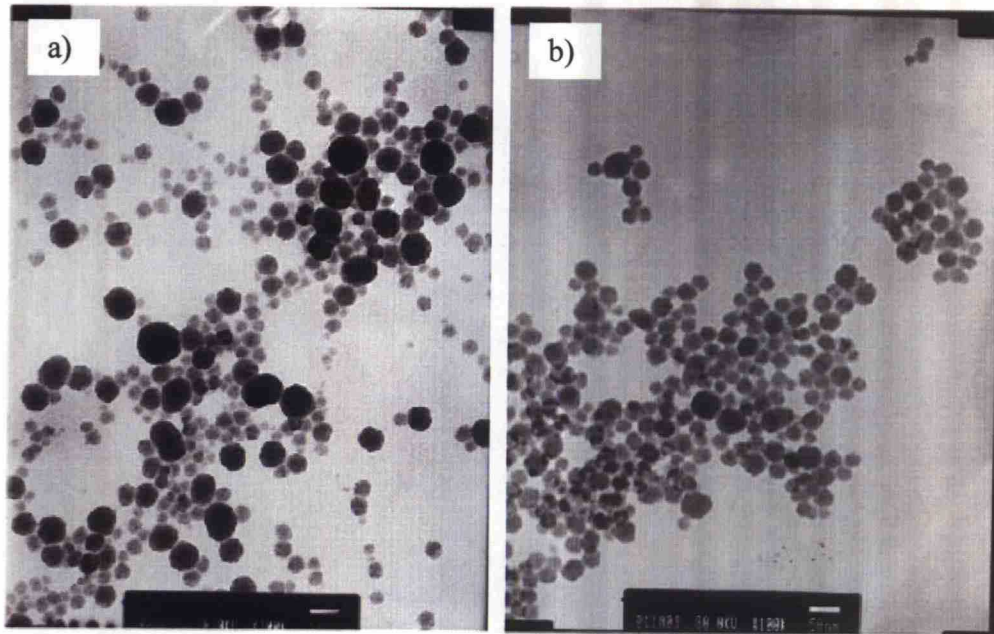


Figure 20. TEM images of colloidal silica created in the buildup process; a) a new family of smaller particles has been formed; b) added silica has been completely deposited on existing particles, resulting in a uniform particle size distribution (Tsai *et al.* 2005b)

## 5 Aggregation of Particles

### 5.1 Terminology

The word *aggregation* is used for all the ways in which colloidal particles link together. Iler (1979) distinguishes the following four forms of aggregation:

- *Gelling*, where the particles are linked together into a three-dimensional network that fills the whole volume of sol so that there is no increase in the concentration of silica in any macroscopic region in the medium. Instead, the overall medium becomes viscous and is then solidified by a coherent network of particles, which, by capillary action, retains the liquid.
- *Coagulation*, where the particles come together into relatively close-packed clumps in which the silica is more concentrated than in the original sol, so the coagulum settles as a relatively dense precipitate.
- *Flocculation*, where the particles are linked together by bridges of the flocculating agent, which are sufficiently long that the aggregated structure remains open and voluminous. There is no sharp distinction between coagulates and flocculates.

- *Coacervation*, in which the silica particles are surrounded by an adsorbed layer of material which makes the particles less hydrophilic, but does not form bridges between particles. The particles aggregate as a concentrated liquid phase immiscible with the aqueous phase.

The basic difference between coagulation or flocculation of particles and gelling is illustrated in Figure 21.

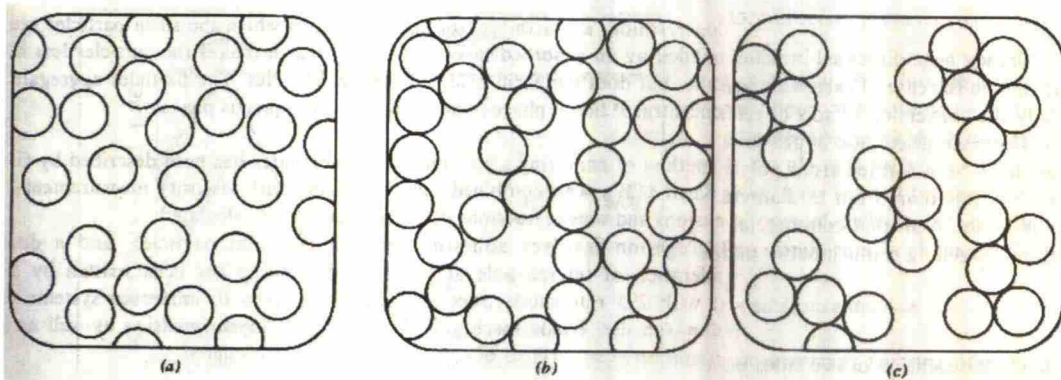


Figure 21. The difference between a gel and coagulates or flocculates. a) silica sol; b) a gel; c) coagulates or flocculates. (Iler 1979, p. 365)

## 5.2 Coagulation Mechanisms

Coagulation is considered to be the result of van der Waals attraction which draws two particles together at the moment of collision, unless hindered by two factors (Iler 1979, p. 373):

- The hydration of the surface of the particles by a layer of water molecules, hydrogen-bonded to the SiOH groups.
- The negative ionic charge on the particles above about pH 3.5 and the surrounding cloud of positive counter cations such as  $\text{Na}^+$ , forming a "double layer".

In the pH range 7-10 silica sols are stable if electrolyte concentration is low, but are coagulated when salts are added. Two mechanisms for this have been suggested (Iler 1979, p. 373):

- Particle-to-particle attraction by van der Waals forces. In this case the repulsion force between particles with similar ionic charges is simply reduced by the addition of salt coagulant when a critical coagulation concentration (c.c.c) is exceeded.



- Particle-to-particle bridging by the flocculating agent. This is a rather complicated mechanism.

The critical coagulation concentration for sodium was given by Iler (1979, p. 378) as

$$N = 0.26 - 0.005C - 0.002(T - 40), \quad (5)$$

where

$N$  is the normality of the sodium salt,

$C$  is the concentration of silica in g/100 ml, and

$T$  is the temperature in °C.

### 5.3 Aggregation Models and Experimental Work

The aggregation stage has been investigated by many authors. Smoluchowski (1917) was the first to systematically develop a theory of aggregation. He distinguished *perikinetic aggregation* (when collisions are brought about by Brownian motion of very small particles) from *orthokinetic aggregation* (when collisions are brought about by fluid motion). Smoluchowski was also the first to derive equations for the aggregation mechanisms, based on simple two-body collisions.

Schaer *et al.* (2001) investigated the aggregation process in colloidal silica by destabilizing a commercial silica sol (Ludox HS 30, containing monodisperse, 12 nm silica particles) by the addition of sodium ions. The influences of various parameters were investigated by the use of population balances. They found that the aggregation process in colloidal silica goes through the stages of perikinetic and orthokinetic aggregation. The perikinetic aggregation mechanism was dominant for aggregates with mean number sizes lower than 250 nm. Only physico-chemical factors affected the perikinetic aggregation mechanism, allowing the scale-up of the process from laboratory or pilot scale data. The orthokinetic mechanism was found to apply for particles with mean number sizes larger than 250 nm.

Schaer *et al.* studied the influence of the following variables on the aggregation process:

- *Stirring speed.* Stirring speed had no influence on particle size distribution during the first stage of the aggregation process, when particles were smaller than about



100 nm. Even after that, the influence of stirring speed was minimal and affected mainly the breakage of larger aggregates.

- *Sodium concentration.* An increase in electrolyte concentration was found to enhance the aggregation process.
- *Temperature.* An increase in temperature enhanced aggregation during the first stage of the process, since the collision efficiency increases with temperature in the perikinetic aggregation stage.
- *Silica concentration.* An increase in total silica concentration was found to enhance the perikinetic aggregation rate.

The influence of primary particle size was not investigated.

Schlomach and Kind (2004a) developed a simulation model to predict aggregate structure, whereby aggregates were modeled as fractals. For fractal systems, the relationship between aggregate diameter and the number of primary particles in the aggregate is given by the equation

$$x_{Ai} = \left( \frac{i}{\alpha} \right)^{\frac{1}{d_f}} x_p, \quad (6)$$

where

$x_{Ai}$  is the aggregate diameter,

$x_p$  is the primary particle diameter,

$i$  is the number of primary particles in the aggregate,

$\alpha$  is a coefficient normally close to 1, and

$d_f$  is the fractal dimension.

The fractal dimension is 1 for a chain of particles and 3 for an ideally compact aggregate. For silica aggregates the fractal dimension was found to be close to 2. Figure 22 shows simulation results for aggregate structures with 1000 primary particles. Equation (6) can be used to estimate the number of primary particles per aggregate if the diameters of the aggregate and the primary particles are known. (Schlomach and Kind 2004a, 2004b)



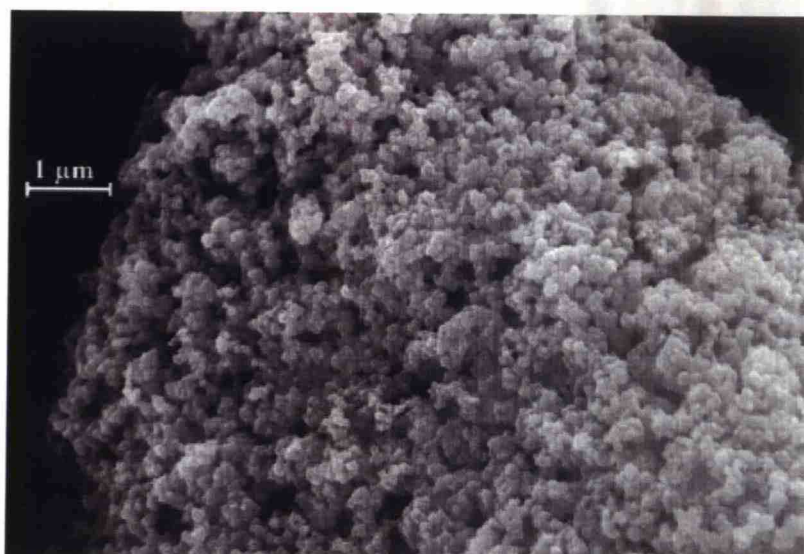


Figure 24. SEM image of the dried product obtained by Schlomach and Kind (2004b); the image shows a uniform primary particle size of about 22.7 nm

## 5.4 Break-Up and Dispersion of Aggregates

### 5.4.1 High-Shear Mixers

In a high-shear rotor-stator mixer, liquid is radially dispersed as jets through a rapidly spinning central rotor. As it travels across a small gap between the high-speed rotor and the stationary stator, the fluid is forced into a pattern of slots, holes, or other perforations in the stator, causing high mechanical and hydraulic stresses (Shelley 2004). High-Shear mixers are used for example for the preparation of paper coatings and the dispersion of fumed silica (see Paragraph 8) (Silverson Machines 2003, 2005). The dispersion process is shown in Figure 25.

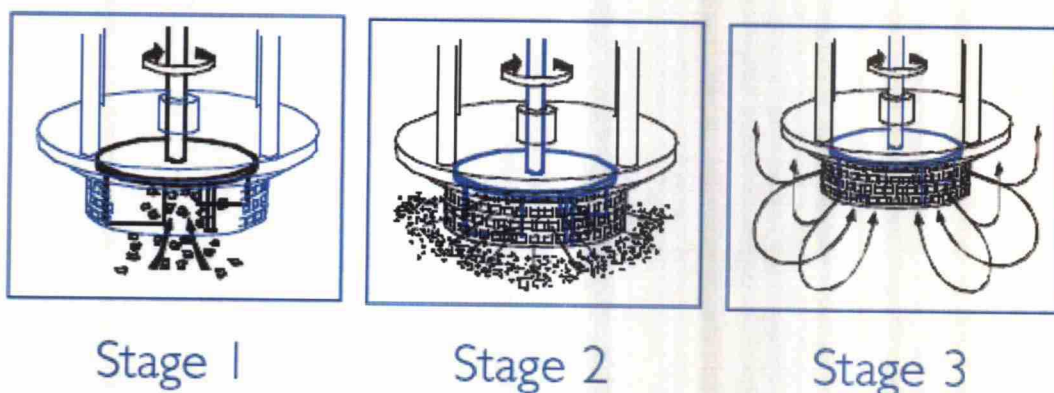


Figure 25. Dispersion of solids using a high-shear mixer. Stage 1: The suction created by the rotor draws both liquid and solid ingredients into the workhead. Stage 2: Centrifugal force drives the materials to the periphery of the workhead where they are subjected to a milling ac-



tion in the gap between the rotor and the stator. Stage 3: The product is expelled from the head and projected back into the body of the mixer (Silverson Machines 2005)

High-shear mixers are available as batch mixers, often with interchangeable work-heads, inline mixers, and ultra high-shear inline mixers (Shelley 2005). Typical particle size distributions generated by these three types are shown in Figure 26. The figure shows that submicron sizes are achievable with high shear mixers, but the mean particle (aggregate) size remains approximately one order of magnitude larger than the primary particle size.

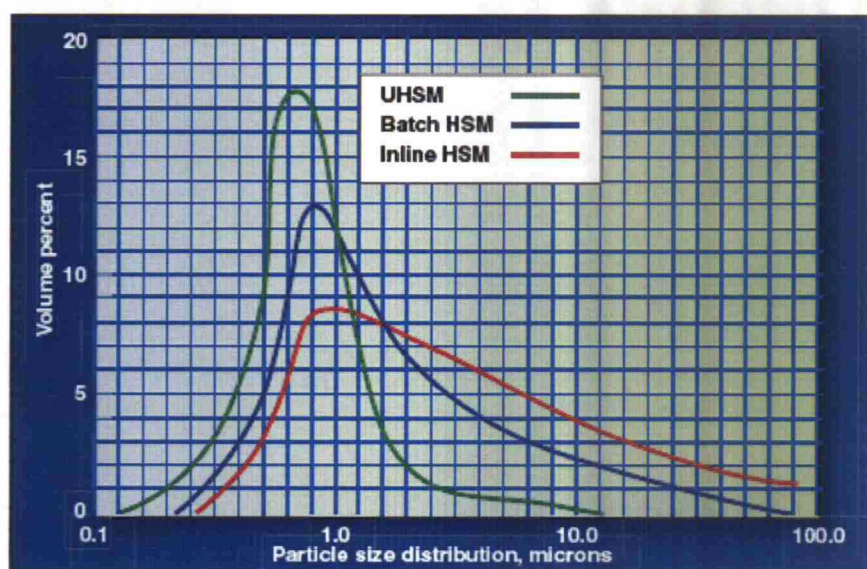


Figure 26. Typical particle size distributions generated by different types of high-shear mixers (Shelley 2005)

### 5.4.2 Bead Mills

Bead mills, also called stirred media mills, have raised an increasing amount of interest in recent years, as bead mills suitable for grinding materials to the nanometer scale have been developed. A fine bead mill is a very effective piece of equipment for grinding crystalline materials and disaggregating solids, including silica, even down to nanometer sizes. According to Way (2007), they are reasonably simple, scalable, and low-cost.

A bead mill can be run in a single-passage operation, a cyclic operation, or in a circulation mode of operation (Figure 27). With the choice of the right bead size, the milling time can be reduced down to a few minutes (McLaughlin 1999, Way 2007). Bead mills can be used in either batch or continuous operation. In continuous operation, the residence time required should equal the residence time in the mill so that milling

can be performed in a single-passage operation. In this case, the flow inside the mill should be close to plug flow. To achieve near plug flow, high throughput rates that result in uniform velocity of particles through the mill are required (Mende *et al.* 2006).

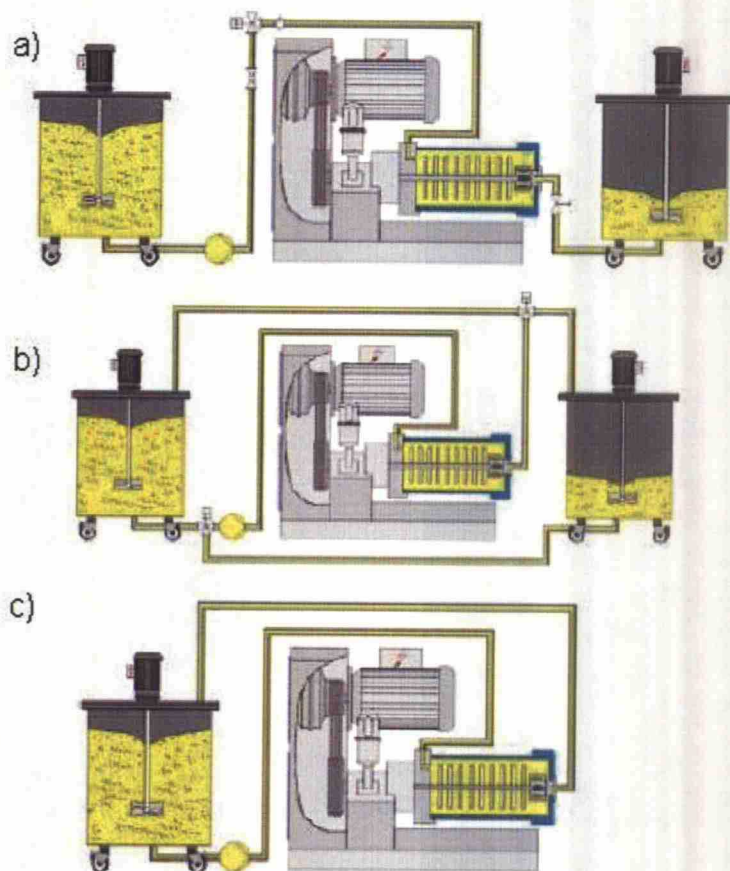


**Figure 27. Modes of operation in bead milling; a) single passage; b) cyclic mode; c) circulation mode (Kolb and Scherer 2002)**

Bead mills have a vertically or horizontally arranged cylindrical tank which is filled between 70 and 90 % with grinding beads. The beads are normally made of steel, glass or ceramic materials. An agitator with suitable agitation elements provides intensive movement of the grinding material, while the product suspension is continuously pumped through the grinding chamber. The suspended solids are ground or dispersed between the grinding and beads by impact or shearing forces. The product and the beads are separated by a separator gap, sieve or a centrifugal system at the discharge outlet of the mill. (Kolb and Scherer 2002)

The theoretical basis of the grinding technology has been described by Kwade and Schwedes (2002). According to their theory, the transmitted grinding energy is pro-



portional to two basic values, the number of stress events (contacts) and the stress intensity at each stress event. The number of contacts decreases with decreasing initial particle size. This can be compensated by using smaller beads. Thus very fine beads and a mill that is able to use these beads are required to grind materials down to nanometer scale. (Kolb and Scherer 2002, Mende *et al.* 2006) Bead sizes of 100 to 200  $\mu\text{m}$  are usually used. 100  $\mu\text{m}$  glass beads have been successfully used to disaggregate silica particles down to a mean particle size of 40 nm. (Mende *et al.* 2006) For dispersion or disaggregation, the ratio between bead size and final particle size should be between  $10^2$  and  $10^4$  (Kolb and Scherer 2002). For a primary particle size of 40 nm, this corresponds to a bead size of 4-400  $\mu\text{m}$ . By using appropriately sized beads, the residence time required can be reduced to even less than a minute under optimal conditions (McLaughlin 1999).

A distinction must be made between disaggregating of aggregates and actual grinding of crystalline materials. In the case of the silica particles, only disaggregating is desired. In fact, too high stresses inside the mill can lead to undesired change in the crystalline structure of the product and its properties. (Mende *et al.* 2006) The key to the dispersion of nanoparticles is a technique called “mild dispersion”, whereby small beads and slow agitator tip speed are used to create multiple, low-energy contacts between the grinding media and the particles (Way 2007). The low agitator speed also results in low energy consumption of the mill.

### 5.4.3 Ultrasonic Dispersing

A third approach to dispersing aggregates is ultrasonic disaggregation. Pohl and Schubert (2003) have compared the effects of rotor-stator systems and ultrasonic dispersing on mean aggregate size. With ultrasonic dispersion, the resulting aggregates normally show a very broad size distribution. With milling, the achieved particle size distribution is often much narrower. Pohl *et al.* (2004) have investigated the dispersion characteristics of fumed silica (Aerosil 90 by Degussa, primary particle size 21 nm) in ultrasonic dispersing. They found that the main parameter affecting particle size was specific energy. Remarkable effects were achieved at specific energies higher than  $10^6 \text{ kJ/m}^3$ .



## 6 The Sol-Gel Process

The term sol-gel process is applied to describe fabrication of inorganic materials by preparing a sol, gelling, and then drying the gel (Scherer 1994). Figure 28 shows the stages and possible end products of the sol-gel process.

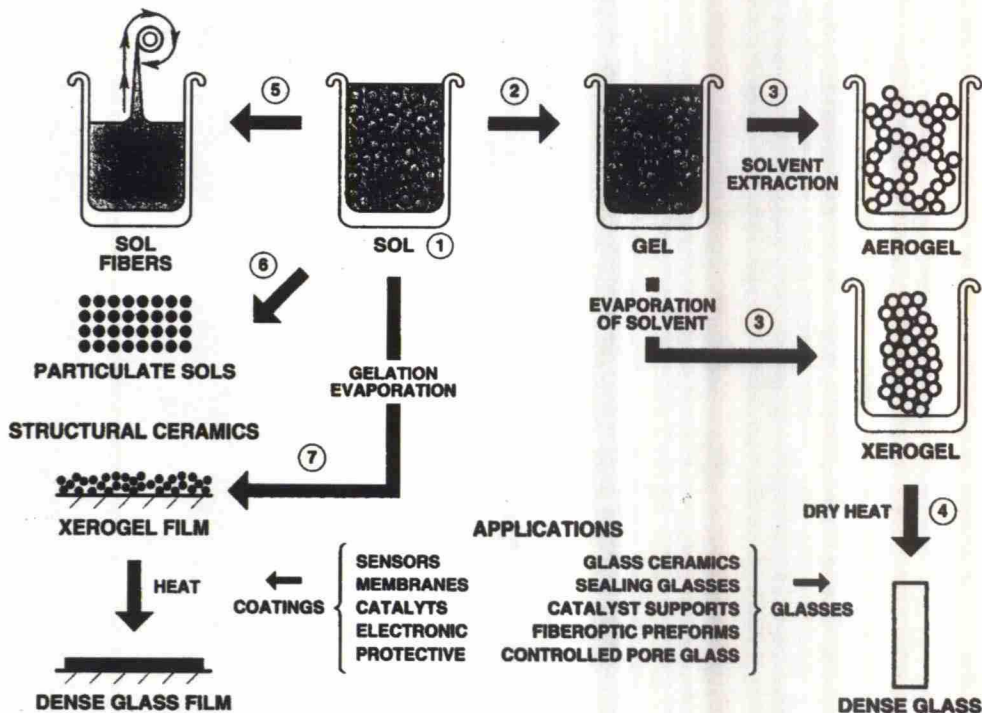


Figure 28. The various stages of the sol-gel process (Brinker 1994)

What makes the sol-gel technology particularly interesting is the fact that it combines the control over the molecular structure of the material as well as the ability to shape it at room temperature, for example by casting it into molds (Brinker 1994). Synthetic silica powders can be obtained by grinding the dried gel.

The term sol-gel process is normally applied to a process where silica alkoxydes, such as tetra-ethyl-ortho-silicate (TEOS,  $\text{Si}(\text{OC}_2\text{H}_5)_4$ ), but also aqueous solutions of metal silicates, such as water glass, are used as precursors. (Brinker 1994) The aqueous sol-gel process was investigated by Scломach and Kind (2004b), as mentioned before.

Using TEOS as the precursor, extremely large primary particles of perfect spherical shape can be obtained, with diameters of hundreds of nanometers (Hench and West 1990, Khan *et al.* 2004). However, TEOS as raw material is too expensive in industrial production (Lee *et al.* 2006). The precipitation is normally done in an ethanol

solution using ammonia. Ghosh and Pramanik (1997) have suggested that a nano-sized ceramic powder similar to silica particles could also be precipitated from an aqueous solution by using metal formates instead of metal alkoxides as the raw material.

TEOS-derived silica particles are often used as model particles and for calibrating measuring equipment. Their properties can be easily and exactly controlled by varying the reaction conditions. (Gellermann *et al.* 2007) Figure 29 shows a TEM image of typical spherical silica particles obtained by the sol-gel method using TEOS as precursor.

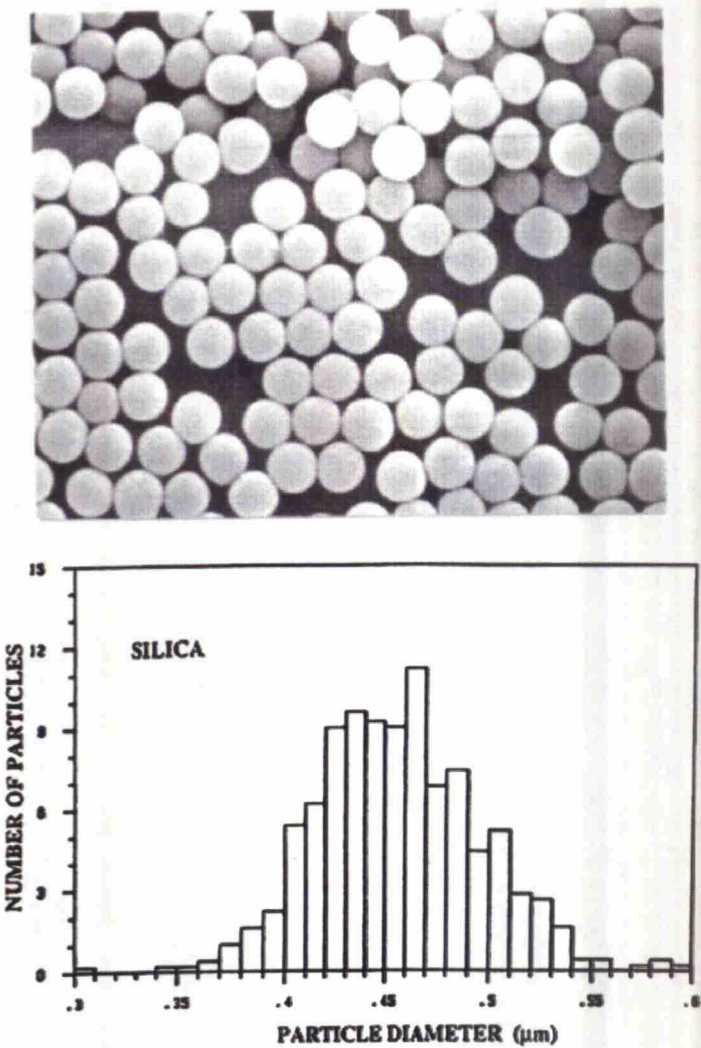


Figure 29. TEM image and particle size histogram of a typical batch of spherical silica particles produced by the sol-gel method using TEOS as precursor (Hench and West 1990)

## 7 Precipitated Silica

### 7.1 Production

Precipitated silica is a synthetic, finely divided, white, amorphous form of silicon dioxide. It has only been produced commercially since the 1940s, but in the meantime it has become the most important group of silica products on the basis of the amounts produced. (Flörke *et al.* 2005)

The formation of precipitated silica is essentially a neutralization process. It is very similar to the acid neutralization process discussed in Paragraph 4.4, with the difference that the final salt concentration exceeds the critical coagulation concentration. Raw materials for the production of precipitated silica are aqueous alkali metal silicate solutions, most commonly water glass, and acids, generally sulfuric acid. Precipitation with other acids has also been proposed but those are of minor economic interest (Flörke *et al.* 2005). Thornhill and Allen (1955) and Hüter and Steenken (1962) have made a particularly interesting proposition to use carbon dioxide as the acid in the precipitation process.

In the process for making precipitated silica, the silica precipitates according to Equation (1):



In contrast to silica gels, which are produced under acidic conditions, precipitation is carried out in neutral or alkaline media. The properties of the precipitated silica can be influenced by the design of the plant equipment and by varying the process parameters. (Flörke *et al.* 2005) The process involves the following steps (Iler 1979, p. 556):

- Forming and growing colloidal particles.
- Coagulating particles into aggregates forming a suspended precipitate, controlled by pH and  $\text{Na}^+$  ion concentration.
- Reinforcing the aggregates to a desired degree without further nucleation.

An industrial production process consists of the following steps (Flörke *et al.* 2005):

- Precipitation



- Filtration
- Drying
- Grinding
- Compacting and granulating (optional).

Precipitation is most commonly carried out in a batch process, although continuous processes have also been proposed (Société Française des Silicates Spéciaux Sifrance 1972, see Paragraph 9). Figure 30 shows the basic process scheme. (Flörke *et al.* 2005)

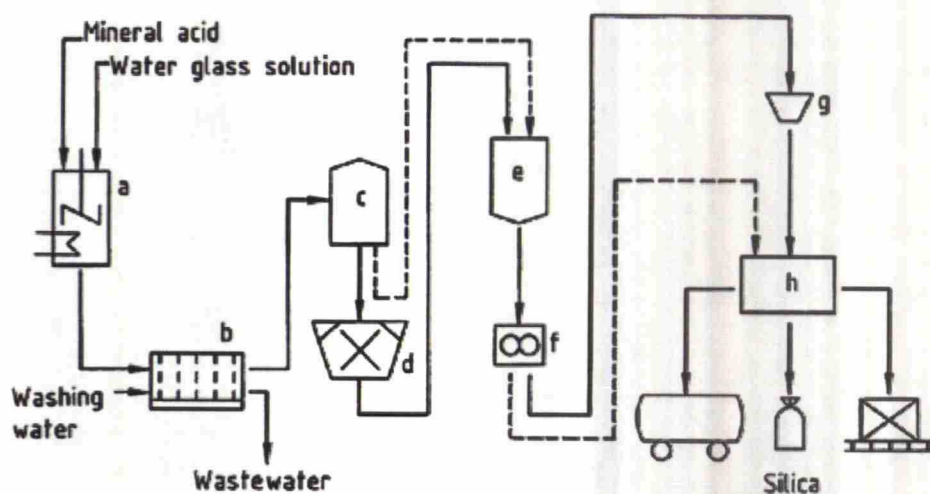


Figure 30. Basic process scheme for the production of precipitated silicas; a) Precipitation; b) Filtration; c) Drying; d) Grinding; e) Storage; f) Compacting; g) Granulation; h) Packaging (Flörke *et al.* 2005)

## 7.2 Chemistry

There is a close relation between the formation of silica gel and precipitate. In precipitation, the silica concentration is lower and the particles are brought together into aggregates by forces of coagulation. In the absence of a coagulant, silica is not precipitated from solution at any pH. (Iler 1979, p. 554)

As discussed before in Paragraph 3.2, under acidic conditions silicic acid polymerizes to small particles which network together to form a continuous gel throughout the water. Under alkaline conditions, silica polymerizes to discrete colloidal particles which grow to sizes larger than about 5 nm in diameter and remain as a stable sol. A simple way to differentiate between a precipitate and a gel is that a precipitate encloses only part of the liquid in which it is formed. (Iler 1979)

Above pH 7 and up to 10.5, where silica begins to dissolve, the silica particles are charged negatively and repel each other. Therefore, they do not collide, and particle growth continues without aggregation. When silica particles are present in hot suspension at pH 9-10, they are coagulated when the concentration of sodium ions exceeds the critical coagulation concentration, or c.c.c. (In a solution of sodium silicate with the commonly used ratio 3.3  $\text{SiO}_2\text{:Na}_2\text{O}$  the sodium ion normality is 0.1  $C$ , where  $C$  is the silica concentration in g/100 ml.) During this aggregation stage particles form colloidal fractal structures. The resulting aggregates can be reinforced by the addition of active silica, which is usually formed by the addition of more water glass and acid (Figure 31). The active silica is then deposited on the surface of the aggregates in a similar manner as in the buildup process (see Paragraph 4.5.3). (Iler 1979)

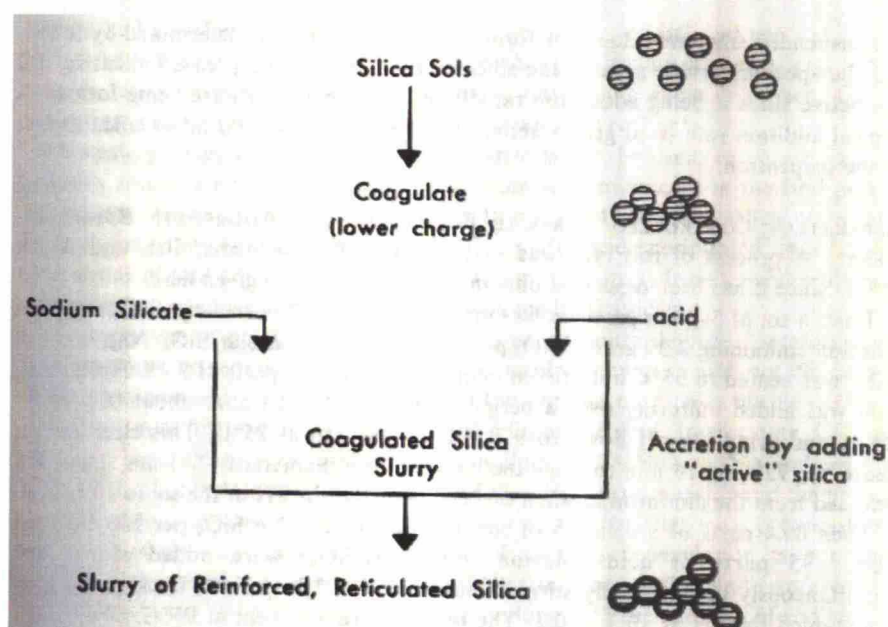


Figure 31. Reinforcement of aggregates by adding active silica (Iler 1979, p. 557)

## 7.3 Enhanced Precipitation

### 7.3.1 Precipitation from Emulsion Systems

Jesionowski (2001, 2002a, 2002b) has investigated the precipitation of silica from emulsion systems of an aqueous sodium silicate solution and cyclohexane. Cyclohexane was removed from the product by distillation. Sulfuric (Jesionowski 2001) and hydrochloric acids (Jesionowski 2002a, 2002b) were used for precipitation. Both the acid solution and the water glass solution were emulsified in cyclohexane and

then mixed together. Figure 32 shows the flow diagram. The effects of various emulsifiers and dispersing media on particle size and morphology were examined. Ionic and non-ionic surfactants were used as emulsifiers and a top stirrer, a homogenizer, and an ultrasonic bath were used as dispersing media. Under optimal conditions, particles in the range of a few hundreds of nanometers with very narrow particle size distributions were obtained. Best results were achieved by using a non-ionic surfactant as the emulsifier and a homogenizer as the dispersing medium (Jesionowski 2002b). The obtained particles showed similar characteristics to those precipitated from TEOS systems.

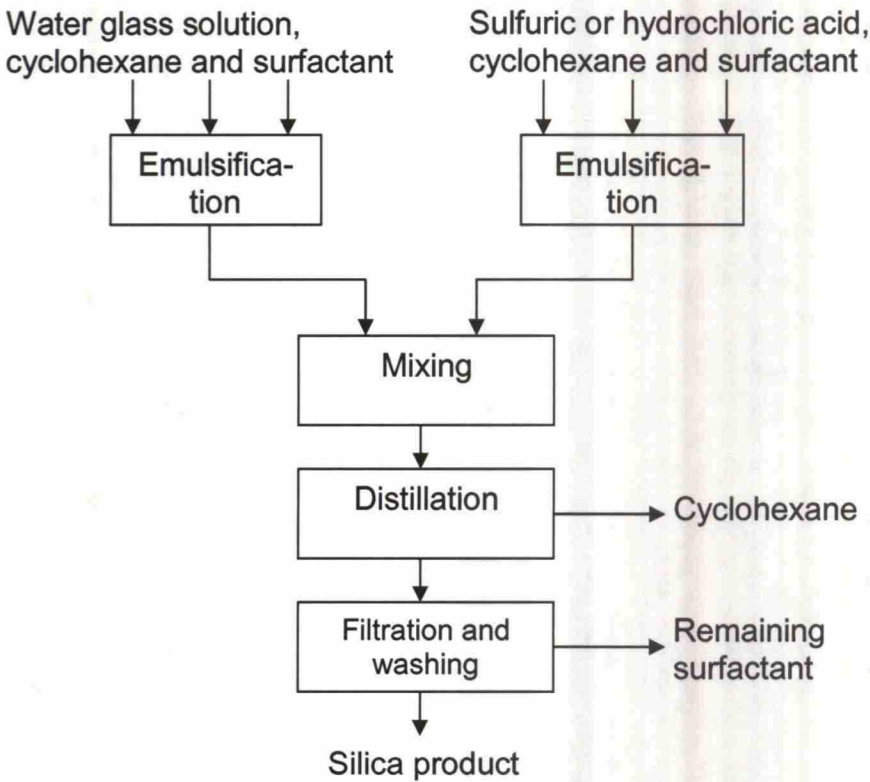


Figure 32. Flow diagram of the coagulant process used by Jesionowski (2001, 2002a, 2002b)

### 7.3.2 Precipitation Using Coagulants

The first type of precipitation using coagulants is described in the patents by Moyer (1945), Baker and Frankle (1965), and Tamenori *et al.* (1987). In this process, first a coagulant, also called clustering agent (Baker and Frankle 1965), is added to a solution of water glass to coagulate the silica aggregates in the water glass to micelles of desired size. Then an acid is added to remove the sodium ions from the micelles and to precipitate the silica particles. The flow diagram is shown in Figure 33. The acid is



also sometimes called insolubilizing agent (Baker and Frankle 1965). By this method, very fine precipitates of globular shape can be obtained. According to Baker and Frankle (1965), the coagulant has to be a hydrophilic material which tends to reduce the effective charge on the colloidal particles in the sodium silicate solution or reduces the dielectric constant of the medium between the particles. Among possible coagulants are completely water-miscible organic liquids such as alcohols, ammonium hydroxide, and its water soluble derivatives and highly soluble uni-univalent or uni-divalent salts, such as NaCl or Na<sub>2</sub>SO<sub>4</sub>.

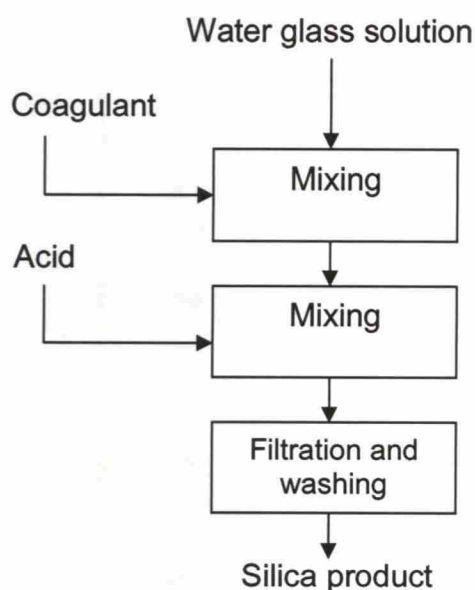


**Figure 33. Flow diagram of the Baker and Frankle (1965) coagulant process**

To obtain a proper product, the coagulant quantity must be exactly controlled. The reference point is set by the so-called opalescence point, which is the amount of coagulant that is just enough to cause a faint opalescence in the water glass solution. This indicates the formation of micelles in the solution. The coagulant amount is expressed relative to the opalescence point. Then the acid, for example sulfuric acid or carbon dioxide, is added quickly to the solution to remove the sodium ions from the micelles, and to precipitate the silica particles. Depending on the size of the particles, the silica either stays in colloid suspension or a solid precipitate is formed. According to the patent, particle sizes of 7-100 nm could be obtained.

A patent by Tamenori *et al.* (1987) describes a very similar process for the production of high-purity solar cell grade silicon, with the exception that the acid is added slowly to form larger precipitates.

A second type of coagulant process patented by Acker and Winyall (1977) produces loosely aggregated precipitated silica, consisting of primary particles of 200-500 nm in diameter, which can be easily disaggregated by milling. In their method, an alkali metal silicate solution is neutralized by addition to an ammoniated carboxylic acid solution, or an ammoniated alkali metal silicate solution is neutralized by addition of carboxylic acid. Figure 34 shows the two possible flow diagrams.

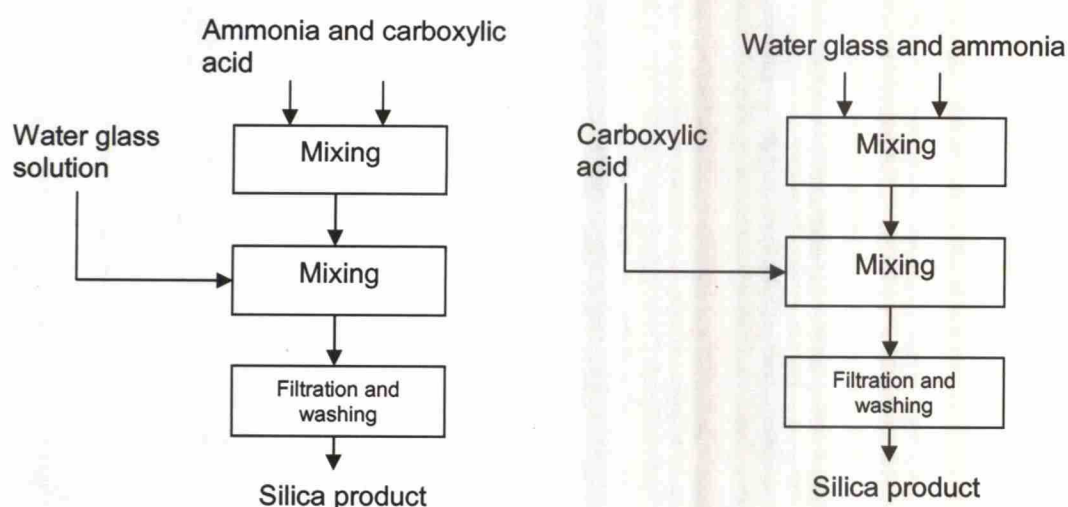


Figure 34. Variants of the Acker and Winyall (1977) coagulant process

## 8 Fumed Silica

Fumed silica, or pyrogenic silica, is another form of nanostructured silica. It is made from silicon tetrachloride at high temperatures by a flame-hydrolysis oxidation process. In the process, silicon tetrachloride is continually vaporized, mixed with dry air and then with oxygen, fed to a burner, and hydrolyzed according to the equations



The gases leaving the reactor contain all of the silica in form of an aerosol. The silica is separated from the sour gas by cyclones or filters. The process is shown in Figure 35. Fumed silica is characterized by its specific surface area, being normally in the range 50–400 m<sup>2</sup>/g, corresponding to a primary particle size between 10 and 100 nm. Figure 36 shows typical particle size distributions of fumed silicas with various specific surface areas. Aqueous silica sols can be made by dispersing fumed silica in water. (Flörke *et al.* 2005)

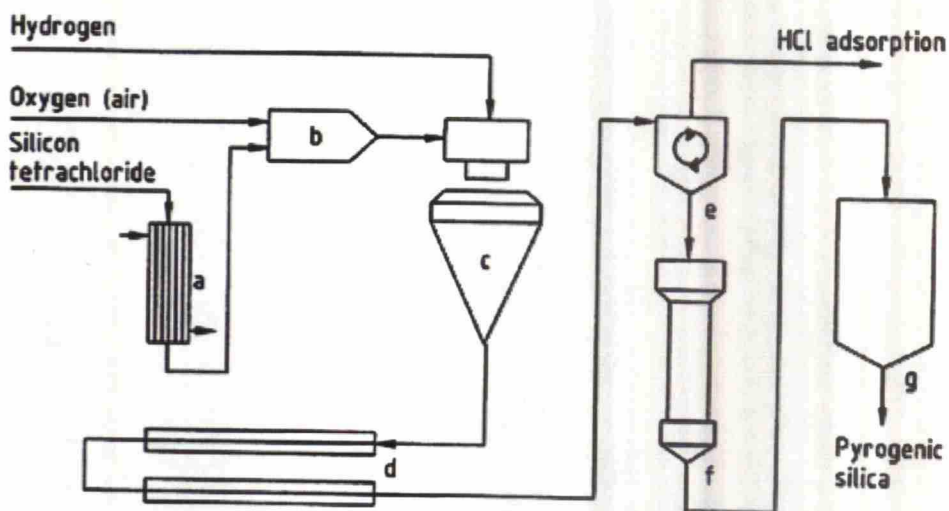


Figure 35. Industrial process for fumed silica production; a) Vaporizer; b) Mixing chamber; c) Burner; d) Cooling section; e) Separation; f) Deacidification; g) Hopper (Flörke *et al.* 2005)

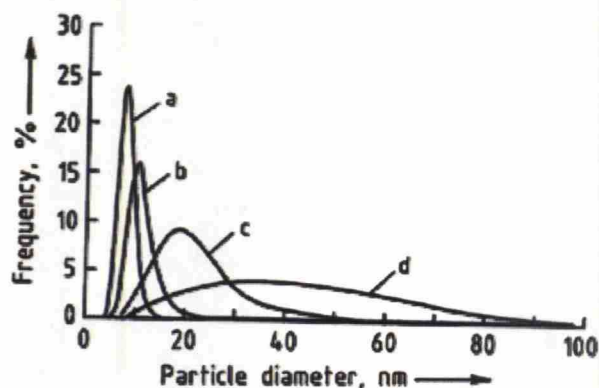


Figure 36. Primary particle size distribution of fumed silicas with various specific surface areas; a) 300 m<sup>2</sup>/g; b) 200 m<sup>2</sup>/g; c) 90 m<sup>2</sup>/g; d) 50 m<sup>2</sup>/g (Flörke *et al.* 2005)

## 9 Continuous Processes

### 9.1 Overview

So far, almost all processes that have been introduced either for silica sol or precipitated silica production are batch or semibatch processes. For silica sols there are, however, a few continuous processes that have been described mostly in patents. Some of these are discussed in paragraph 9.2. Furthermore, EKA Chemicals claims to have a continuous process for manufacturing their Bindzil Colloidal Silica products (EKA Chemicals 2007). However, no public information about this process is available, except that it is said to produce any particle size between 5 and 100 nm.

Concerning precipitated silica and precipitated nanoparticles in general, there has been quite a lot of research in recent years. In paragraph 9.3, the most interesting ex-



perimental works are described as well as one patent on continuous precipitation of silica.

## 9.2 Silica Sols

A few continuous processes have been described for silica sol manufacturing in the patent literature. Nalco Chemical Company (1963) seems to be the first to have a patent on a continuous process, based on ion exchange. Weldes *et al.* (1969) patented a process where a silicic acid solution is mixed with an alkaline solution in a continuous stirred tank reactor.

Brekau *et al.* (1999) patented a continuous process for Bayer. The process is basically the buildup process described in Paragraph 4.5.3, but it uses a multi-stage cascade reactor, where each reactor is fed with overflow from the preceding stage. The process starts with a heel of silica sol, to which silicic acid is added in the reactors. pH is controlled by alkaline addition and reaction volumes are controlled by evaporation of water. Operating conditions of the reactors are given in Table 3. The authors claim that their process could produce silica sols with an average particle size between 27 and 72 nm.

**Table 3. Operating conditions of the reactors in the patent by Brekau *et al.* (1999)**

	pH	Particle Size (nm)	Average Residence Time (h)	Average SiO <sub>2</sub> Concentration (wt-%)
First Reactor	10.7-11.7	14-27	0.5-2	9-16
Second Reactor	9.8-11.3	15-41	0.5-2	11-30
Third Reactor	9.9-10.8	18-49	0.5-2	16-40
Fourth Reactor	9.4-10.5	20-68	1.5-2	22-45
Fifth Reactor	9.0-10.5	27-72	1.5-2	28-50

Although being not very practical, the method proposed by Brekau *et al.* seems to be the only feasible method for making silica sols with exactly tailored particle sizes in a continuous process. It can be assumed that various commercial silica sol manufacturers, including EKA Chemicals, have developed similar processes, without publishing any information on them.

## 9.3 Precipitated Silica

A first continuous process for making precipitated silica has been patented by Société Française des Silicates Spéciaux Sifrance (1972). The flowsheet is shown in

Figure 37. Apparently, this is not a very practical process because of the multiple continuous stirred tank reactors in series.

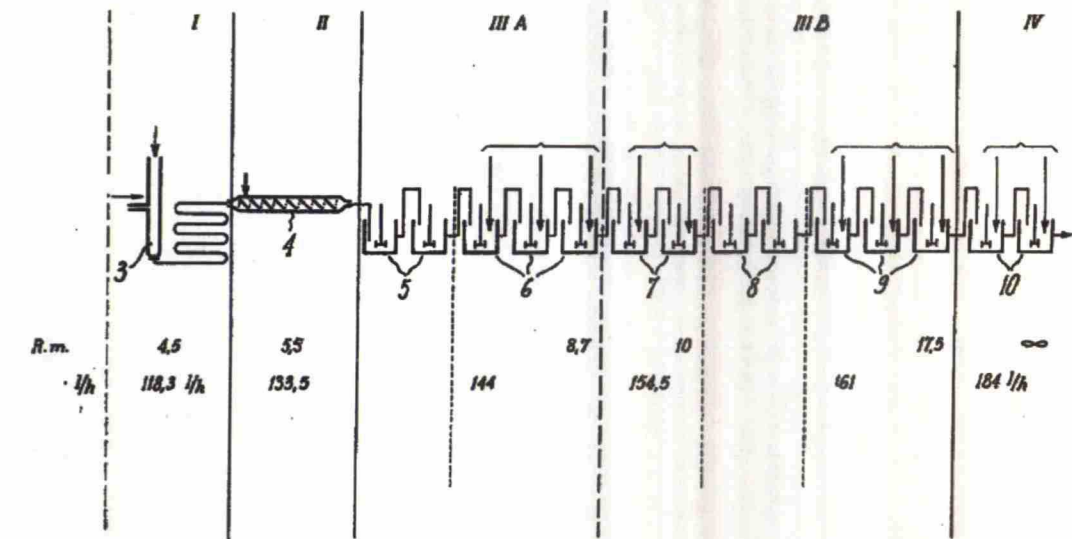


Figure 37. Continuous process for making precipitated silica (Société Française des Silicates Spéciaux Sifrance 1972)

An apparatus for continuous flow precipitation was described by Matijević (2006). According to the author, the apparatus could be used for making yttrium dioxide, silica, aluminum hydroxide, and barium titanate particles. A schematic presentation of the apparatus is shown in Figure 38.

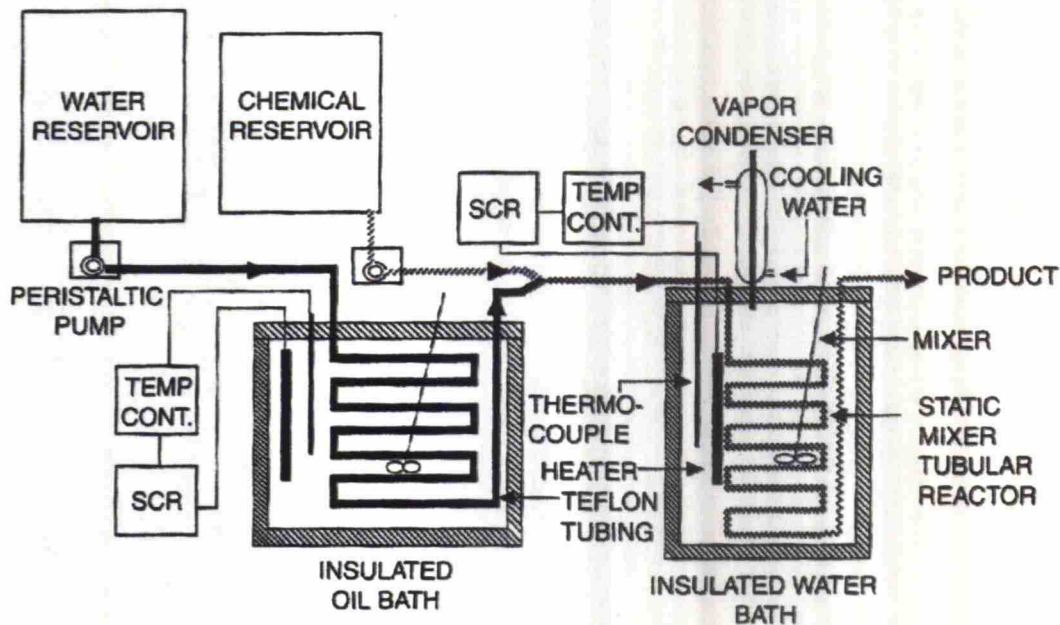
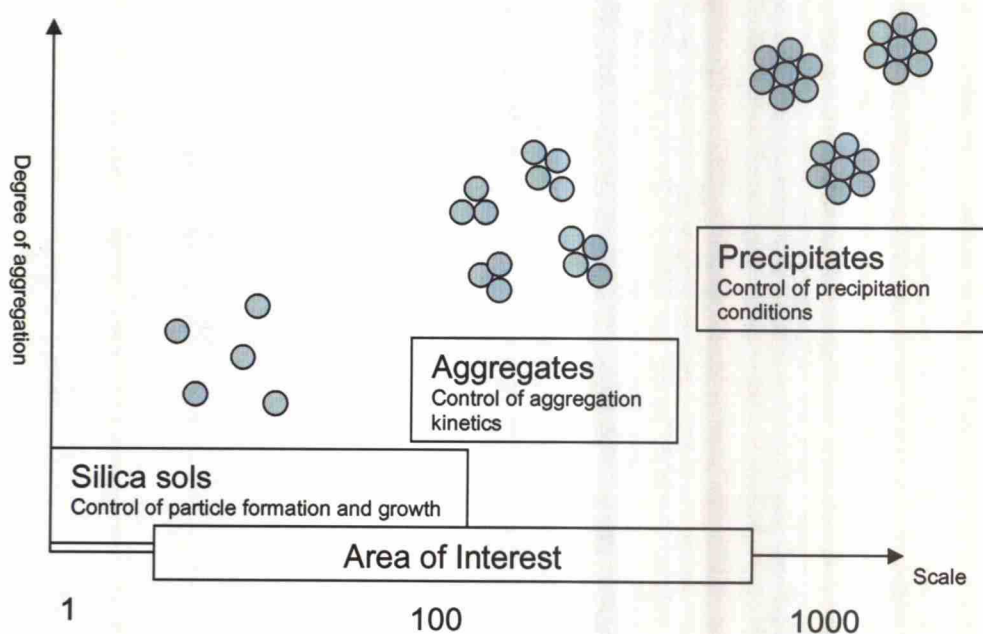


Figure 38. Schematic presentation of the apparatus for continuous flow precipitation (Matijević 2006)

## 10 Conclusions from the Literature Review

The formation of colloidal silica has been studied quite extensively over the years. A detailed discussion of the polymerization behavior of silica and particle formation is given in Iler (1979). For a brief introduction to particle formation and manufacturing of colloidal silica, the articles by Roberts (2006) and Yoshida (1994) can be recommended. Recent experimental work has been done by Tsai *et al.* (2004, 2005a, 2005b).

There is also a lot of published material on aggregation and precipitation of silica. Again, the basics can be found in Iler (1979). Among the most interesting experimental works are the ones by Schaer *et al.* (2001) and Schlomach and Kind (2004b). Also an article by Schlomach *et al.* (2006), in which parallels between the precipitation of calcium carbonate and silica are drawn, is considered interesting. An overview of all the topics can also be found in Ullmann's Encyclopedia of Industrial Chemistry (Flörke *et al.* 2004). The size ranges of silica structures together with the parameters that affect their formation are summarized in Figure 39.



**Figure 39. Size ranges of silica structures and the parameters that affect their formation**

So far, only methods based on ion exchange seem to be in industrial use for the manufacturing of silica nanoparticles in the form of colloidal silica. Autoclaving and sol-gel methods based on TEOS chemistry have been used in the laboratory. Methods based on acid neutralization are mainly used for the production of precipitated



silica. Some methods presented in the Literature Review Part that produce discrete silica particles are roughly categorized according to their product's size range and their estimated complexity in Figure 40. Precipitated and fumed silica are not included because the products produced by those methods are quite different.

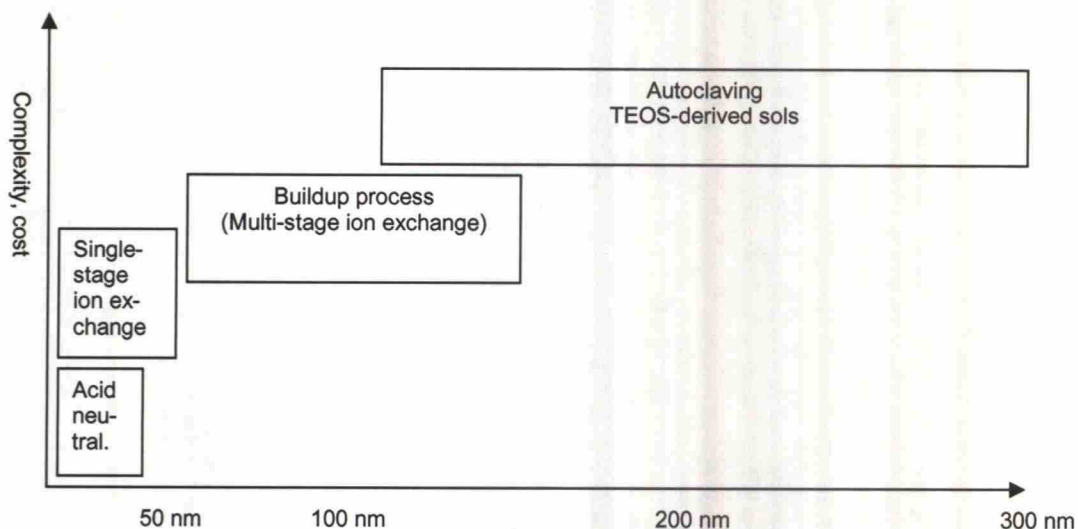


**Figure 40. Classification of methods that produce discrete silica particles**

Figure 40 shows that the complexity of the process increases quite rapidly with increasing particle size. Acid neutralization and precipitation techniques, possibly followed by a disaggregation stage, seem to be the most promising methods for the low cost on-site manufacturing of silica nanoparticles. Presumably, some degree of aggregation in the product has to be taken into account when using such a process. Stability of the product is not an issue if the product is to be used within the next few hours or even minutes. The aim of the experimental and process design parts is to explore these methods and evaluate their usability for industrial production.

## EXPERIMENTAL PART

### 11 Introduction to the Experimental Part

The aim of the experimental work was to find out what types of nanoparticles can be made using water glass and acid, and testing different processes in a semi-batch reactor arrangement. Three processes were tested experimentally: Sol via Acid Neutralization, Precipitation, and the Baker and Frankle (1965) Coagulant Process. A list of experiments is presented in Appendix A.

The Sol via Acid Neutralization –Process consists of neutralizing a dilute, hot water glass solution so that no gel is formed (see Paragraph 4.4). In order for this to be possible, the sodium sulfate concentration in the product has to be kept under a critical limit which was given by Iler (1979). All processes that are introduced here are basically acid neutralization processes. However, the term Acid Neutralization Process is used in the literature to refer to a process at low silica concentration. Thus it is used here in that sense as well.

The Precipitation Process is a very similar process, but in this case the silica concentration is substantially higher (see Paragraph 7.2). Gel formation during the reaction will occur, but any gel is broken up using high stirrer speed. The product suspension contains large aggregates of silica particles. The precipitation process can be seen as a variation of the sol-gel-process.

In the Coagulant Process, a coagulant is added to the water glass solution before neutralizing it with acid (see Paragraph 7.3.2). The addition of the coagulant results in the formation of micelles in the water glass solution, from which the sodium ions are removed by the addition of an acid. This results in substantially different precipitation characteristics than in the above mentioned two other processes.

### 12 General arrangements

The experiments were performed at the Laboratory of Chemical Engineering during May and June, 2007. The reactor used was a 2 l spherical glass reaction vessel. The batch was mixed with a Heidolph RZR 2020 mixer. A six-blade impeller which was placed near the bottom of the reactor was used for agitating and mixing. For heating, an electric dry bath was used. Temperature was measured directly from the reaction

mixture. In most experiments acid was fed into the batch using a diaphragm pump. In some experiments acid was also poured by hand. The flow rate of the pump could be varied by changing the stroke volume and the stroke frequency. Acid feed was monitored with a scale placed under the acid container. pH was not monitored during the reaction but it was measured from the batch after the reaction was complete. The experiment setup is shown in Figure 41.

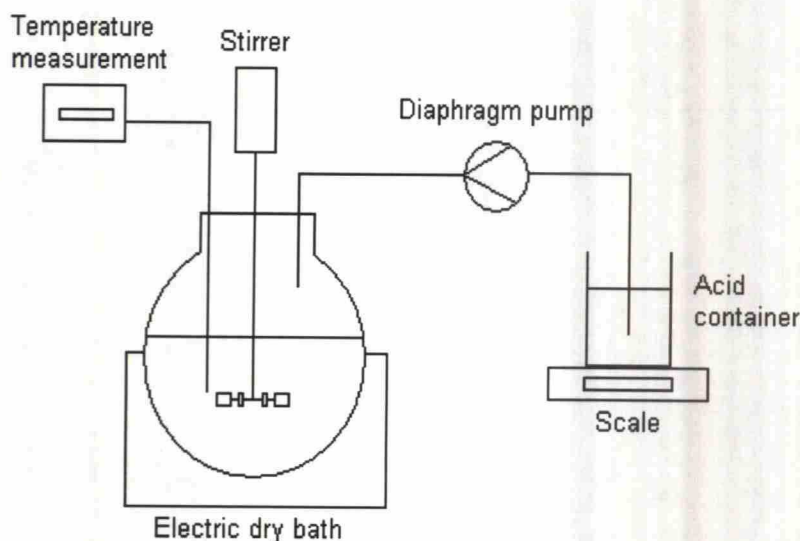


**Figure 41. The semi-batch reactor arrangement used in the experiments**

The water glass used in the reaction was Zeopol 33, manufactured by J.M. Huber Finland Oy. It is a sodium silicate solution with an Si:Na mole ratio of 3.3 and a silica concentration of approximately 28 %. The sulfuric acid was a 95-98 % sulfuric acid obtained from Sigma Aldrich. It was diluted to 20 % in most of the experiments. Tap water was used as solvent in all experiments.

## 13 Sample Analysis by Dynamic Light Scattering

### 13.1 Theory

The primary means of sample analysis was a Malvern Zetasizer ZS Nano instrument, which performs size measurement using a process called Dynamic Light Scattering (DLS). The same or a comparable instrument has been used by many researchers (Schaer *et al.* 2001, Schlomach and Kind 2004b, Tsai 2004, Tsai *et al.* 2005a, Tsai *et al.* 2005b) and it is considered very reliable. Sample analysis concentrated on particle size. Other potentially interesting characteristics like zeta potential or specific surface area were not measured.



DLS (also known as Photon Correlation Spectroscopy, PCS) measures Brownian motion and relates it to the size of the particles. A laser beam is shot through the sample and the particles in the suspension will scatter the light in all directions. A detector that is placed close to the sample will measure an interference pattern. Due to the Brownian motion of the particles the pattern is not stationary. The intensity fluctuation of the scattered light depends on the size of the particles. From the intensity fluctuations, the velocity of the Brownian motion can be determined, and the particle size distribution can be calculated using the Stokes-Einstein relationship. The instrument reports a size that has the same hydrodynamic properties as a sphere of equal hydraulic diameter. (Malvern Instruments 2005)

The fundamental size distribution generated by DLS is an intensity distribution. This can be converted into volume and number distributions. To do this, the refractive index of the material has to be known. 1.46 was taken as the refractive index for silica (Siliconfareast.com 2004). However, one must be very careful when interpreting number distributions because small errors in the intensity distribution will lead to huge errors in the number distribution. If a sample contains large and small particles, the small particles will show only very weakly in the intensity and volume distributions. This is because the intensity of scattering of a particle is proportional to the sixth power of its diameter and the volume of a particle is proportional to the third power of its diameter. (Malvern Instruments 2005) Figure 42 shows a real-life example.

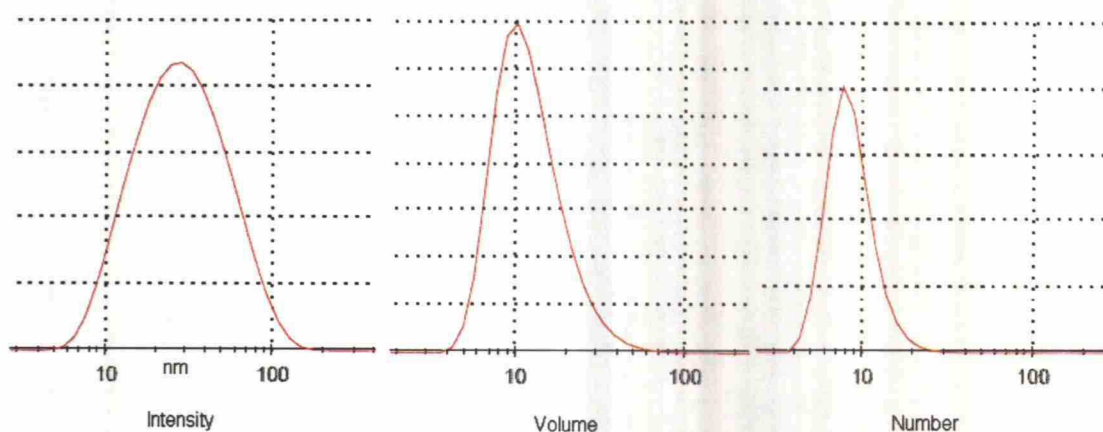


**Figure 42. Intensity, volume and number distributions of a sample (Sample A5)**

There are some limitations to DLS analysis that became evident when analyzing the samples. Firstly, the suspension must be almost clear and colorless for the laser beam

to pass through. Secondly, the particles have to remain in suspension and must not settle. With these two limitations, the limit for the maximal particle size for silica was found to be about 1000 nm. For larger particles, for example a Malvern Master-sizer, which uses conventional Fourier optics, could be used (Schaer *et al.* 2001).

The results were averaged from three measurements, every measurement consisting of ten measurement runs, meaning that every result was calculated by the system as an average from a total of 30 measurement runs. The intensity and number peaks were considered as the most important numbers produced by the instrument. Also size distribution graphs were considered interesting, although graphical presentations of particle sizes in this manner are problematic (Sommer 2000). Other numbers produced by the system are the polydispersity index (PDI) and Z-average size, which is an intensity-weighted average size. Z-average size is normally the most stable number produced by the system and should be used for quality control purposes, but it does not necessarily relate to the real particle size unless the size distribution is very narrow (Malvern Instruments 2005).

### 13.2 Measurements of Commercial Silica Sols

For testing purposes, the particle size distributions of a few commercial sols were measured. The results are shown in Table 4.

**Table 4.** Size measurements of commercial silica sols

Product	Particle size given by manufacturer / nm	Intensity peak	Measured particle size / nm		
			Volume peak	Number peak	Z-Average size
Product 1	6	24.4	7.56	5.08	16.5
Product 2	25	37	28.1	23.1	33.4
Product 3	10 - 100	130	102	69.3	113
Product 4	15	42.2	17.1	12.6	28.6
Product 5	40	131	103	68.4	113
Product 6	N/A	137	110	73.8	117

The results show that the values closest to the particle size given by the manufacturer are the volume peak and the number peak. The manufacturer's value lies between these two numbers in all measurements except Product 5. In this case there might be some aggregation. All samples showed a more or less wide distribution similar to Figure 42 instead of a sharp peak. If the number given by the manufacturer is assumed to be correct, then volume and number peaks seem to give good estimates for

the mean particle size, the volume peak giving slightly larger and the number peak giving slightly smaller values. In the following paragraphs, the number peak was chosen as the most important number to characterize particles. If microscopic images are to be taken, it is most likely to see particles of that size on the pictures.

## 14 Sol via Acid Neutralization

### 14.1 Experimental Procedure

In the first experiments, stable silica sols were produced at lower silica concentrations by acid neutralization. This could be achieved when total silica concentration was kept below about 3 % (mass-percent).

A dilute water glass solution was partially neutralized with sulfuric acid to a pH of about 9-10. The reactor was first charged with water and water glass solution and the batch was then heated until reaction temperature was reached. The acid was then added to the batch using the pump while stirring. Temperature was kept at 80-83 °C during the reaction. Stirrer speed was set at 400 rpm. The basic block diagram is shown in Figure 43. Samples were taken from the batch and analyzed by DLS. Approximate gel times of the samples were determined by observing the bottled samples for several days.

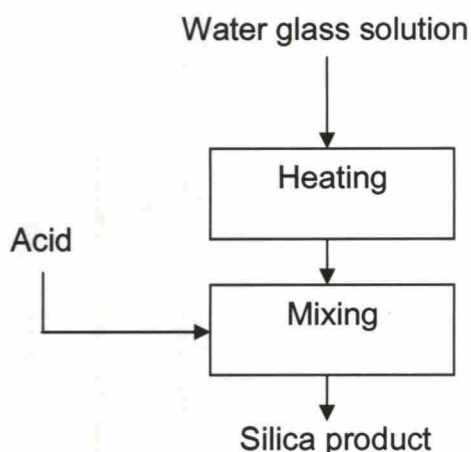


**Figure 43.** Basic block diagram for the acid neutralization experiments



## 14.2 Neutralization of Water Glass

The neutralization curve of the water glass solution is presented in Figure 44. It was measured in experiment A1. Measured quantities of sulfuric acid were successively added to a water glass solution and pH was measured after each addition.

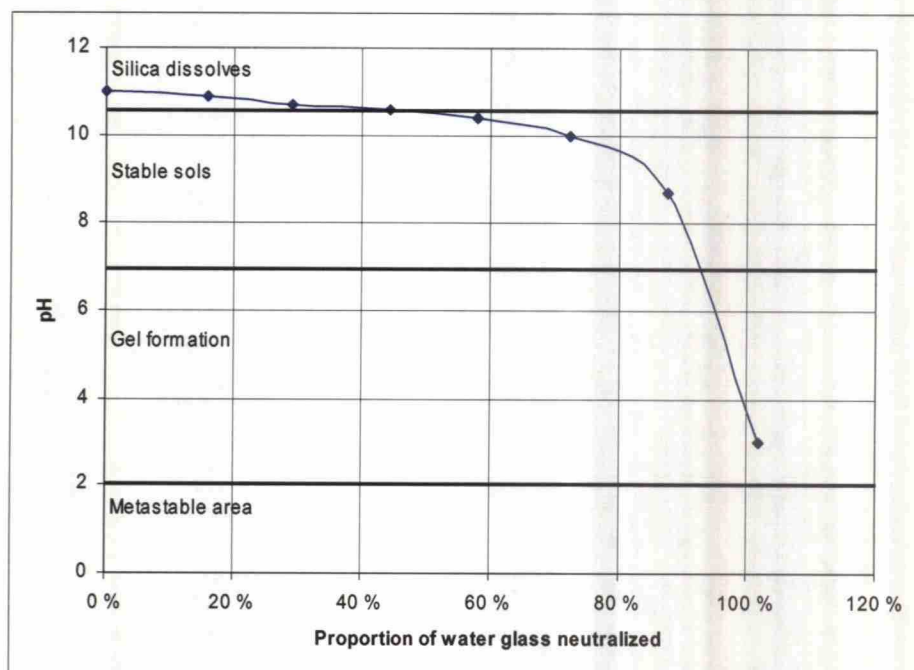


**Figure 44. Neutralization curve of the water glass solution**

From Figure 44 it can be seen that in order to remain in the stable area, the appropriate proportion of neutralization is 50-90 %, calculated from reaction stoichiometry. Dropping of the pH below 7, even locally, must be avoided because gel formation at pH 5-7 is almost instantaneous. If the pH drops into the gelling range even locally, then microgel will be formed which then is dispersed throughout the batch and acts as seed for gel formation throughout the liquid. This is illustrated in Figure 45. The pH can be lowered into the metastable area if acid addition and mixing are very quick while crossing the gel formation area. To get into the metastable area, a proportion of sulfuric acid of about 120 % of the amount sufficient to neutralize the water glass is needed.

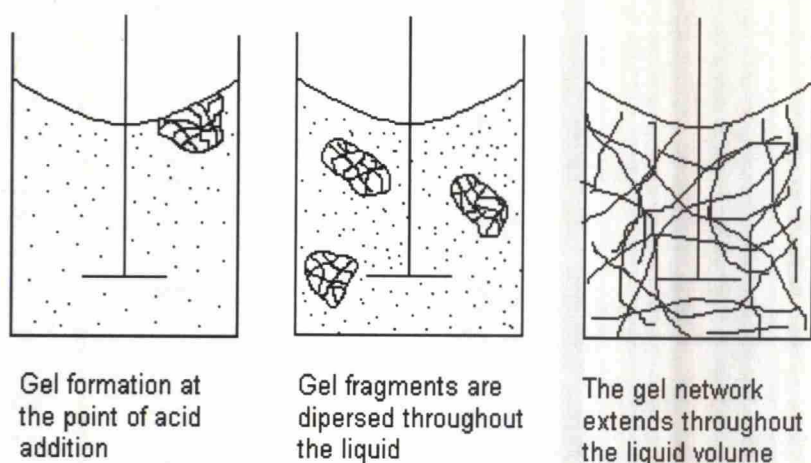


**Figure 45. Formation of gel fragments and gel extension throughout the liquid volume**

### **14.3 Results**

Results from the successful acid neutralization experiments A4-A9 are listed in Table 5. More detailed information on the experiments is presented in Appendix B. Original outputs of the particle size measurements are shown in Appendix F. Stable sols could be obtained when acid addition rate was slow enough and the quantity of acid added was kept moderate at a proportion of about 70 % of the quantity which would have been necessary to completely neutralize the water glass. Else, gelling of the product was the result. If acid addition rate was lowered, then more acid could be added without the risk of gelling, as can be seen in experiment A9. This was probably due to the reasons discussed in Paragraph 14.2. Very high acid addition rates led to immediate gelling.

All stable sols were clear liquids. Particles with number mean diameters around 10 nm were obtained in these experiments. At higher concentrations the particle size distributions were broader and showed slightly more larger-sized particles. This is probably due to the aggregation of particles because of the sodium sulfate that was being formed in the reaction. Acid addition rate did not have an effect on mean particle size, but at lower acid addition rate the particle size distribution was slightly narrower. (Compare the DLS results for samples A5 and A8 in Appendix F.)

**Table 5. Acid neutralization experiments in the stable sol area**

Experiment	A4	A5	A6	A7	A8	A9
<b>Batch</b>						
total SiO <sub>2</sub> concentration (by mass)	2.1 %	2.5 %	3.0 %	3.6 %	2.6 %	2.6 %
total Na <sub>2</sub> O concentration (by mass)	0.7 %	0.8 %	0.9 %	1.1 %	0.8 %	0.8 %
<b>Sulfuric acid addition</b>						
H <sub>2</sub> SO <sub>4</sub> addition rate/gs <sup>-1</sup>	0.12	0.12	0.12	0.12	0.02	0.02
proportion neutralized	71 %	72 %	72 %	71 %	72 %	86 %
<b>Measurements</b>						
mean number particle size / nm	6.82	8.62	11.9	N/A	7.29	12.2
final pH	10.1	10.0	10.0	10.1	10.2	9.3
<b>Calculated</b>						
free SiO <sub>2</sub> concentration (by mass)	1.4 %	1.8 %	2.1 %	2.4 %	1.8 %	2.1 %
total Na-norm	0.19	0.23	0.27	0.32	0.23	0.23
free Na-norm	0.13	0.17	0.19	0.23	0.16	0.20
critical Na-normality calculated from Iler's formula	0.18	0.18	0.18	0.18	0.18	0.18

Another area of interest was the stability of the products, which relates to the Na<sup>+</sup>-concentration in the suspension. The samples with Na<sub>2</sub>SO<sub>4</sub>-concentration higher than about 1.3 % gelled within a few days to a few minutes. The sols with lower Na<sub>2</sub>SO<sub>4</sub>-concentrations were stable for long periods of time. The dependence between Na<sub>2</sub>SO<sub>4</sub>-concentration and gel time is illustrated in Figure 46. The stability decreases exponentially with increasing Na<sub>2</sub>SO<sub>4</sub>-concentration, as was predicted by Iler (1979).

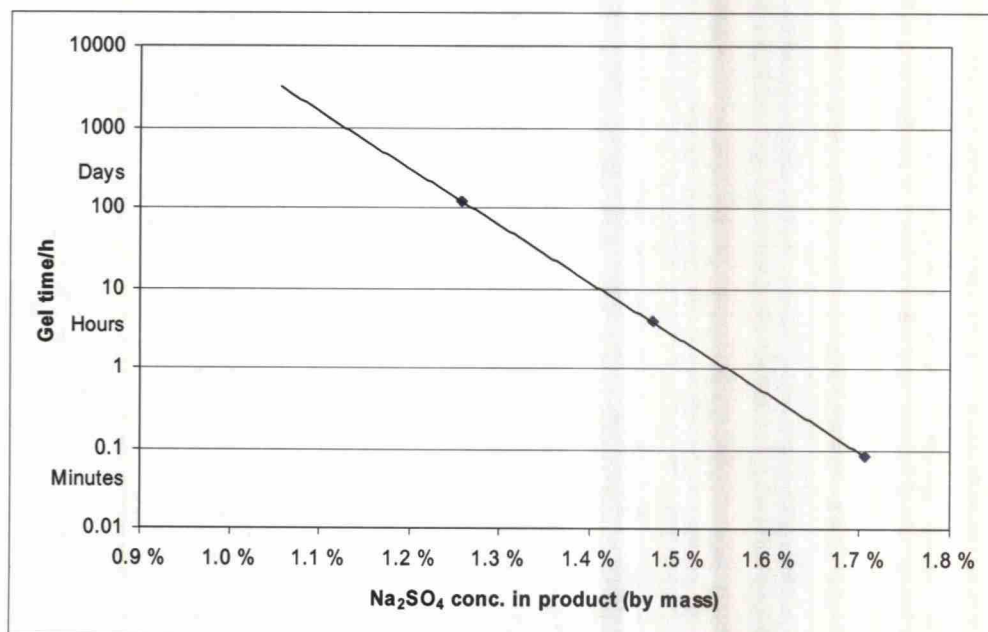


**Figure 46. Stability of the silica sols obtained in the Acid Neutralization Process**



## **14.4 Conclusions**

Particles of about 7-12 nm in diameter were obtained by acid neutralization in the stable sol area. This is in good accordance with the equilibrium particle sizes given by Iler (1979, p. 242-243) for temperatures lower than 100 °C. The particle size seems to grow slightly with increasing silica concentration.

The stability of the sols decreases rapidly with increasing product concentration, as could be expected. From Table 5 it can be seen that sodium normality exceeded the threshold calculated from Iler's formula (calculated as  $0.1 C$ ,  $C$  being is the silica concentration in g/100 ml) at a  $\text{Na}_2\text{SO}_4$ -concentration of about 1.5 %, which is also the concentration at which the samples were not stable anymore. Thus it can be said that Iler's formula is reasonably accurate for predicting product stability. The value given by the formula seems to apply for the normality calculated from free sodium concentration (sodium present as  $\text{Na}_2\text{SO}_4$ ), whereas the value 0.3 N, which was also given by Iler, seems to apply for the normality calculated from total sodium ion concentration (sodium present as  $\text{Na}_2\text{SO}_4$  and sodium silicate).

It is obvious that large particles cannot be obtained by this method. Also, low product concentrations and rapidly decreasing stability at higher concentrations can be expected to cause problems when applying this method to practice.

## **15 Precipitation**

### **15.1 Experimental Procedure**

In order to make particles larger in diameter, precipitation experiments at higher silica concentrations were performed. The procedure was very similar to the acid neutralization experiments: The reactor was first charged with a batch of water and water glass solution, which then was heated until reaction temperature was reached. Then acid was added by pumping. If a gel was formed, it was broken up with high stirrer speed. 400 rpm were not sufficient to break up the gel, but at least 800 rpm were necessary. In most of the experiments, stirrer speed was set at 1000-1300 rpm. Acid addition rate was kept very low in most experiments. The quantity of acid added was controlled so that product pH was above 8. A quantity enough to neutralize 80-90 % of the water glass was added to the batch. Figure 47 shows the basic principle. Using the given reactor, the highest practical silica concentration was found to be about 10

%. At higher concentrations, crystallization of the product on the reactor walls became a problem, affecting reactant concentrations and heat transfer.

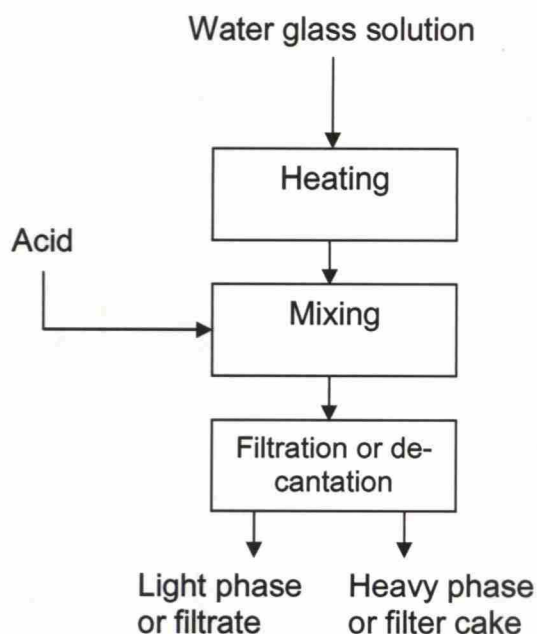


Figure 47. Basic block diagram for the precipitation experiments

The acid addition rate had to be kept very low in order to avoid gelling. At high acid addition rate, an extremely rigid gel, which could not be broken up, was formed almost instantly. The temperature during the reaction was kept at 80-85 °C.

## 15.2 Stirrer Speed and Power Input

In the Precipitation Process, violent agitation is crucial for rapid mixing-in of the acid and for keeping gelling and aggregation under control. Power input can be estimated from stirrer speed using a power law. Correlations for unbaffled vessels are given for example in Peters *et al.* (2003, p. 539-542). Approximated values, based on the properties of water (viscosity 1 mPas, density 1000 kg/m<sup>3</sup>), are presented in Table 6.

Table 6. Stirrer speed and approximate power consumption in the batch

Stirrer speed / rpm	Power input / kW m <sup>-3</sup>
400	0.07
600	0.26
800	0.64
1000	1.3
1300	3.0

In most experiments, stirrer speed was between 1000 and 1300 rpm, corresponding to a power input of 1-3 kW/m<sup>3</sup>. Schlomach and Kind (2004b) used a power input of 0.163 kW/m<sup>3</sup> before the gel point and 0.765 kW/m<sup>3</sup> after the gel point, based on the viscosity of water.

### 15.3 Measurement of Primary Particle Size

Primary particle size was measured from the samples by the following procedure: Some of the well-dispersed product suspension was diluted with water and the larger particles were allowed to settle. Then a sample was taken from the slightly turbid top phase and passed through a 450 nm filter into a cuvette. In most cases, the suspension passed easily through the filter. The sample could then be analyzed by DLS. The method is illustrated in Figure 48.

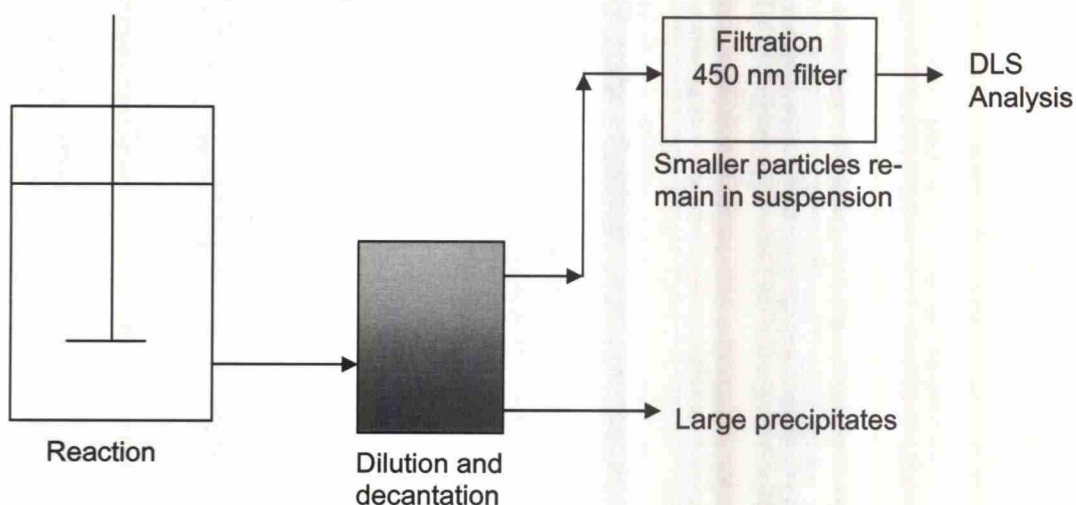


**Figure 48. Determination of primary particle size from precipitates**

In most cases, the particle size distributions showed two peaks, of which the smaller peak was interpreted as the primary particles, while the larger peak was interpreted as aggregates of two or three particles. This can be clearly seen in Figure 49, which shows the analysis result for sample B3. The primary particle size could be measured in experiments B2, B3, B4, B6, and B7.



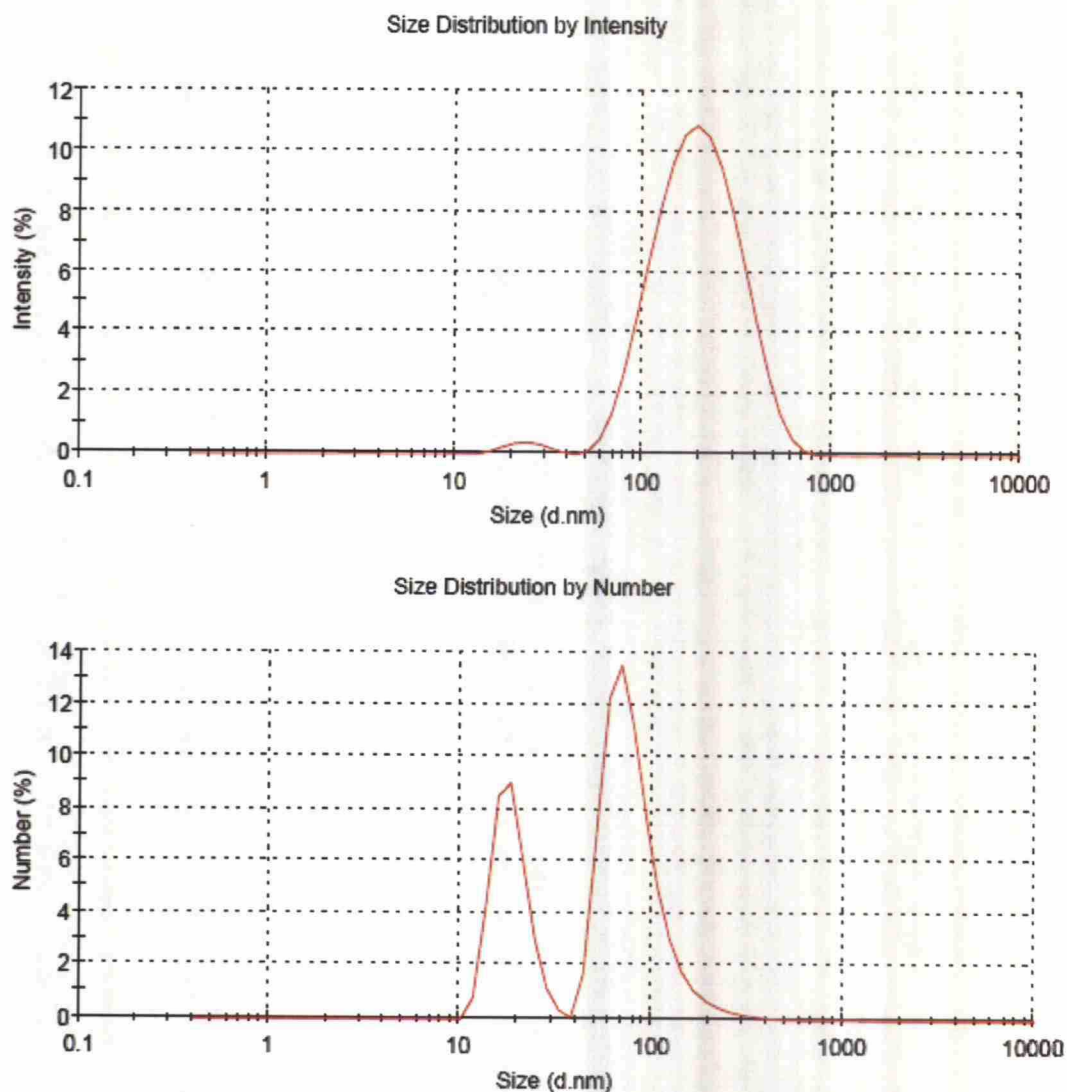


Figure 49. DLS analysis in the procedure from Figure 48 shows two peaks in the number distribution. The smaller peak corresponds to the primary particles (Sample B3)

## 15.4 Results

The most important data for experiments B2-B7 are shown in Table 7. Complete measured and calculated data for those experiments are listed in Appendix C. The original output of the instrument is presented in Appendix G.

**Table 7. Results of the precipitation experiments**

Experiment	B2	B3	B4	B5	B6	B7
total SiO <sub>2</sub> concentration (mass)	3.3 %	4.3 %	7.3 %	8.5 %	8.6 %	10.9 %
Proportion neutralized	80.9 %	84.2 %	76.6 %	80.8 %	82.4 %	83.1 %
characterization	gel-like precipitate	white, powder-like precipitate	white, powder-like precipitate	white, powder-like precipitate	white, powder-like precipitate	white, powder-like precipitate
free silica concentration in product (by mass)	2.6 %	3.6 %	5.6 %	6.8 %	7.1 %	9.0 %
primary particle size/nm	10.5	18.4	32.5	N/A*	34.5	50

\* Primary peak not observed in the measurements

At silica concentrations lower than about 4 %, a gel-like precipitate was formed, which gelled again within a few days of storage. At higher concentrations, white powder-like precipitates were formed, which were stable for long periods of time.

At silica concentrations lower than 4 %, acid addition was complete before gel formation, and a gel-like precipitate was formed. At higher concentrations acid addition was continued during gel formation and breakup, and a powder-like precipitate was obtained. The stability of the precipitates was probably due to the reinforcement of aggregates by the addition of additional silica to the aggregate surface.

The precipitation process goes through the stages shown in Figure 50. All of these stages could be observed visually. In the beginning, the solution was a clear liquid. The formation of aggregates was indicated by an increase in turbidity. When the gel point was reached, the liquid became completely turbid and its viscosity increased rapidly. When the gel was broken up, the viscosity decreased again, and the dispersion became white. At higher silica concentrations, the stages of gel formation and breakup were very fast. After the gel breakup was complete, there was no further change in product consistence, even when acid addition was still continued. The observations were basically the same that were described by Schlomach and Kind (2004b). They also measured quantitatively the compaction of the gel fragments by measuring the fractal dimension, but that could not be done in these experiments because there was no instrument available that could handle such large particles. The fractal dimension of the aggregates can be measured using static light scattering (Schlomach and Kind 2004b).

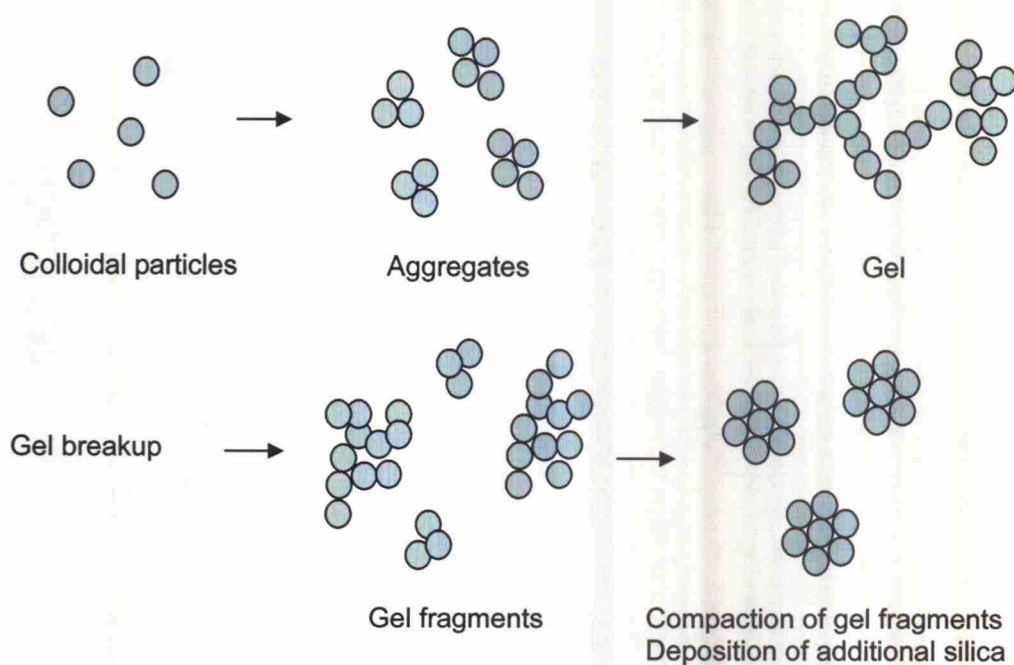


Figure 50. Stages in the precipitation process. The figure is not to scale

### 15.5 Microscopic Analysis

Samples B3 and B4 were sent to the Laboratory of Forest Products Chemistry for microscopic analysis. The samples were first centrifuged, and the light phase was then applied to a silicon wafer by spin coating. Then Atomic Force Microscope (AFM) images of the surfaces were taken. The results are shown in Figure 51.

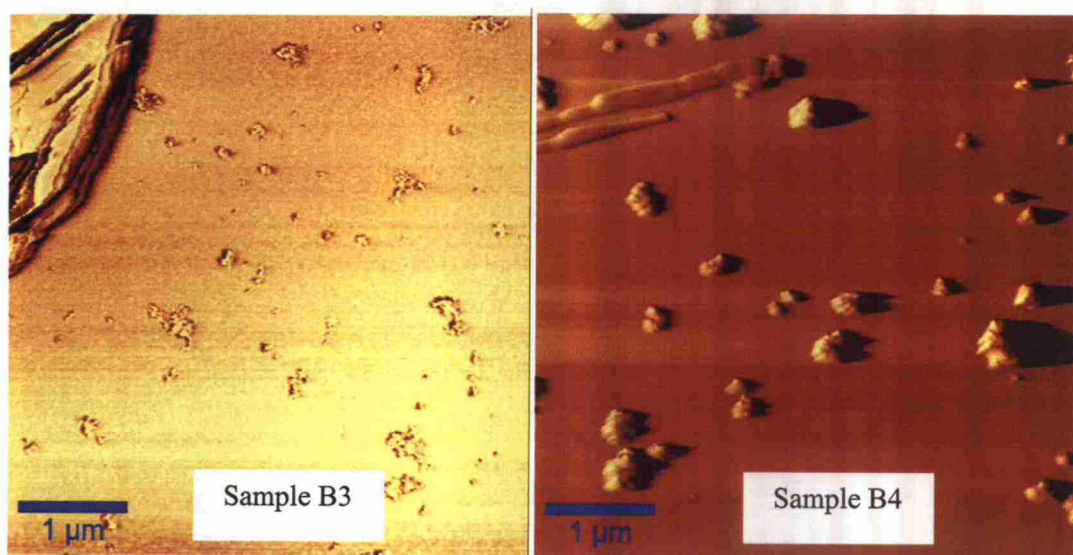


Figure 51. AFM images of surfaces prepared with samples B3 and B4. Spin coating parameters (speed and acceleration): B3: 3000 rpm, 1420 rpm/s; B4: 4000 rpm, 1420 rpm/s (taken by Tiina Nypelö at TKK Laboratory of Forest Products Chemistry)



The image of sample B3 shows aggregates up to approximately 500 nm in diameter and primary particles between 10 and 20 nm. The crystal in the top left corner of the image of sample B3 is probably crystallized sodium sulfate. The image of sample B4 also shows aggregates up to 500 nm in diameter and primary particles in the range 30-40 nm. The primary particles are uniform in size as observed by Schlomach and Kind (2004b). The difference between the particle sizes is clearly visible, and the images are consistent with the results of the DLS analysis. Keeping in mind that the only difference between samples B3 and B4 was the silica concentration, the images seem to confirm that primary particle size can be controlled by varying the silica concentration.

Scanning Electron Microscope (SEM) images of sample B6 were taken at the Laboratory of Materials Science. Figure 52 shows the sample in two magnifications.



**Figure 52.** SEM images of sample B6 (taken by Eero Haimi at TKK Laboratory of Materials Science)

The primary particle size for sample B6 was 34.5 nm in the DLS measurements. The SEM images show a primary particle size between 30 and 40 nm, which is consistent with the DLS measurements. The images are shown in full scale in Appendix I.

## 15.6 Conclusions

In these experiments, product structure and the primary particle size were considered especially interesting. It was also tested whether it was possible to obtain nanometer-sized aggregates by varying the precipitation conditions. The two most important parameters that affected the outcome of the experiments were:

- *Silica concentration.* At low silica concentrations (lower than about 3 %), silica sols could be obtained, which were stable for at least a few hours. At concentrations of 3-4 %, a gel-like precipitate was formed, which gelled again within a few days of storage. In this case, acid addition was finished before gel formation, and the gel was broken up with high stirrer speed. At concentrations above 4 %, a white powder-like precipitate was formed that did not gel upon standing. In this case, acid addition was not completed before gel formation, but instead was continued during gel formation and breakup.
- *Acid addition rate.* Precipitates were only formed at a low acid addition rate. A high acid addition rate resulted in the formation of a very rigid gel, which could not be broken up. It is hard to specify a high or a low acid addition rate because it depends on reactor type, mixing intensity, and reactant concentrations. In these experiments, the low acid addition rate was specified as about 0.02 g H<sub>2</sub>SO<sub>4</sub>/s and the high acid addition rate as about 1.3 g H<sub>2</sub>SO<sub>4</sub>/s.

The products formed at different combinations of these parameters are summarized in Figure 53.

Other important parameters are temperature and stirrer speed. Temperature has to be kept high enough during the reaction because at lower temperatures gelling is preferred. In the experiments a temperature of about 80 °C was found to be high enough. Stirrer speed must be high enough to break up any gel as soon as it is formed. At least 800 rpm, better more than 1000 rpm, are required to break up any gel, corresponding to a power input of about 0.6 to 1 kW/m<sup>3</sup> (see Paragraph 15.2). Sinnott (1999, p. 471) recommends at least 2 kW/m<sup>3</sup> for violent agitation in fine slurry suspensions.

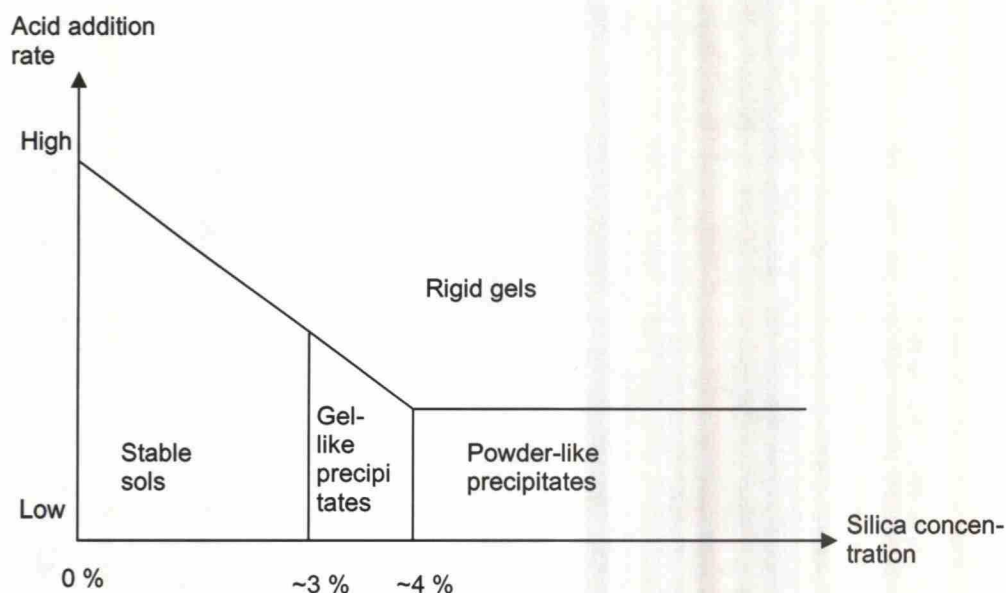


**Figure 53. Possible products from acid neutralization when a hot solution of sodium silicate is neutralized with sulfuric acid at pH above 7**

The results for the primary particle size are shown as a function of the product's free silica concentration in Figure 54. The results indicate that a primary particle size of at least about 50 nm is achievable in a precipitation process. This is an important result, since there has been no published data of this kind so far.

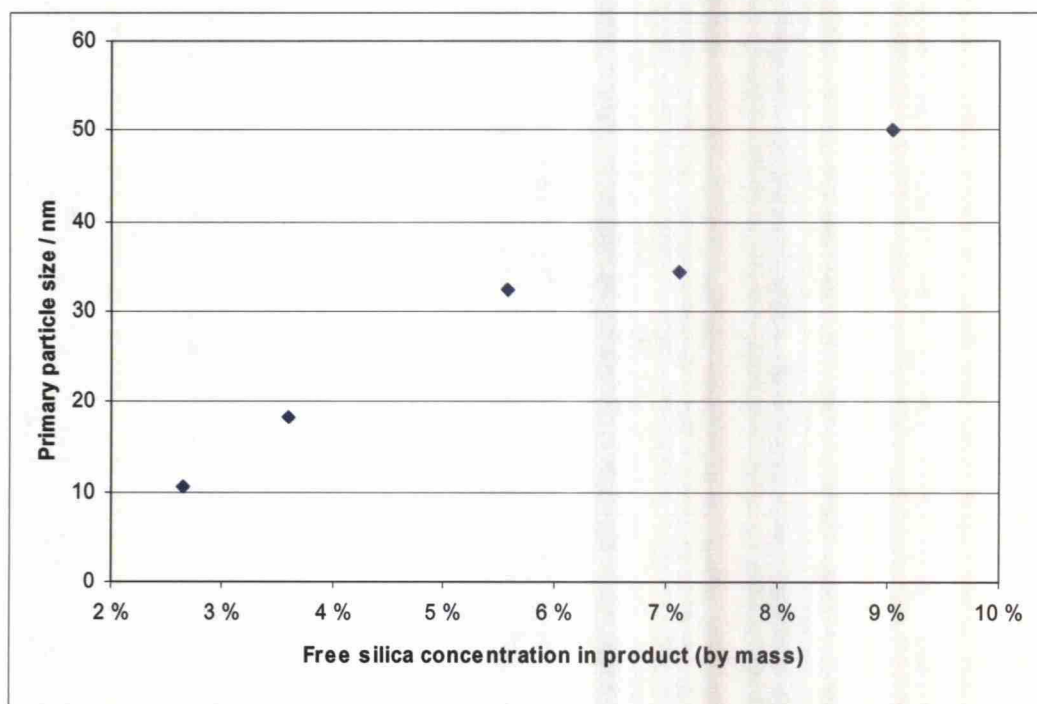


**Figure 54. Measured primary particle size as a function of product free silica concentration when a hot solution of water glass is neutralized to a pH of about 9-10**



These particles, however, come always aggregated in precipitates or in a gel. Thus if primary particles are the desired product, these aggregates must be broken up in some way during precipitation or afterwards; It might also be possible to control the aggregate size during precipitation by applying high shear force. However, Schaer *et al.* (2001) have suggested that at small scale (smaller than about 250 nm) hydrodynamics have only very little effect on the particle size distribution. Thus it may not be possible to obtain primary particles or very small aggregates directly. So far, there have been no public studies on disaggregating nanoparticles by high-shear mixing.

It is probable that the aggregates in the product show a certain size distribution, ranging from the nanometer area with aggregates of a few particles to the millimeter area. However, this distribution could not be measured in the experiments because there was no suitable instrument available.

## 16 Coagulant Process

### 16.1 Experimental Procedure

The coagulant process as described by Baker and Frankle (1965) was also tested experimentally. NaCl and Na<sub>2</sub>SO<sub>4</sub> were used as coagulants.

The reactor was first charged with water and water glass solution and then heated to a slightly elevated temperature, about 45-50 °C. Then the coagulant was added slowly, and the mixture was allowed to stabilize for a few minutes. Then a measured quantity of acid enough to drop the pH to 1-2 was added to the solution. The basic block diagram is shown in Figure 55.

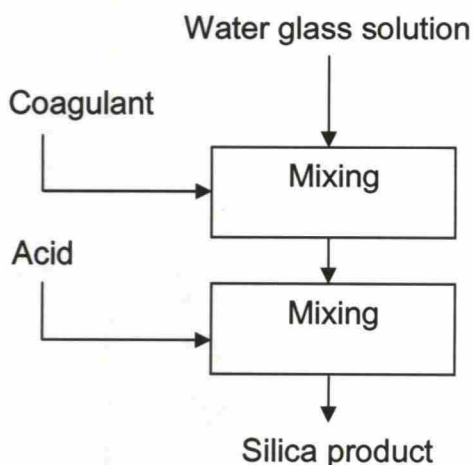


Figure 55. Basic block diagram for the coagulant process experiments

In a preliminary experiment it was tested how much of the coagulant was necessary to cause a light turbidity in the water glass solution. It was found that for NaCl, the mass concentration had to be at least twice as high as the silica mass concentration.

## 16.2 Results

Results of the experiments are summarized in Table 8. More detailed records are presented in Appendix D. Original outputs for samples C4 and C5 are presented in Appendix H.

**Table 8. Details for the coagulant experiments with NaCl as coagulant**

Experiment	C1	C2	C3	C4
Coagulant conc. (by mass)	13.31 %	7.62 %	3.33 %	4.94 %
Total SiO <sub>2</sub> conc. (by mass)	6.65 %	4.53 %	2.03 %	1.65 %
Characterization	wax-like precipitate upon salt addition	rigid gel	clear liquid	slightly turbid liquid
Coagulant type	NaCl	NaCl	NaCl	NaCl
Coagulant conc. g/l	162	86	35	53

Experiment	C5	C6	C7	C8
Coagulant conc. (by mass)	5.52 %	5.59 %	6.60 %	10.01 %
SiO <sub>2</sub> conc. (by mass)	1.95 %	1.87 %	1.90 %	1.49 %
Characterization	slightly turbid liquid	white precipitate	clear liquid	clear liquid
Coagulant type	NaCl	NaCl	Na <sub>2</sub> SO <sub>4</sub>	Na <sub>2</sub> SO <sub>4</sub>
Coagulant conc. g/l	59	60	72	113

In most cases, the solution turned slightly turbid at the point of coagulant addition. If the amount of coagulant was too low, no change was observed at this point. This happened in experiments C7 and C8. If the amount of coagulant was too high, a wax-like precipitate was formed at this point. This was observed in experiment C1. Coagulant addition rate seemed to have no influence on the product.

In most experiments, the acid was added practically instantaneously. Experiment C6 was done with slow acid addition rate. During acid addition, stirrer speed was increased to promote effective mixing. Baker and Frankle (1965) specified that the mixing-in of the acid should be completed in less than 5 seconds.

At high acid addition rate and rapid mixing, in most cases a stable slightly turbid sol was formed which passed easily through a 450 nm sieve. Experiments were done us-

ing low silica concentrations, so the results were comparable to those obtained from the acid neutralization experiments at low concentrations.

The particle size intensity distributions showed two families of particles, one in the range of 10 nm and another in the range of 100 nm, which is visible in the intensity distribution. Figure 56 shows the particle size intensity and number distributions for sample C5.

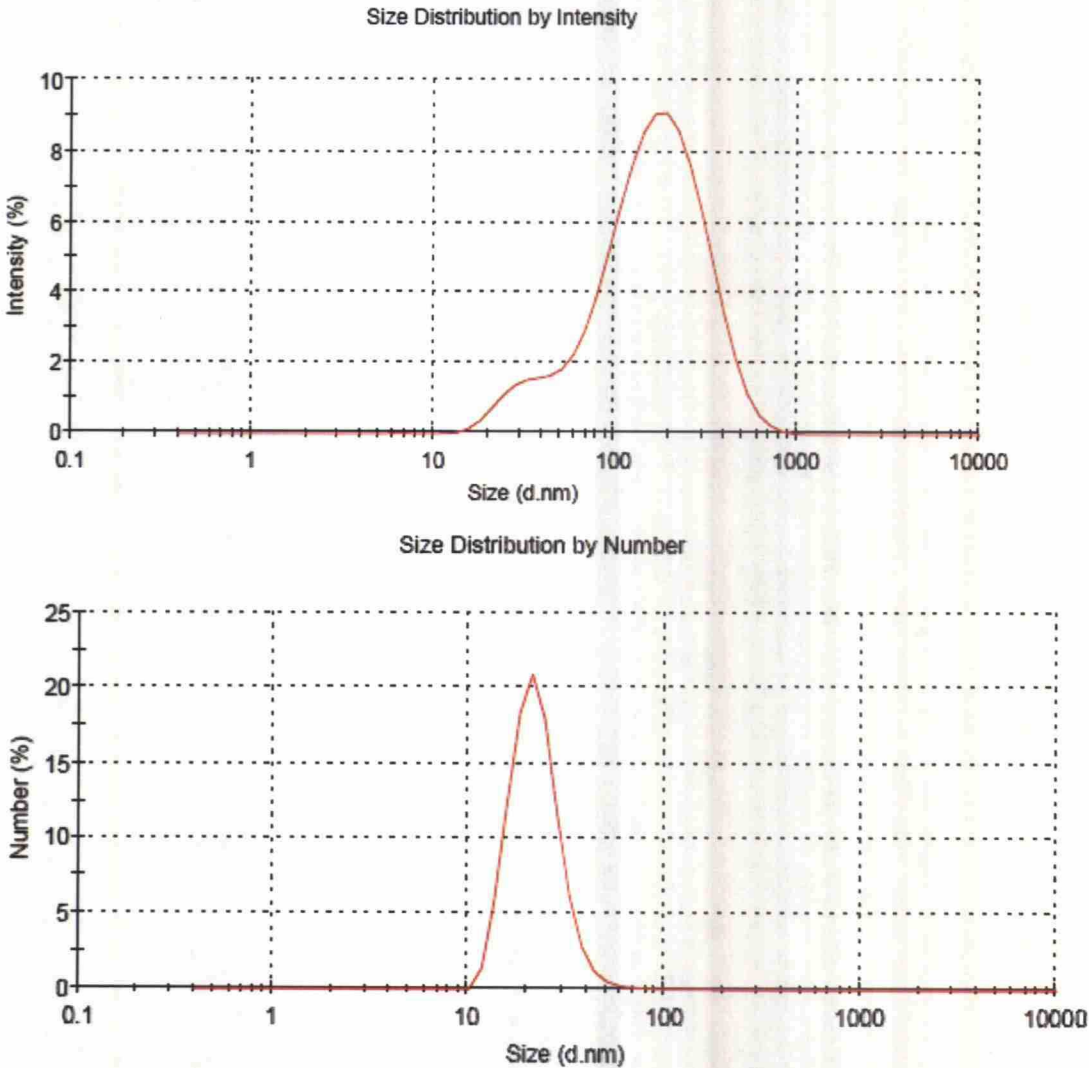
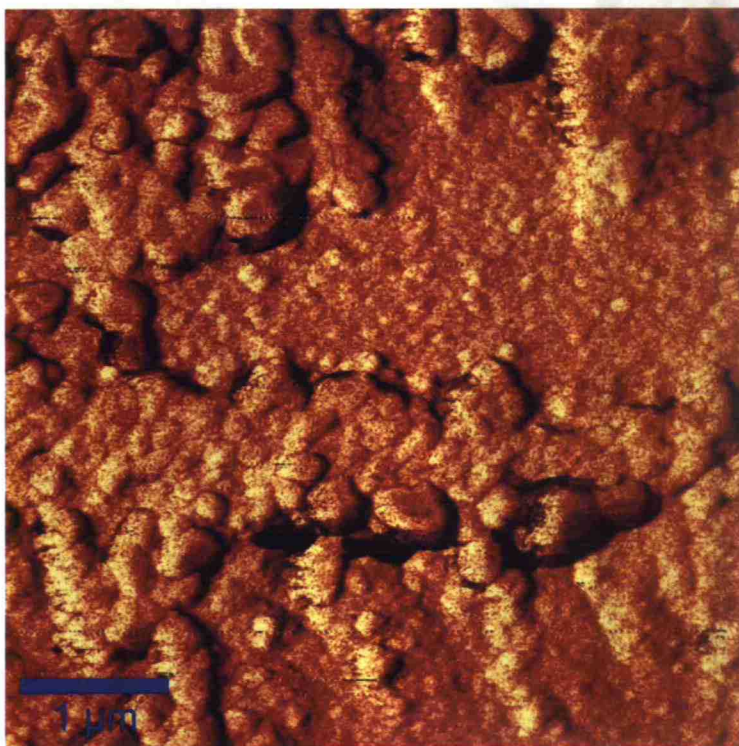


Figure 56. Particle size intensity and number distributions for sample C5. The two particle families are clearly visible in the intensity distribution

### 16.3 Microscopic analysis

Spin coating surfaces and AFM images of sample C5 were prepared. The images mainly show only crystalline NaCl, which covers all silica particles on the surface. Figure 57 shows an image of a surface prepared with high speed, which seems to show silica particles of about 100 nm under a layer of crystalline NaCl.





**Figure 57.** An AFM image of a spin coating surface prepared with sample C5. Parameters: 5000 rpm, 1420 rpm/s (taken by Tiina Nypelö at TKK Laboratory of Forest Products Chemistry)

## 16.4 Conclusions

With the aid of coagulants, substantially different results than those in acid neutralization experiments could be obtained. However, the NaCl concentration had to be at least twice as high as the silica concentration in order to have an effect on the particle size distribution. Na<sub>2</sub>SO<sub>4</sub> concentration should have been even higher and a sufficient concentration was not found in the experiments. If a salt is used as the coagulant, then the solubility of the salt could turn out to be limiting at high silica concentrations.

The particle size distributions were hard to interpret. The number distributions showed similar results than in the Acid Neutralization Experiments, which could be expected since the silica concentration range was the same. In the intensity distributions, however, a second family of larger particles was clearly visible. No parameters that would clearly affect the particle size distribution were found, but then again the number of experiments was so low that no reliable conclusions can be drawn.

The samples obtained in experiments C3-C5, C7 and C8 were stable sols that showed a slight turbidity, indicating the presence of larger particles. Those samples were sta-

ble for unexpectedly long periods of time, despite of their high salt concentration. This was probably because of an altered surface charge of the particles. This could give hints for how the modification of the particles should be done, but still more research in this area is required.

Stable sols were only obtained if acid addition was practically instantaneous. If the acid addition rate was slow, a very fine white powder-like precipitate was formed. This observation is in accordance with the patents by Baker and Frankle (1965) and Tamenori *et al.* (1987).

## 17 Additional Experiments

The main focus of the experiments was to investigate what products could be obtained by neutralizing a hot solution of water glass with acid at a pH higher than 7. However, some additional interesting experiments, mainly connected to the precipitation experiments, were performed:

- Experiment D1 was closely connected to the precipitation experiments. It was tested whether nanometer-sized precipitates could be made by forming gel fragments of desired size by first applying high shear and then adding additional water glass and acid to add a layer of reinforcing silica on the gel fragments to stabilize the product. This was tested by first mixing water glass and acid until just before the gel point. Then the slightly turbid suspension was agitated with a high-speed kitchen mixer. Additional water glass was added to the solution and acid addition was continued. The result was a very smooth paste-like gel, but not a suspension as was expected. This experiment is considered interesting because it shows that the product properties can be changed by varying the precipitation conditions. In this experiment, one would have expected a result similar to the result of experiment B3, but instead a smooth paste-like gel was obtained. More details of the experiment are presented in Appendix E.
- In experiment D2 it was tested whether the precipitation reaction could be stopped before the gel point by quickly neutralizing the solution with acid before gelling occurs. It turned out to be possible, but measured particle sizes were not very large, so there were only few large aggregates present in the solution.



- In experiments D3-D4 it was also tested whether a similar product could be obtained by the inverse route, i.e. by adding water glass to a sulfuric acid solution under acidic conditions. In these cases, the product was rather a gel than a precipitate. The viscosity of the product was quite low in the beginning when water glass addition was complete, but then increased steadily until the product turned into a rigid gel. If an impurity, for example a piece of dry silica gel, was introduced into the suspension, then gelling was very rapid. This experiment shows that precipitation should be performed by adding a sulfuric acid solution to a water glass solution, and not vice versa.

## **18 Conclusions from the Experimental Part**

### **18.1 General Conclusions**

The synthesis of large silica nanoparticles using only water glass and sulfuric acid without using ion exchange or autoclaving at high temperatures proved to be quite challenging. The performed experiments should be seen as a starting point for further research with more sophisticated equipment.

However, some good results could be obtained in these experiments already, and at least the following conclusions can be drawn:

- Acid neutralization before the gel point does not produce desired particle sizes.
- With precipitation at higher concentrations, more favorable particle sizes can be obtained. These particles, however, come always aggregated and must be dispersed in some way.
- Coagulant processes can be used for producing larger particles in colloidal suspensions, but they are impractical because of the large coagulant concentrations needed.

### **18.2 Key Variables**

The following key variables that have an influence on product properties were identified:

- *Silica concentration.* The silica concentration is maybe the most important parameter that characterizes the whole process. It is the most important parameter



that affects particle size and product appearance. In the Precipitation Process, varying the silica concentration can be used to control the primary particle size at least in the range of about 7-50 nm, which corresponds to product silica concentrations of about 1.5-10 %. Within this range, the relation between silica concentration and particle size is almost linear. Figure 58 shows primary particle size as a function of the product's silica concentration throughout the whole measured concentration range.

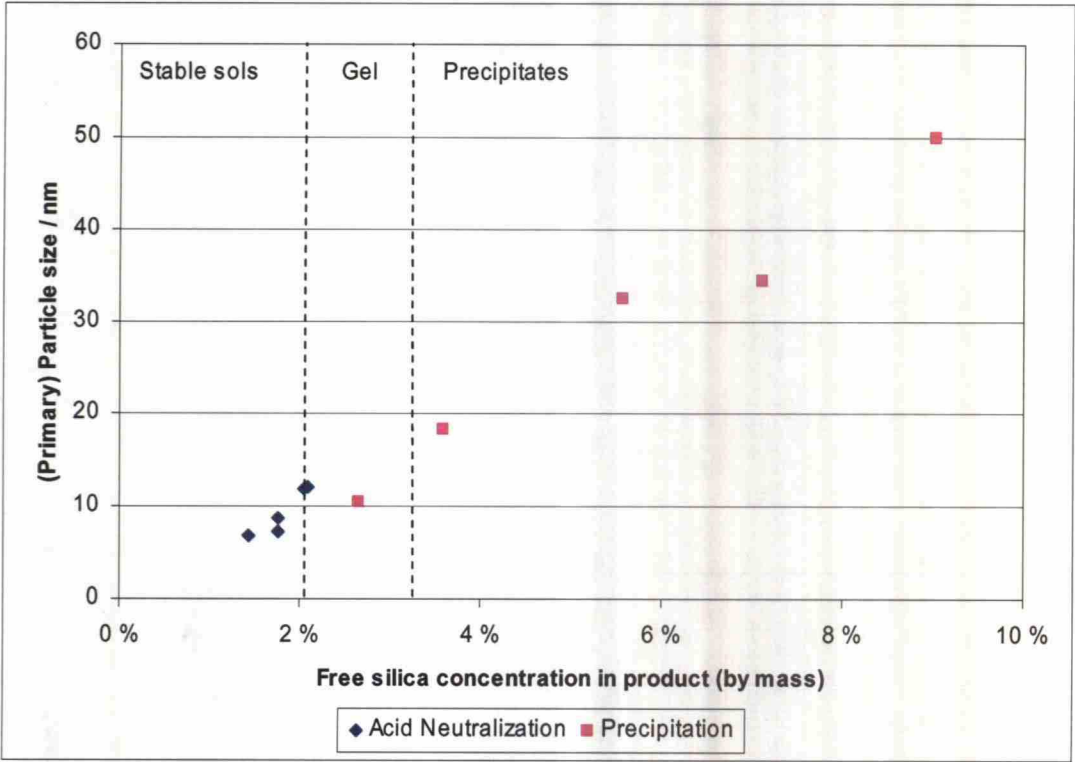


**Figure 58.** The relation between (primary) particle size and product silica concentration throughout the measured concentration range when a hot solution of water glass is neutralized to a pH of about 9-10

- *Acid addition rate.* Acid addition rate is a very important parameter in all of the processes. In the Acid Neutralization and Precipitation Processes, slow acid addition is the key to obtaining proper products (stable sols or precipitates). Rapid acid addition results in gel formation. Acid addition has to be done in such a way that pH is maintained as uniform as possible throughout the reactor volume. In the Coagulant Process, the acid addition rate determines the product characteristics: Stable sols can be obtained by quick acid addition, while slow acid addition results in the formation of a precipitated powder.

- *Stirring intensity.* Stirring intensity is an important issue in all of the three processes. In the Acid Neutralization and Coagulant Processes, efficient stirring is necessary to maintain a constant pH in the batch. In the Precipitation Process, another important function of stirring is to break up any gel that is formed during the reaction. In the experiments a power input of at least  $1\text{-}3\text{ kW/m}^3$  was found appropriate.
- *Temperature.* Temperature has to be sufficiently high in all processes. In the Acid Neutralization and Precipitation Processes, temperature should be at least  $70\text{ }^{\circ}\text{C}$ , more favorably  $80\text{ }^{\circ}\text{C}$ . Attempts to make products at low temperature result easily in gelling. In the Coagulant Process, temperature is not such an important parameter, but it was discovered that the risk of gelling can be reduced by performing the reaction at elevated temperature, about  $45\text{-}50\text{ }^{\circ}\text{C}$ .

### **18.3 Product Stability**

Product stability is an issue only in the Acid Neutralization Process. This is discussed in more detail in Paragraph 14.3. In the Precipitation and Coagulant Processes, the obtained products are stable for long periods of time, even weeks to months. Normally, some aggregation will occur but gelling or other changes in the visual appearance of the products are not observed. In any case, there will be no or little change in the primary particle size distribution but only in the degree of aggregation.

### **18.4 Suggestions for Further Research**

Still more research is required in the following fields:

- More experiments are needed to verify whether aggregate size can be influenced during the precipitation stage if sufficiently high shear forces were applied. The stirred tank reactor used in these experiments is not suitable for that because the flow field in the reactor is not homogenous. A Taylor-Couette reactor (Marchisio *et al.* 2001, Judat *et al.* 2004) or even an ultrasonic reactor (Machunsky and Peucker 2007) could be more appropriate (see Paragraph 22.2). A further possibility is to test whether the aggregation of particles can be prevented by the use of some additives. However, there has been no published information on this and there is yet no clue what these additives might be.

- More experiments are also needed to find the optimal reaction conditions. The exact parameters for reactant addition rate, temperature, and reactant concentrations depend heavily on the type of reactor and cannot be specified universally. In these experiments, the maximum silica concentration was about 10 % due to the crystallization of material on the reactor walls at higher concentrations.
- More experiments at higher concentrations are needed to find the maximum primary particle size that can be achieved.
- Research is required to find out at what stage of the process the modification of the nanoparticles should be done and whether the modification process is compatible with the precipitation process. Since there is yet practically no information how the modification is going to be done, there is still a significant uncertainty factor in the whole process.



## 19 Evaluation of Process Alternatives

### 19.1 Introduction

One aim of this thesis was to compare different processes that could be used for silica nanoparticle production. The following processes were chosen for comparison:

- Acid Neutralization
- Precipitation
- Coagulant Processes
- Emulsion Process
- Ion Exchange.

An industrial process concept, based on own experiments and literature, was created in each of the cases and is briefly presented in the following paragraphs. The processes are represented as block diagrams whereby each block represents one unit operation.

### 19.2 Processes

#### 19.2.1 Acid Neutralization

The simplest process is the Silica Sol via Acid Neutralization –process, which was also tested experimentally (see Paragraph 14). The process consists of mixing-in of the acid and then possibly separation of the sodium salt by ultrafiltration or another membrane operation, and concentration of the product. Figure 59 shows the basic flow diagram. In this process, the silica concentration has to be very low, less than about 3 %, so that no aggregation or gelling occurs.

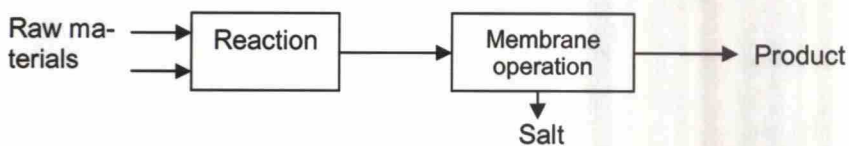


Figure 59. Flow diagram of the Acid Neutralization process

### 19.2.2 Precipitation

The Precipitation Process operates at a considerably higher concentration than the Acid Neutralization Process, and aggregation of the product is taken into account. Different process variants, depending on the desired product, can be imagined. Figure 60 shows three different possibilities. If a reactor can be designed where aggregation can be kept under control (using high shear) then size reduction may not be needed. This is discussed in Paragraph 22. Else, size reduction by grinding or ultrasonic dispersing is needed. It can be placed either before or after washing and salt separation. If washing takes place before size reduction, then normal filtration can be used because of the large size of the aggregates. If the washing step is placed after size reduction, then ultra- or microfiltration is required.

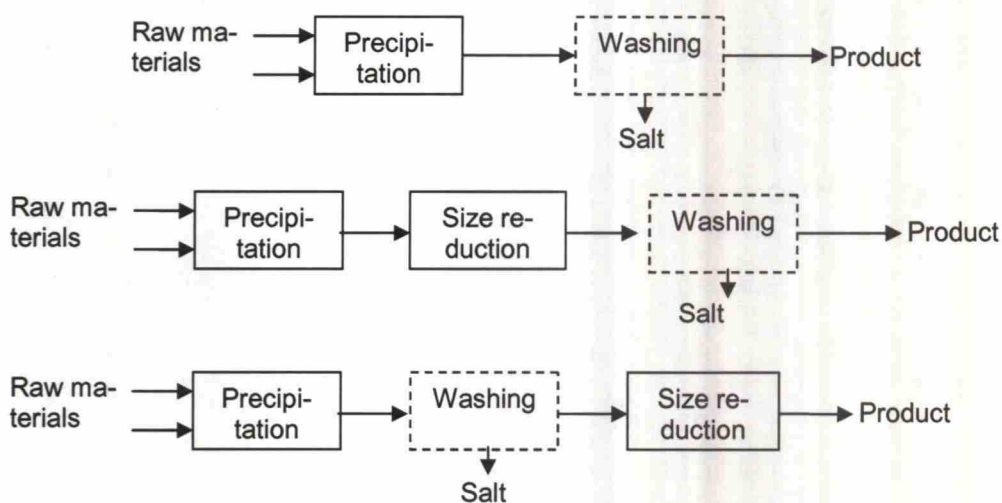
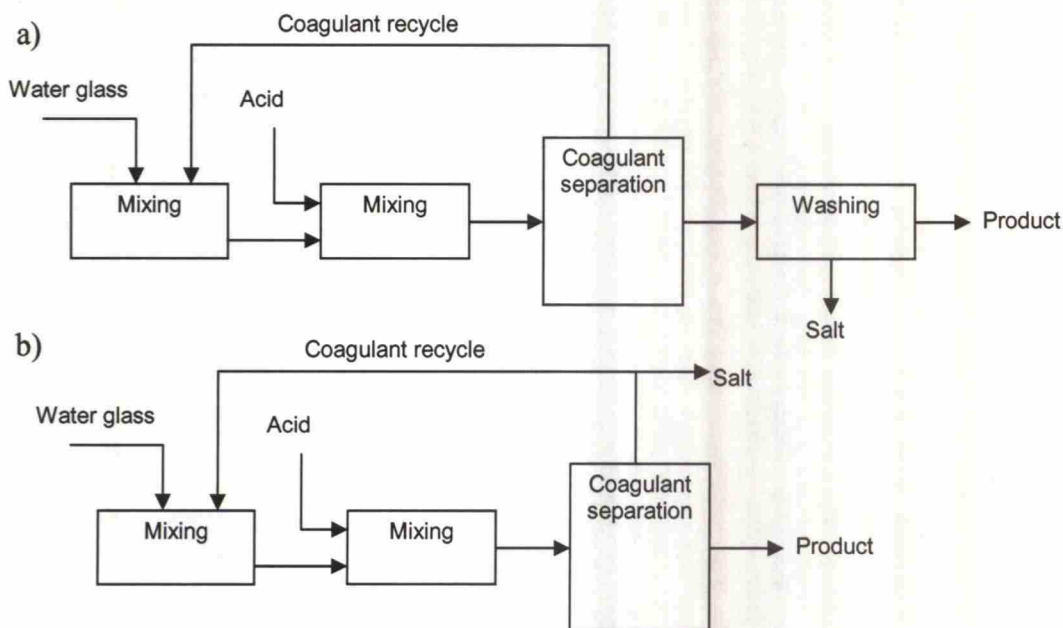


Figure 60. Alternative flow diagrams for the precipitation process

### 19.2.3 Coagulant Processes

In the Coagulant Processes described by Baker and Frankle (1965) and Acker and Winyall (1977), an additional component is introduced into the flow sheet (see paragraphs 7.3.2 and 16), and thus coagulant separation and recycle are needed. Figure 61 shows two possible flow sheets.

The water glass is mixed with the coagulant, which effects the formation of micelles in the solution. Then acid is mixed in rapidly to effect precipitation of the micelles, whereby the particles retain the size and shape of the micelles. Then the coagulant is removed from the product if needed and recycled.



**Figure 61. Possible flow diagrams of coagulant processes; a) This diagram applies as well to the Baker and Frankle (1965) process as to the Acker and Winyall (1977) process; b) This diagram applies if the same salt is used as coagulant that is being formed in the neutralization reaction**

#### 19.2.4 Emulsion Process

Figure 62 shows the flow diagram for the Emulsion Process described by Jesionowski (2001, 2002a, 2002b, see Paragraph 7.3.1). Acid and water glass are mixed with an emulsifier to make two emulsions which are then mixed together in the precipitation step. The acid effects the precipitation of the silica particles, which retain the shape and the size of the emulsion droplets.

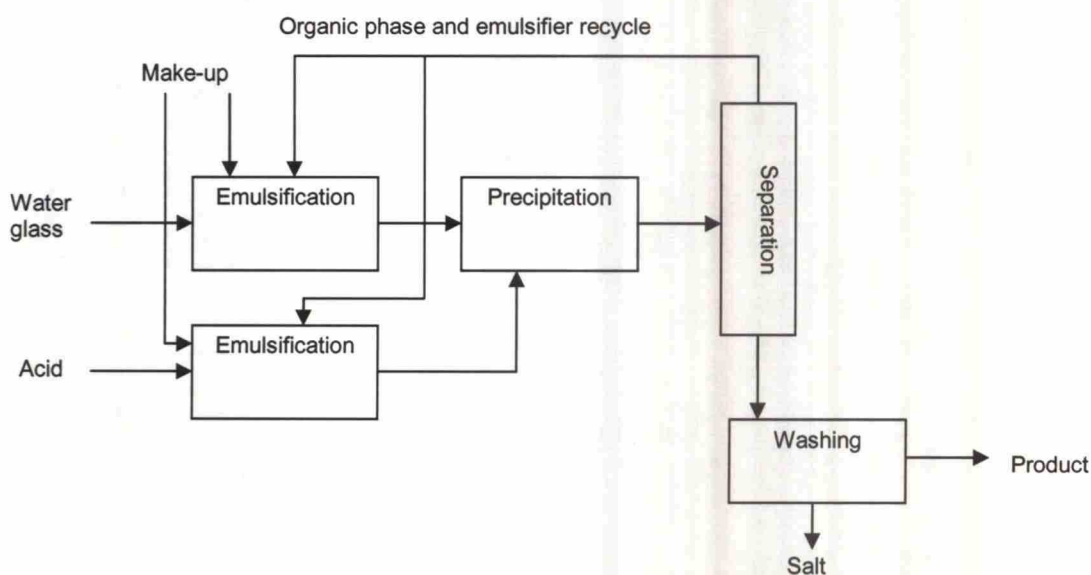


**Figure 62. Flow diagram of the emulsion process described by Jesionowski (2001, 2002a, 2002b)**



### 19.3 Comparison of the Processes

Table 9 shows a comparison between the different process variants using various criteria. The particle size ranges and shapes are taken from own experiments or from the literature. The complexity of the processes was defined as the number of unit operations (number of blocks in block diagram) plus the number of additional components (in addition to water, water glass and an acid) in the flow sheet. Also, a conventional state-of-the-art ion exchange process (Figure 63) is taken as a benchmark. Sol-gel-processes using TEOS as raw material are not included in the comparison because only processes that produce the product in an aqueous phase are considered.

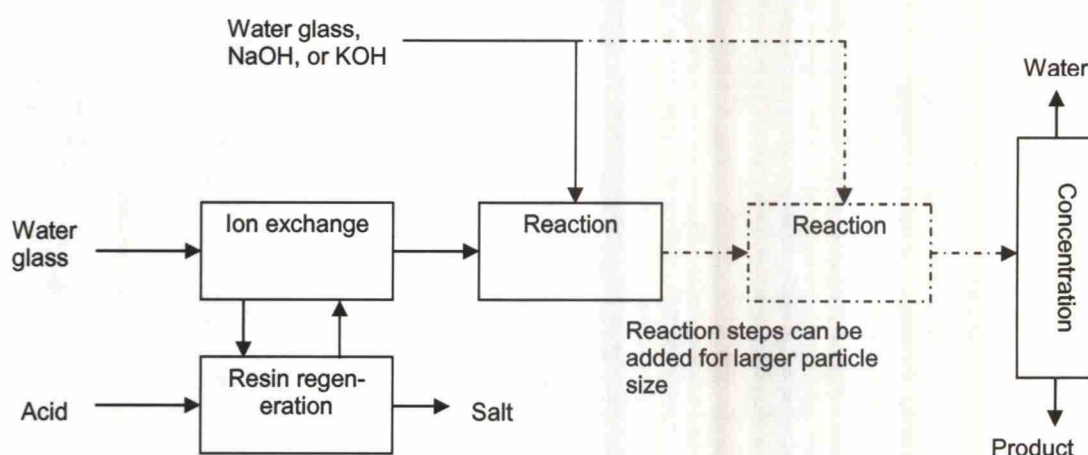


Figure 63. Flow diagram of an ion exchange process

Figure 64 shows a graphical representation of the comparison with the process complexity and the product particle size as criteria. It can be seen that for producing very different products, completely different processes are needed. It is not possible to have a single process that could produce any desired particle. One should notice that the comparison of the precipitation process with the other processes is not completely fair since the products are quite different. When talking about Precipitation Processes, one should not confuse aggregate size and primary particle size.

Table 9. Comparison of processes. Complexity index is defined as the number of unit operations + the number of additional components in the flow sheet

	Particle size	Particle shape	Additional components	Unit operations	Complexity index
Acid neutralization	About 10 nm	Globular	None	2	2
Precipitation	Aggregates: hundreds or thousands of nm; Primary part.: at least 10–50 nm	Aggregates: irregular, fractal Primary particles: Globular	None	2-3	2-3
Coagulant (Baker and Frankle 1965)	At least up to 100 nm, maybe larger	Globular	1 (Coagulant (salt, alcohol or ammonia))	3-4	4-5
Coagulant (Acker and Winyall 1977)	200 – 500 nm	Globular, loosely aggregated	1 (Ammonia, mineral acid is replaced by carboxylic acid)	4	5
Ion Exchange	10-100	Globular	0-1 (NaOH or KOH)	4-9, depending on particle size	4-10
Emulsion	200 – 1000 nm	Globular or irregular	2-3 (Organic phase, emulsifier, possibly coagulant)	5	7-8

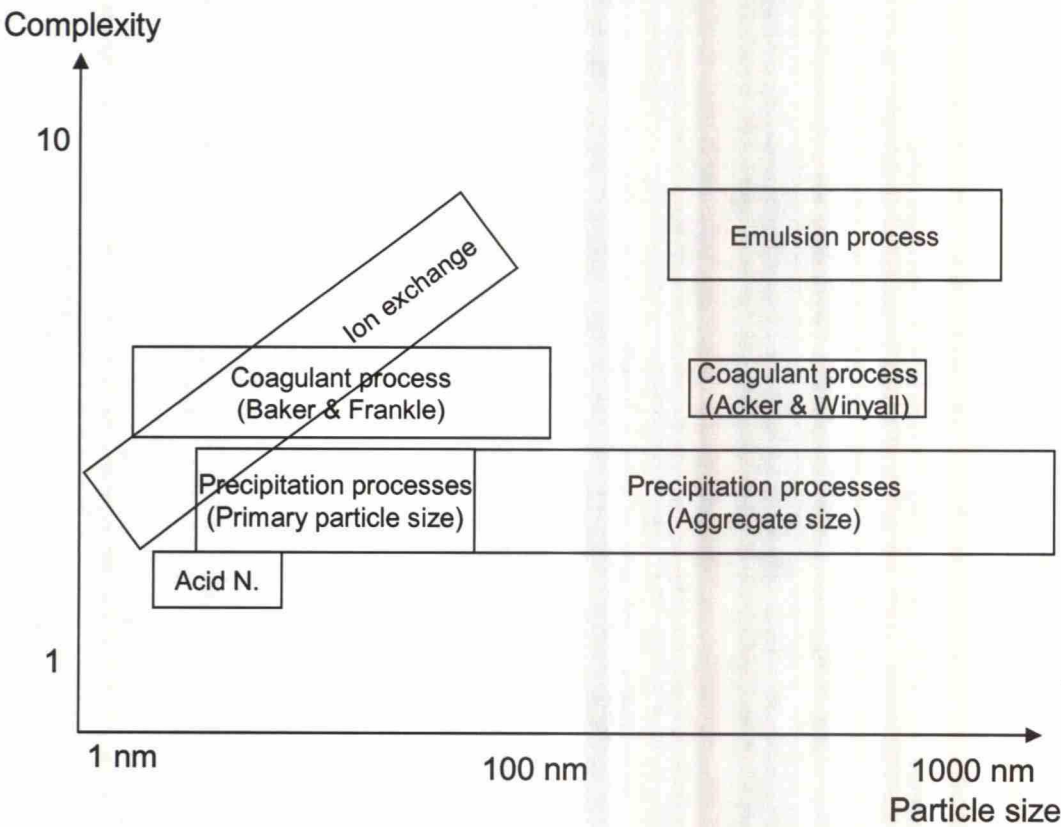


Figure 64. Process comparison with particle size and process complexity as criteria

## **19.4 Selection of a Process**

The comparison in the previous paragraph shows that precipitation and ion exchange are the processes that are best suitable for industrial mass production. Those are also the ones that are already being used in industrial production. Acid neutralization could also be considered for producing small particles, but the very low product concentration makes the process impractical. Coagulant processes can be problematic because of the high coagulant concentrations and the difficulties that arise from coagulant separation and recycle. Coagulant processes can be considered if a coagulant is found that is easily separable or has not to be separated at all. Emulsion processes are most suitable for the small-scale production of highly specialized products. In emulsion processes, problems arise from the separation of the organic phase. Furthermore, the use of flammable solvents like cyclohexane is not favored.

Since the Precipitation Process is a new and promising approach for the production of silica nanoparticles, it is chosen as the basic principle for the pilot and industrial processes to be designed. The main advantages of the Precipitation Process are the following:

- Simplicity, compared to other processes.
- The reaction can be performed at a significantly higher concentration than in ion exchange processes, making separation of water by evaporation or membrane separation unnecessary.
- Particle size can be controlled quite easily in the range of at least 10-50 nm varying the reactant concentrations. In state-of-the-art ion exchange processes, particle size can only be varied by varying the number of reaction steps.

The main disadvantages are:

- The aggregated nature of the product which may be difficult to deal with.
- The considerable amount of sodium sulfate or other salt in the product, which has to be eventually separated. Separation may not be required in the pilot process, but most probably it has to be done in industrial scale.
- Since equipment for size reduction in the nanoscale is not yet in wide industrial use, it might still be expensive and not yet fully reliable. This is expected to change with ongoing research and development at the equipment manufacturers.



## 20 Pilot Process Design

### 20.1 Introduction

For the first pilot-scale process, a semi-batch process that can be built by combining existing equipment is recommended. At this stage, there is not yet enough knowledge to design a continuous process, with the greatest challenge being probably in reactor design. The pilot process is based on the Precipitation Process principle, but it can also be used for testing other process schemes, like the Coagulant Process.

A stirred tank reactor, which is operated in semi-batch mode, is chosen as the reactor. The reactor is followed by size reduction equipment, which may be a stirred media mill (bead mill), an ultrasonic probe or a homogenizer. The size reduction equipment can be designed to be interchangeable so that test runs with different equipment can be performed.

Filtration and washing equipment are not included in the pilot process, because the amounts of sodium salt produced are not very high and it is not yet known at what stage of the process the washing should be done. If filtration and washing are needed, there are two ways to do it in the process:

- A conventional filter can be placed right after the reactor, when the aggregates are still large. Presumably, the filtration has to be a batch operation where the aggregates are collected in a filter cake and then washed with water.
- Ultra- or microfiltration equipment can be placed after the size reduction step when aggregates are already smaller in size and conventional filtration is not possible anymore. This kind of filtration and washing is easier to perform in a continuous or semi-continuous mode of operation.

Separation could also be done after the application of the nanoparticles to the surface if the sodium sulfate does not cause any problems in the previous stages of the process. In that case the salt can be separated from the waste water if needed. If an additive or a coagulant is used, then its separation should be considered individually.

### 20.2 Capacity

The design capacity of the pilot process is 0.9 g/s  $\text{SiO}_2$ . The capacity of the reactor also depends on the desired  $\text{SiO}_2$  concentration of the product suspension. It is as-

sumed that the minimum practical  $\text{SiO}_2$  concentration in the process is about 4 %. The usage calculations are presented in Table 10.

**Table 10.  $\text{SiO}_2$  usage in the pilot process**

<b>Total <math>\text{SiO}_2</math> usage</b>	
g s <sup>-1</sup>	0.9
g h <sup>-1</sup>	3060
kg h <sup>-1</sup>	3.06
kg h <sup>-1</sup> 10 % solution	30.6
kg h <sup>-1</sup> 4 % solution	76.5

The reaction time in larger scale is not yet known. In the patent by Sifrance (1972), which features a similar system, a reaction time of 40-180 minutes is recommended. Scaling up from the experiments, where the acid addition rate was 0.02 g  $\text{H}_2\text{SO}_4$ /s, a reaction time of about 40 minutes can be estimated, based on a constant feed of acid per unit volume. Thus, a 40 minutes reaction time can be assumed to be a good estimate.

### **20.3 Description of the Process**

Figure 65 shows the preliminary flow sheet of the pilot process. A more detailed flow sheet with controls and valves is presented in Appendix J. Table 11 shows a list of the equipment in the pilot process together with the most important technical data, based on a reaction time of 40 min. The individual items are also discussed briefly in the following paragraphs.

Water glass is charged into the reactor DC-101 and then diluted with water to the desired concentration. The batch is then heated with the immersed heater EB-101 to a temperature of about 80 °C. Acid is fed to the reactor with the acid feed pump GA-101 while constant temperature is maintained in the reactor. When the desired acid quantity has been added to the reactor, the acid feed is stopped. The reactor discharge valve is then opened and the mill feed pump GA-102 and the mill KA-101 are started. Grinding in the bead mill produces additional heat, so the mill will normally be equipped with a cooling jacket. Milling can be done either in a single passage or a circulation mode of operation (see Paragraph 5.4.2). Also, milling during the reaction is possible. In that case, the reaction mixture is being pumped through the mill while acid is being added. When the desired disaggregation stage is achieved, the slurry is pumped into the storage tank FA-101 using the pump GA-102, and a new batch can

be prepared. The storage tank is equipped with an agitator to keep the particles in suspension. The two-tank system allows quasi-continuous operation where a new batch is being prepared while the other one is being consumed. From the storage tank, the suspension is pumped to the process using the pump GA-103.

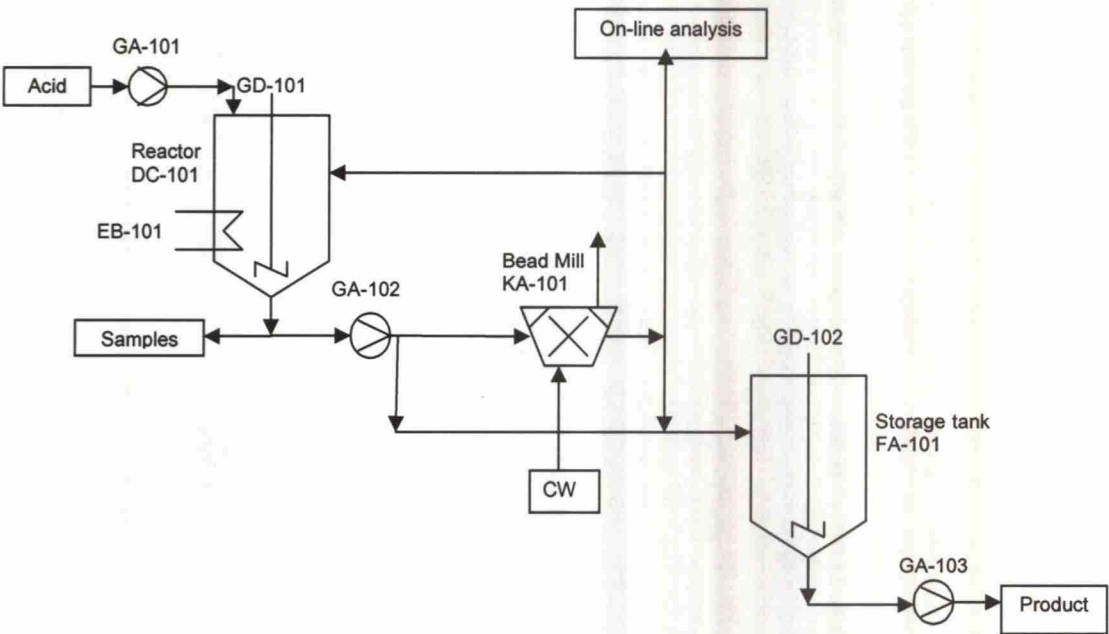


Figure 65. Flow sheet of the pilot process

Table 11. Equipment list for the pilot process

Label	Name	Material	Technical data	Remarks
DC-101	Reactor	PP or GRP	0.1 m <sup>3</sup> volume, 0.5 m diameter	
EB-101	Reactor heater	Hastelloy or similar	30 kW	
FA-101	Storage tank	PP or GRP	0.1 m <sup>3</sup>	
GA-101	Acid feed pump	Special*	0.134 l/min	Peristaltic pump
GA-102	Reactor discharge pump	Silicone*	6 – 20 l/min	Peristaltic pump
GA-103	Product discharge pump	Silicone*	0.4 – 1 l/min	Peristaltic pump
GD-101	Reactor agitator	Hastelloy or similar	0.2 kW shaft power	Rushton turbine
GD-102	Storage tank agitator	Stainless steel	0.2 kW shaft power	
KA-101	Bead mill	Stainless steel	4 l grinding chamber vol- ume, 15 kW	

\*tubing material

### 20.4 Reactor DC-101 and Heater EB-101

For the pilot plant, a stirred tank reactor is chosen despite its limitations because it is versatile, easy to scale-up, and low-cost. The stirred tank reactor allows testing of different reaction conditions and also the use of additives or coagulants. It also al-



lows frequent product changes and the use of different modification agents, assuming that the surface modification takes place in the reaction step.

A baffled tank with  $0.1 \text{ m}^3$  (100 l) volume is chosen for the reactor, based on the assumption of batch sizes between 30 and 80 kg. Such a DIN standard vessel has 0.508 m diameter (Vogel 2005) and is available in many materials, and it can be obtained from various manufacturers. The reactor must withstand basic and acidic conditions at the reaction temperature ( $80^\circ\text{C}$ ) and should be easy to clean. One would intuitively think of a glass reactor, but it is not a good choice because glass is not compatible with sodium silicate. Sulfuric acid, on the other hand, is incompatible with the most metallic materials of construction. Therefore, polypropylene, which can be used for temperatures up to  $120^\circ\text{C}$ , is chosen as the reactor material. Also glass-fiber reinforced plastics (GRP) can be used, but then chemical compatibility has to be checked first. Further, polytetrafluoroethylene (PTFE) lined stainless steel can be considered. (Sinnott 1999)

Heating of the reactor can be done via a jacket or an immersed coil either by steam, water, or heat transfer oil, or electrically via an immersed heater. An immersed heater is preferred over a jacket because of its higher heat transfer coefficient. The heater should be able to maintain a constant temperature in the reactor during the reaction. Most heaters can be equipped with a thermostat which can provide this task. If 10 min are allowed for heating a 70 kg batch, the heater must have a duty of 30 kW, based on the heat capacity of water. The heater should be made of a material that can withstand the sulfuric acid, for example Hastelloy or aluminum bronze. Another possibility could be to use hot water for diluting the water glass for bringing in a part of the heat needed. The reactor should have some insulation to prevent excessive heat loss. Figure 66 shows a schematic drawing of the reactor with two different heat transfer possibilities.

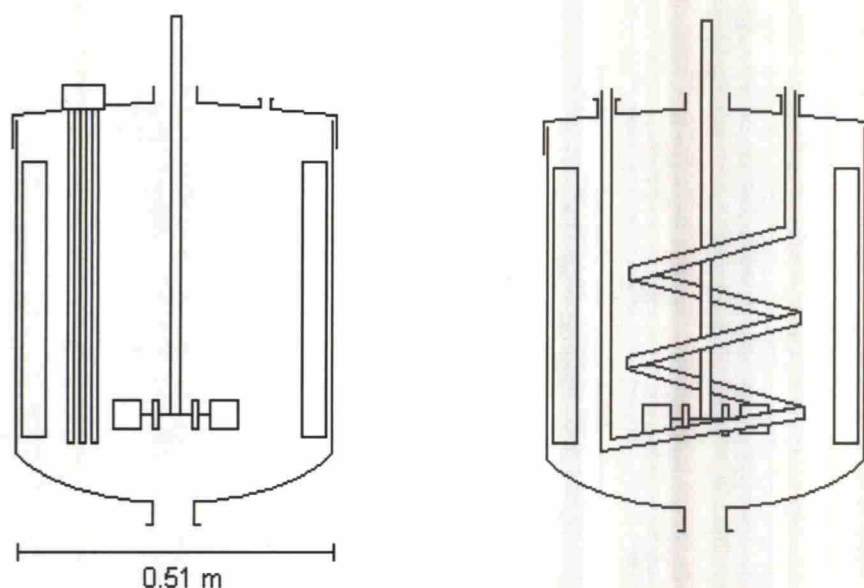


Figure 66. Schematic drawings of the reactor with different heat transfer possibilities; left: electric immersed heater; right: immersed coil for heat transfer fluid

## 20.5 Bead Mill KA-101

In the precipitation reactions tested so far, the formed precipitates have had sizes up to the millimeter scale, thus requiring size reduction. The bead mill KA-101 is used to perform this task. Specially designed machines for nanoparticle disaggregation have been developed by the German company Netzsch-Feinmahltechnik GmbH. Especially the models Zeta RS and Zeta LMZ are recommended for pilot and industrial scale use. Figure 67 shows the two machines. The Zeta RS model is especially designed for the “mild dispersion” of nanoparticles as described by Way (2007), while the Zeta LMZ model can also be used for actual milling of crystalline materials. The LMZ model can be used for bead sizes down to 150  $\mu\text{m}$ , while the RS model can even be used for 50  $\mu\text{m}$  beads. Grinding in the bead mill sets free additional heat and thus all bead mills are equipped with a cooling jacket. (Netzsch) Sizes and power requirements of the LMZ series mills are given in Table 12.

Table 12. Sizes and power requirements of Netzsch’ LMZ series bead mills (Netzsch-Feinmahltechnik 2006)

Machine size	LMZ 2	LMZ 4	LMZ 10	LMZ 25	LMZ 60	LMZ 150
Grinding chamber volume / l	1.6	4	10	25	62	151
Batch size approx. / l	10	100	500	2000	> 2000	> 4000
Drive power of the agitator mill / kW	4	13.5 - 15	17.5 - 22	36 - 45	70 - 90	160

From Table 12 it can be seen that for the pilot process with a maximum batch size of 100 l, a mill with a 4 l grinding chamber volume and 15 kW power is sufficient. The Zeta RS mill has the same operation parameters.

Because the mill is not in contact with sulfuric acid, stainless steel can be chosen as the material of construction. For the beads, various materials and sizes are available. 100  $\mu\text{m}$  glass beads have been successfully used for disaggregating silica aggregates (Mende *et al.* 2006), but ultimately, test runs at the manufacturer should be performed to find the optimal bead size and material.

Another uncertainty is the time required for milling. According to McLaughlin (1999), there is a rapid drop in the particle size in the first few minutes of the milling process, after which size reduction is only very slow. Therefore, long term milling to achieve smaller particles is economically inefficient. Using 100  $\mu\text{m}$  beads, time estimates for achieving a mean particle size of 100 nm range from 2 minutes (McLaughlin 1999) to 10 minutes (Netzsch-Feinmahltechnik 2005). Therefore, 10 minutes are taken as a first estimate. Again, test runs at the manufacturer are required to achieve certainty.



Figure 67. Netzsch Zeta LMZ and Zeta RS bead mills (Netzsch-Feinmahltechnik 2006)



## 20.6 Agitators

### 20.6.1 GD-101

The task of the agitator GD-101 is to keep the solids in the reactor DC-101 in suspension and maintain a uniform pH throughout the reactor volume by efficient mixing-in of the acid. A standard flat six-blade turbine (Rushton turbine), as used in the experiments, is chosen as the agitator. The agitator must withstand sulfuric acid and must therefore be made of an appropriate material, for example Hastelloy.

Figure 68 shows a typical flow pattern for the impeller. From the figure it can be seen that the acid feed point should be somewhere next to the impeller where the mixing intensity is the highest possible. Therefore, an acid feed tube must be inserted into the tank.

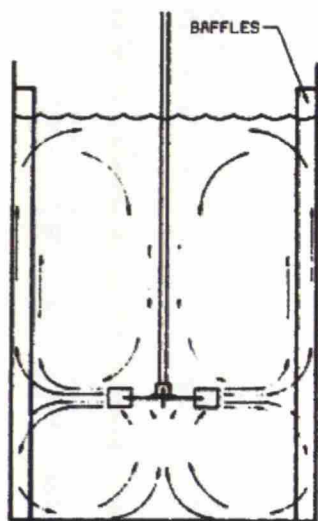


Figure 68. Typical flow pattern for radial-flow impellers (Tilton 1998)

The power required for violent agitation in fine slurry suspensions is at least 2 kW/m<sup>3</sup> (Sinnott 1999). The required shaft power is therefore 0.2 kW for a maximum batch size of 100 l. A power input in this range was also found appropriate in the laboratory experiments (see Paragraph 15.2). Using a turbine with diameter 0.15 m (0.3 times tank diameter), the required speed is about 430 rpm, calculated from a power law between stirrer speed and energy input (for example Sinnott (1999), p. 471)

In this case, only specific power input is used as the scale-up criterion. One must keep in mind that scale-up using only specific power input leads to a different flow

pattern and therefore different mixing characteristics in the reactor, which can affect reactor performance. (Zauner and Jones 2002a).

### **20.6.2 GD-102**

The task of the agitator GD-102 is to keep the solids in storage tank FA-101 in suspension and prevent settling of the particles. As material, stainless steel can be chosen. Special agitators for the suspension of solids are available but also a six-blade turbine can be used. Required power input depends on the stage of disaggregation and mean particle size. If the fluid is a stable colloidal suspension, no agitation at all may be required. If the fluid is a slurry suspension, severe or violent mixing with a power input of  $1.5\text{--}2\text{ kW/m}^3$  may be required (Sinnott 1999). Therefore, an identical agitator to GD-101 is the safest choice.

## **20.7 Pumps**

### **20.7.1 GA-101**

A peristaltic pump is chosen as the acid feed pump GA-101. Because sulfuric acid solution is quite a corrosive fluid, a peristaltic pump is a good choice because the fluid only touches the tubing material. Most peristaltic pumps are programmable and allow monitoring of the flow rate. Another advantage is that they can be used over a wide range of flow rates. A reaction time of 40 minutes was assumed earlier. Assuming, that acid is added continuously over this time, an acid flow rate of  $0.153\text{ kg/min}$  or  $0.134\text{ l/min}$  (for 20 % sulfuric acid) is specified.

### **20.7.2 GA-102**

The pump GA-102 is used to circulate the slurry suspension through the bead mill and discharge the reactor at the end of the cycle. It should be a pump that can handle quite viscous liquids and suspensions, and it should be able to handle the reactor discharge even in case of failure when gel formation has occurred. A peristaltic pump can be used for this task. The pump should be able to discharge the reactor in quite a short time, say 5 to 10 minutes. This corresponds to a flow rate of about 6 to  $20\text{ l/min}$  for batch volumes between 30 and  $100\text{ l}$ .

Some bead mills like the Netzsch Zeta LMZ come complete with a pump and no additional pump is required in this case.

### **20.7.3 GA-103**

The pump GA-103 is used to discharge the storage tank and feed the suspension to the process. It should be able to handle a wide range of flow rates because the required flow rate depends on the silica concentration. For a 10 % SiO<sub>2</sub> suspension, the flow rate is about 30 kg/h or about 25 l/h. For a 4 % suspension, the flow rate is about 70 kg/h or about 60 l/h (about 0.4-1 l/min). A peristaltic pump can be used here as well. For an exactly steady flow rate, also gear, progressing cavity, or centrifugal pumps can be considered.

### **20.8 Storage Tank FA-101**

The storage tank FA-101 is used to buffer the feed to the process. The tank must be able to accommodate the largest possible batch from reactor DC-101, which is 100 l. Since the batch size in normal operation is estimated at 30-70 l, a 100 l (0.1 m<sup>3</sup>) tank is considered sufficient for the storage tank. The material should withstand acidic and basic conditions, but it is not exposed to sulfuric acid. Polypropylene or GRP can be used here as well. Also stainless steel (AISI 304) can be used.

### **20.9 Tubing and Valves**

Because of the low flow rates, tubing diameter is not an issue in this case and should be chosen to fit the fittings on the pumps, vessels, and valves. Tubing in the peristaltic pumps should be chosen to match the flow rates according to the pump manufacturers' recommendations. Tubing and valves must withstand elevated temperatures (up to 100 °C) and acidic and basic conditions. Silicone tubing is an appropriate choice (Sinnott 1999).

For the acid feed line, special tubing that can withstand the sulfuric acid must be chosen. Peristaltic pump manufacturers have special materials for this purpose. Also PVC tubing can be used for sulfuric acid solution at low temperature (Sinnott 1999).

### **20.10 On-line Analysis**

An on-line analysis instrument is useful in the process for measuring the degree of disaggregation during the processing in the bead mill. It should be able to handle a wide range of particle sizes, and one instrument may not be sufficient. For example Schlomach and Kind (2004b) used a Malvern Zetasizer 3000 for measurements be-



fore the gel point, and a Malvern Mastersizer S with a wet sample dispersion unit for large aggregates. The same instrument was also used by Schaer *et al.* (2001). A Malvern Mastersizer laser particle analyzer is also available at the Laboratory of Materials Processing.

## 20.11 Capital Investment

Capital investment estimates for process equipment are presented in Table 13. The total capital investment costs for the pilot process are estimated at about 170,000 €. The by far most expensive individual item is the bead mill with a price of approximately 150,000 € (including beads), accounting for about 88 % of the capital investment cost. The particle size analyzer is not included in this sum because its price depends heavily on its type and functionality. Instrumentation includes temperature, flow rate and pH measurements, and scales for controlling mass balances. Minimum instrumentation requirements are presented in Table 14. Installation of the system is assumed to take 4 weeks or 160 h of work, resulting in an installation cost of about 5000 €.

**Table 13. Capital investment cost estimate for the pilot process. Prices are rough estimates. Price information from Peters *et al.* (2003), Behälter KG (2007), and Netzsh-Feinmahltechnik**

Label	Name	Price estimate / €	%
DC-101	Reactor	1000	0.6
EB-101	Reactor heater	1500	0.9
FA-101	Storage tank	1000	0.6
GA-101	Acid feed pump	1200	0.7
GA-102	Reactor discharge pump	2000	1.2
GA-103	Product discharge pump	3000	1.8
GD-101	Reactor agitator	2000	1.2
GD-102	Storage tank agitator	1000	0.6
KA-101	Bead mill*	150,000	87.6
	Tubing and valves	500	0.3
	Instrumentation	3000	1.8
	Installation	5000	2.9
Total		171,200	100

\*The price of the mill (model Zeta RS, 4 l volume) was given by the manufacturer as 105,000-190,000 €, depending on material, and the price of the beads as 5000-20,000 €, depending on bead size, the smaller beads being the more expensive.

**Table 14. Minimum instrumentation requirements for the pilot process. Additionally, scales are required for controlling mass balances**

Type	Target	Utility value	Measuring range
LIC	GA-101	0.134 l/min	0 - 0.5 l/min
TIC	EB-101	80 °C	0 - 100 °C
LI	DC-101	N/A	0 - 100 %
FI	GA-102	N/A	0 - 30 l/min
LI	FA-101	N/A	0 - 100 %

### 20.12 Alternative Pilot Process Design

In an alternative pilot process design, the bead mill KA-101 is omitted and the conventional agitator GD-101 is replaced with a high-shear mixer, capable to break up the aggregates in a single step during the reaction. The flow sheet of the alternative design is presented in Figure 69. The high-shear mixer that is recommended for this application is a top-entering batch mixer. For example a batch mixer with 1.5 kW power and 3000 rpm can be used (Silverson Machines). The power of the high shear mixer is much more than that of the conventional mixer, but still much less compared to the bead mill, which has 15 kW power. One must, however, take into account that equivalent disaggregation results as with the bead mill are probably not achieved using a high-shear mixer (see Paragraph 5.4).

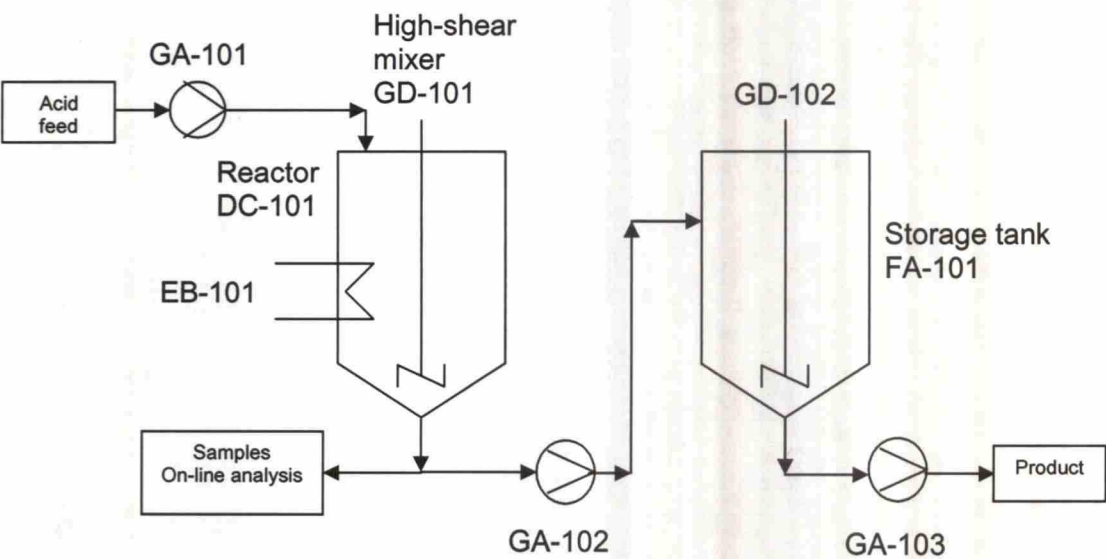


**Figure 69. Alternative pilot process design with high-shear mixer**

Obviously, the flow sheet of the alternative pilot process is much simpler than that of the original design. Savings can also be significant, since the price of a high shear mixer is significantly lower than the price of a bead mill. For comparison, an IKA T

65 D Ultra-Turrax high-shear mixer with 1.5 kW power and 50 l maximum batch size costs about 10,000 €. This price may be at the lower end of the scale but it gives an order of magnitude. Assuming a total price of 20,000 € for the mixer, the pilot process capital investment cost would drop to about 40,000 €.

## 21 Scale-up to Industrial Scale

### 21.1 Process Design

A preliminary scale-up of the existing pilot process to industrial scale was made in order to obtain an estimate for the costs of the industrial production of the silica nanoparticles, although it is probable that this kind of process will not be built in industrial scale. It is, however, that type of process that can be realized with existing equipment and can therefore be used as a benchmark for comparing silica products.

First, the process design of a possible industrial process was created. Figure 70 shows a schematic representation of the process. There are few changes compared to the pilot process: Heating of the reactor is done by a circulation heat exchanger and a filter has been added for  $\text{Na}_2\text{SO}_4$  separation. The type of the filter is not further specified. Equipment was scaled up from the pilot process using shortcut correlations.

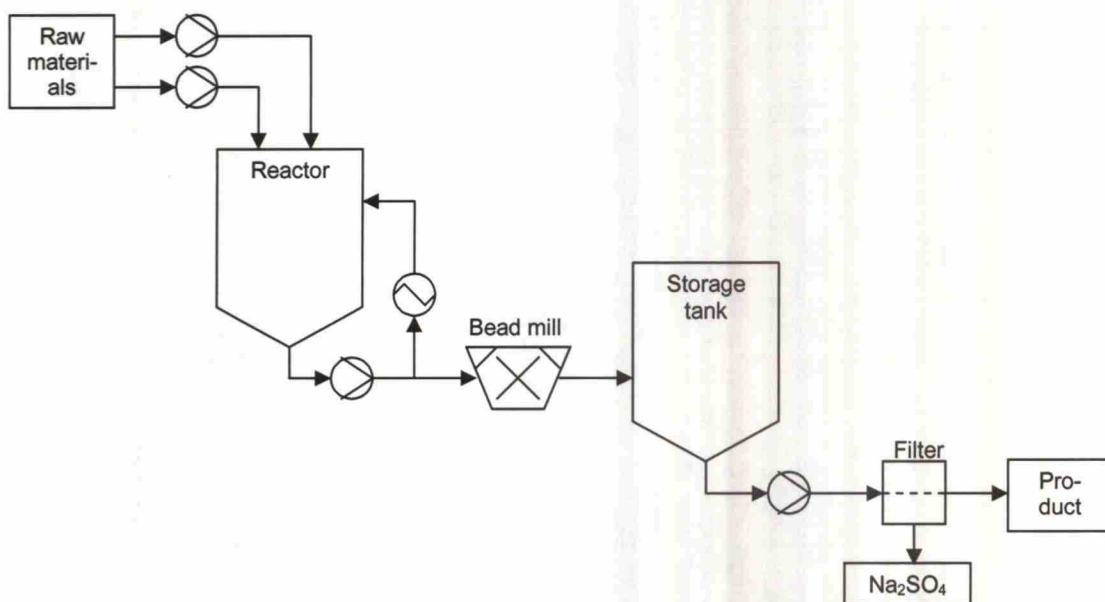


Figure 70. Schematic flow sheet of the industrial process

An industrial process with a design capacity of 370 kg  $\text{SiO}_2/\text{h}$  was assumed. If the silica is prepared as a 10 % suspension, then a 3000 l ( $3 \text{ m}^3$ ) stirred tank reactor with



one batch per hour is appropriate. Whether the batch can really be prepared in this time was not further considered. Further a bead mill with 62 l grinding chamber volume and 90 kW power is needed (see Table 12). A list of equipment with the most important technical data for costing is presented in Table 15.

**Table 15. List of equipment in the industrial process**

Equipment	Technical data
Reactor	3 m <sup>3</sup>
Agitator for reactor	6 kW
Storage tank	6 m <sup>3</sup>
Agitator for storage tank	6 kW
Pumps (4 pcs)	0.2 – 1 kW
Heat exchanger	20 m <sup>2</sup>
Filter	N/A
Bead mill	62 l grinding chamber volume, 90 kW

### 21.2 Capital Investment

Investment costs can be estimated directly using the equipment list given in Table 15. Equipment costs are estimated using correlations given by Peters *et al.* (2003). US Dollar prices were converted into Euros using the factor 1.2 \$/€. Table 16 shows the estimated fixed-capital investment (FCI). Installation, instrumentation, piping, electrical systems, and building and services costs were estimated using factors given by Peters *et al.* (2003, p. 251). Buildings and services in this case refer mainly to raw materials storage facilities. Construction, service facilities, and similar costs were not taken into account because the process is designed to be installed at an existing plant where the facilities are already available. To make the calculation more realistic, only 10 % of the price of the bead mill was taken into account when using the factor method. This is because of the high price of the mill, which does not correlate to the needed amount of instrumentation, piping, et cetera.

**Table 16. Capital investment cost estimate for the industrial process**

Equipment	Cost purchased / €	Remarks
Reactor	33,000	includes agitator
Storage tank	15,000	includes agitator
Pumps (4 pcs)	8000	2000 € each
Heat exchanger	7000	
Filter	83,000	
Mill*	700,000	
Total purchased equipment	846,000	
Basis for factor estimates	216,000	Only 10 % of mill cost included
Other costs	Cost / €	Factor (times basis)
Installation	84,200	0.39
Instrumentation	56,200	0.26
Piping	67,000	0.31
Electrical systems	21,600	0.10
Buildings and services	62,600	0.29
Engineering	69,100	0.32
Total fixed-capital investment (FCI)	1,206,700	

\*Scaled up from the price for the pilot process mill using exponent 0.6

### 21.3 Production Costs

Production costs comprise raw materials, utility, investment, and personnel costs. The estimated unit costs of raw materials, utilities, and labor are presented in Table 17. Their usage estimates are based on a cycle of one batch per hour and a running time of 8000 h/a. A significant uncertainty factor in the production costs is the surface modification agent, which is not yet known. It is assumed to be a specialty chemical with a price of 2000 €/t (Pitt 2002) and its use is estimated at 10 kg/batch, resulting in a yearly use of 80 t. Labor requirements are estimated at 0.1 persons/shift. Equal annual capital cost was calculated assuming a 15 % cost of capital and 10 years economic lifetime, resulting in an annuity factor of 0.19925. The summation of the total manufacturing costs is presented in Table 18.

**Table 17. Unit costs of raw materials, utilities and labor**

Sodium silicate (100 % solids) <sup>1</sup>	700	€/t
Sulfuric acid (100 %) <sup>1,2</sup>	80	€/t
Modification agent <sup>2</sup>	2000	€/t
Steam	30	€/MWh
Electricity	0.07	€/kWh
Process water	0.5	€/m <sup>3</sup>
Waste water	1.2	€/m <sup>3</sup>
Labor	30	€/h

<sup>1</sup>Anon (2005)

<sup>2</sup>Pitt (2002)

Table 18. Total manufacturing costs in the industrial process

Category		Usage		k€ / a	€ / kg 100% SiO <sub>2</sub>	%
Raw materials	Water glass (100 % solids)	3885	t/a	2720	0.92	78.8
	Sulfuric acid (100 %)	1244	t/a	100	0.03	2.9
	Modification agent	80	t/a	160	0.05	4.6
Total raw materials costs				2979	1.01	86.3
Utilities	Steam	1678	MWh/a	50	0.02	1.5
	Electricity	824,000	kWh/a	58	0.02	1.7
	Process Water	25,000	m <sup>3</sup> /a	13	0.00	0.4
	Waste water	20,000	m <sup>3</sup> /a	24	0.01	0.7
Total utilities costs				145	0.05	4.2
Other costs	Labor	876	h/a	26	0.01	0.8
	Maintenance	5 % of FCI		60	0.02	1.7
Total other costs				87	0.03	2.5
Total operating costs				3210	1.08	93.0
Capital; equal annual costs				240	0.08	7.0
Total manufacturing costs				3451	1.17	100

As shown in Table 18, the raw material costs account for about 86 % of the total manufacturing costs. Especially the costs for water glass are dominating with about 79 % of the total manufacturing costs. Figure 71 shows a graphical representation of the total manufacturing costs.

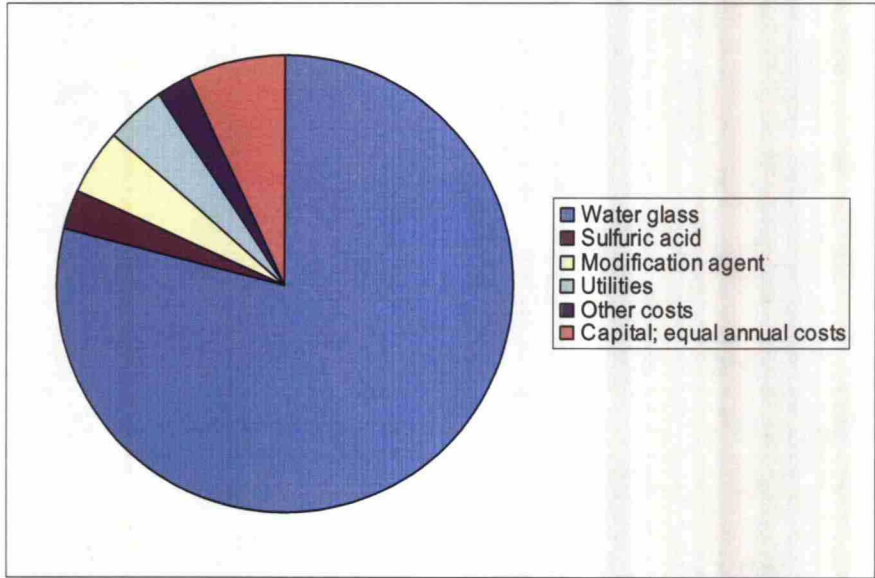


Figure 71. Graphical representation of the total manufacturing costs in the industrial process

Table 19 shows a comparison between the manufacturing costs of the own process and the prices of comparable silica products. As can be seen, the price for silica from



the own process is of the same order of magnitude as the price for precipitated silica, which is logical since the production processes are very similar. The product of the own process, however, is more comparable with silica sol than precipitated silica, which is a filler material and not as such usable for the intended purpose. If the process is installed to replace purchased silica sols or fumed silica, then savings are significant.

**Table 19. Prices of silica products**

	€/kg 100% SiO <sub>2</sub>
Own process	1.17
Precipitated silica <sup>1</sup>	1 -1.5
Silica sol <sup>2</sup>	2.5 – 4
Fumed silica <sup>1</sup>	4 – 7

<sup>1</sup>Lerner (2004)  
<sup>2</sup>Flörke *et al.* (2005)

## 22 Innovative Reactor Design

### 22.1 Introduction

A batch reactor is hardly the best choice for an industrial-scale process. Therefore, alternative and innovative continuous reactor concepts must be developed. In most precipitation reactions, stirred tank reactors are being used. These have also been used in most of the experimental work.

Also, many alternative reactor concepts have already been suggested for nanoparticle precipitation, and especially for continuous operation. Many of the reactors have only been tested for precipitation of barium sulfate nanoparticles. Their suitability for the production of silica nanoparticles has to be evaluated separately. Some of those concepts are presented in Paragraph 22.2.

### 22.2 Reactor Concepts Presented in Journals

#### 22.2.1 Taylor-Couette Reactor

A Taylor-Couette reactor is made of two coaxial cylinders with the inner one rotating. The fluid is contained in a gap between the two cylinders and flows in axial direction. Different fluid dynamic regimes can be achieved depending on the rotational speed of the inner cylinder. (Marchisio *et al.* 2001, Judat *et al.* 2004) Figure 72

shows a Taylor-Couette cell. Taylor-Couette reactors can be used either in batch or continuous operation.

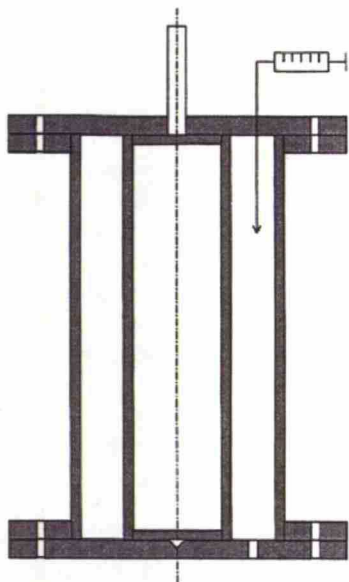


Figure 72. A Taylor-Couette cell (Marchisio *et al.* 2001)

**22.2.2 Sliding Surface Reactor**

Rousseaux *et al.* (1999) have suggested a sliding-surface mixing device for performing fast precipitation reactions. The device consists of a tank which has a rotating disk placed closely over the bottom. The reactants are fed from under the disk into a zone which is called the confined mixing zone, where very high shearing stresses are generated in a very small volume. Above the disk is a zone of moderate mixing where the particles can undergo an aging stage. The sliding-surface reactor can be used in batch or continuous operation. The device is shown in Figure 73.

**22.2.3 Ultrasonic Reactor**

Machunsky and Peuker (2007) have designed an ultrasonic precipitation reactor for continuous operation. The device is shown in Figure 74.

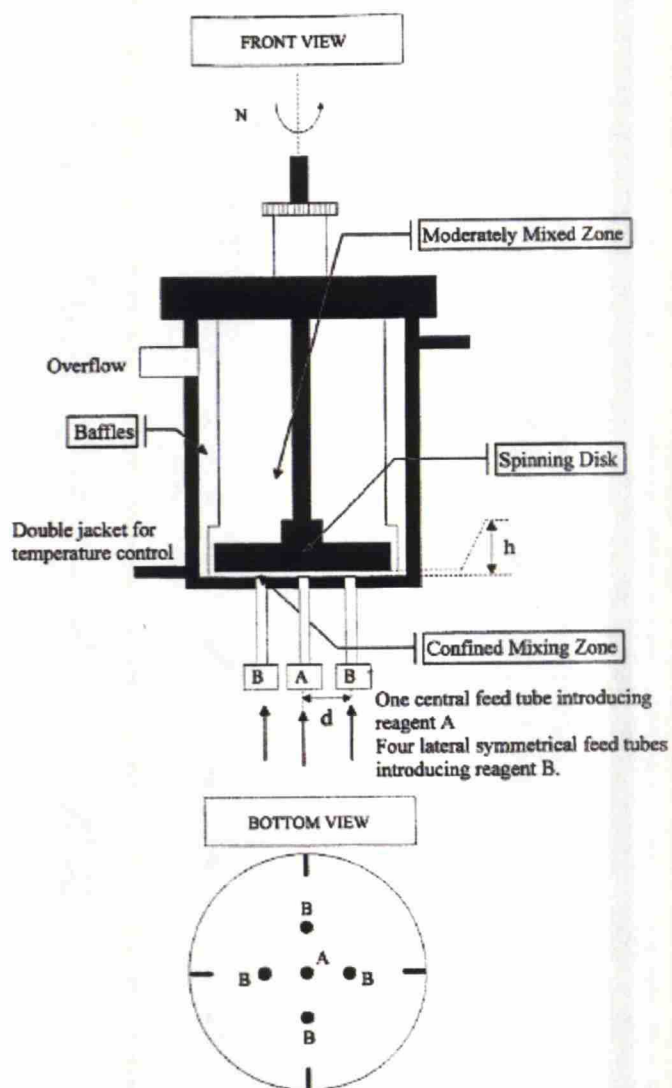


Figure 73. The sliding-surface reactor used by Rousseaux *et al.* (1999)

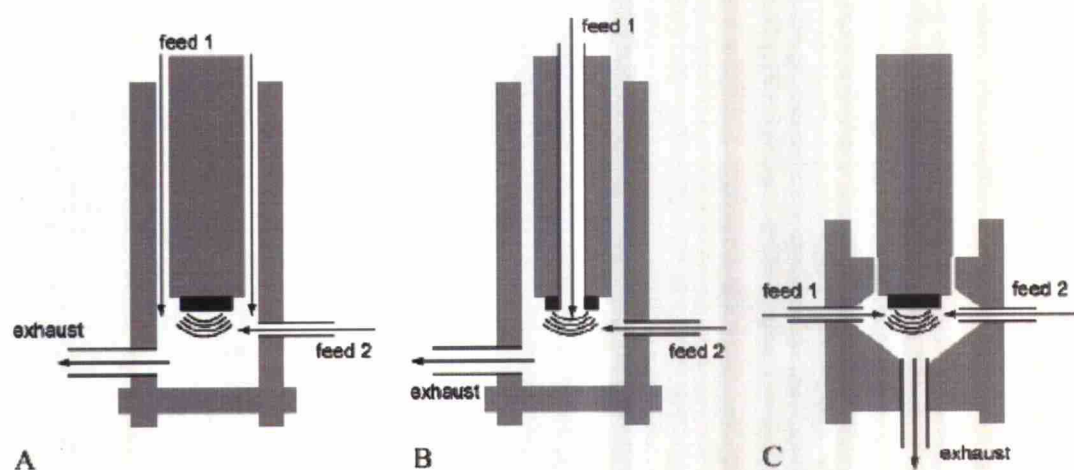


Figure 74. The ultrasonic precipitation reactor designed by Machunsky and Peuker (2007) with different configurations



#### 22.2.4 Y- and T-mixers

Schwarzer and Peukert (2002) made experiments with the precipitation of barium sulfate nanoparticles in a T-mixer. They found that particle size could be controlled by the mixing conditions in the reactor. This could be done independently of the concentrations of the raw materials. A schematic picture of the apparatus is shown in Figure 75 and a photograph in Figure 76. The authors have also developed mathematical and simulation models for the continuous precipitation of barium sulfide nanoparticles (Schwarzer and Peukert 2004, 2005, Schwarzer *et al.* 2006, Gradl *et al.* 2006). The results could possibly be applied to the design of a continuous silica nanoparticle precipitation process as well.

A disadvantage of Y- and T-mixers is that throughput, mixing energy, and geometric parameters cannot be varied independently of each other, making scale-up impossible. Therefore, parallel reactors are necessary for large-scale production. (Machunsky and Peuker 2007) Y- and T-mixers are, however, well suitable for continuous operation.

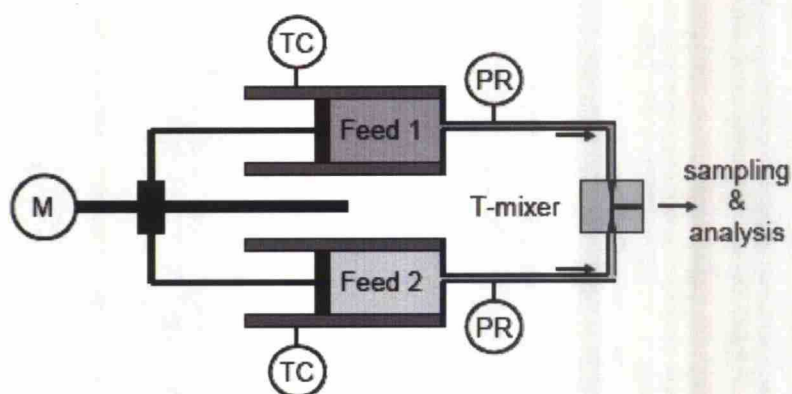


Figure 75. Schematic picture of the T-mixer apparatus used by Schwarzer *et al.* (2006)

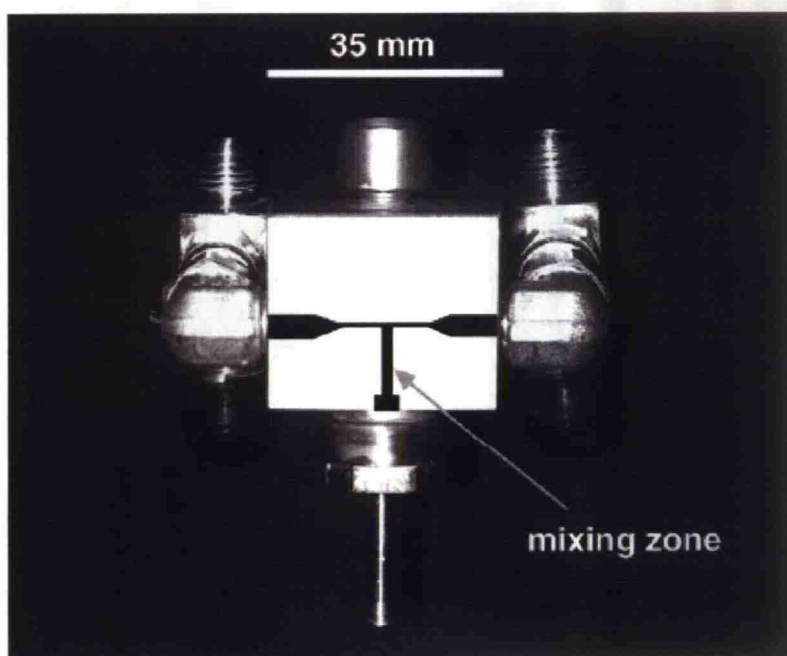


Figure 76. Photograph of the T-mixer used for the precipitation of barium sulfide nanoparticles (Schwarzer *et al.* 2006)

### 22.2.5 Cascade Reactor

Another reactor concept is the cascade reactor in which the acid is added gradually into consecutive stirred tank reactors. Similar designs are featured in the patents by Sifrance (1972, see Paragraph 9.3) for the production of precipitated silica and Brekau *et al.* (1999, see Paragraph 9.2) for the production of silica sols. The basic scheme is shown in Figure 77. Cascade reactors are not very practical in industrial production because of their space and instrumentation requirements.

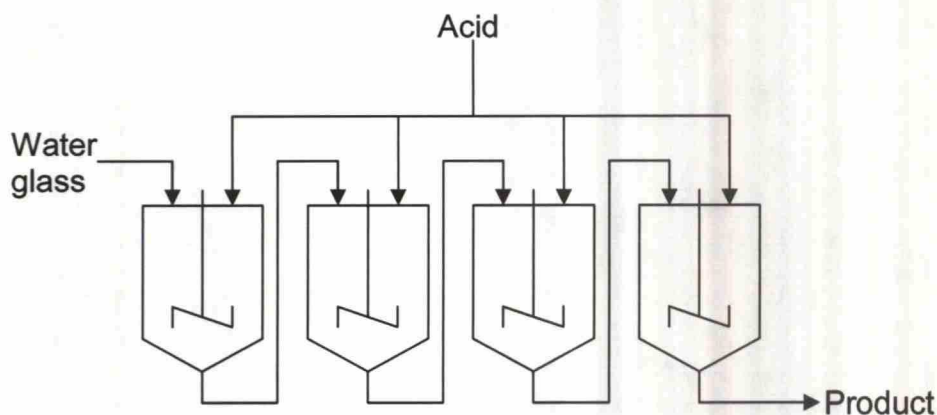
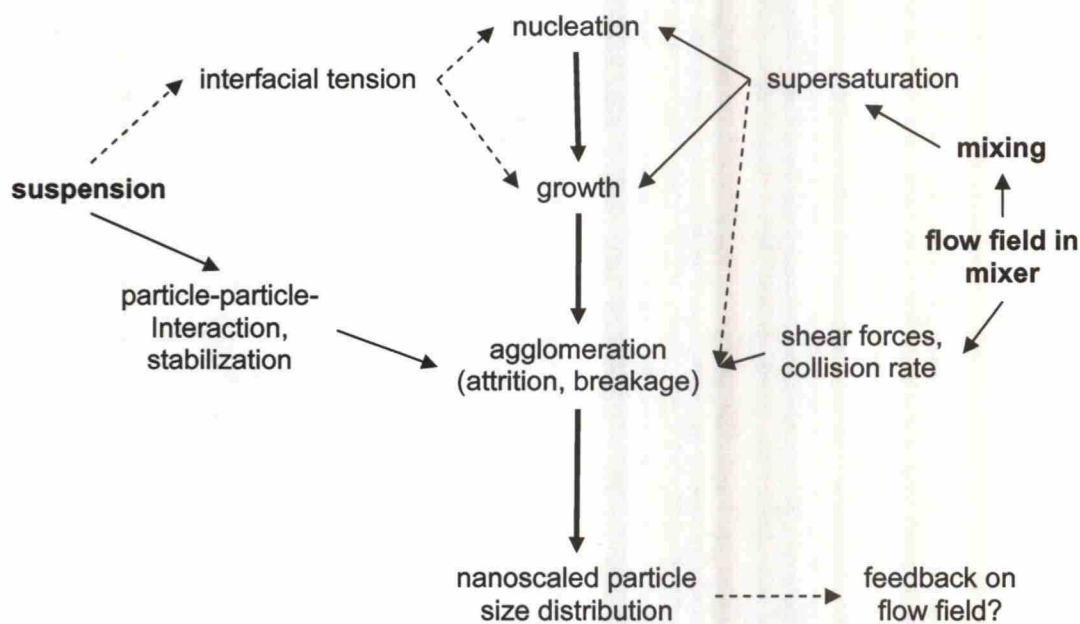


Figure 77. Schematic drawing of a cascade reactor

### 22.3 Ideas for Further Research

The design of the optimal reactor is a difficult task. A simulation model should be developed for theoretical testing of the different ideas before going to practical experiments. For this, kinetic models of particle growth, aggregation and breakage should be developed and combined with Computer Fluid Dynamics (CFD) models of reactor hydrodynamics. Figure 78 shows the different parameters that affect precipitation and particle size distribution. The Segregated Feed Model (SFM) used by Zauner and Jones (2000a) could be a good approach to modeling the precipitation of silica particles. It requires experimental data of particle growth, aggregation, and breakage kinetics that have to be measured in laboratory-scale experiments and combined with population balance and hydrodynamic models. This data, in combination with the simulation model, can then be used for scale-up purposes, according to the methodology shown in Figure 79.

Zauner and Jones (2000b) have developed a methodology to obtain kinetic data in a calcium oxalate system. This could be a good starting point for kinetic measurements in silica systems. Aggregation kinetics for silica has already been determined for aggregation in silica sols (Schaer *et al.* 2001). Some kinetic studies for silica crystallization have been performed by Tavaré and Garside (1993), but these are not sufficient for this purpose.



**Figure 78. Precipitation mechanisms and influencing parameters on particle size distribution (Schwarzer and Peukert 2002)**



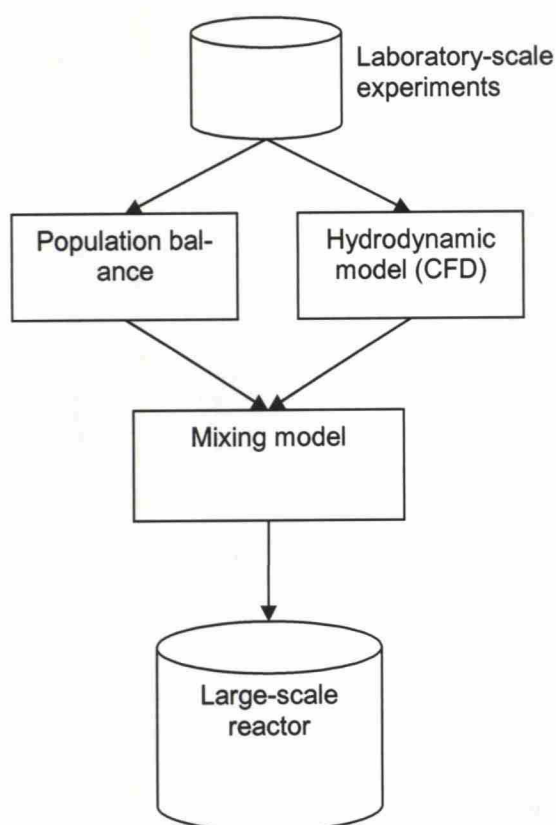


Figure 79. Precipitation process scale-up methodology (Zauner and Jones 2000a)

## 23 Conclusions

The aim of this thesis was to evaluate different possibilities for the production of silica nanoparticles. In the Literature Review Part, most important aspects of silica chemistry and the state-of-the-art production of different silica products are covered. Based on the literature, three processes were chosen for experimental investigations: The Sol-via-Acid-Neutralization Process, the Precipitation Process and the Coagulant Process.

The Precipitation Process proved to be the most promising approach because of its simplicity. In the Precipitation Process, primary particle size can be easily controlled by varying the silica concentration during the reaction stage. However, those particles tend to aggregate very eagerly, and preventing the aggregation of particles in the process is a big challenge that requires further experimental work and innovative reactor design. The state-of-the-art approach is the use of a bead mill or a comparable device after the reaction stage for disaggregating the aggregates. In recent years, bead mills that are capable to handle extremely fine beads have been developed, making milling even down to primary particle size possible.

Based on these facts, a pilot process that features a stirred tank reactor and a bead mill was designed for first tests. The process is operated in batch mode. As an alternative to the bead mill, a high-shear mixer can be used which also lowers the costs significantly. In this case, however, a complete disaggregation of the particles may not be expected. It is explicitly stated that test runs with different equipment must be performed in cooperation with the manufacturers before a purchase decision is made.

Based on the pilot process, an industrial process using the same principle was designed to obtain an estimate for the production costs in an industrial environment. The production costs were estimated at 1.17 €/kg 100 % SiO<sub>2</sub>, which is a competitive price compared to similar silica products. The main cost element is the raw materials, and especially water glass, which accounts for more than 80 % of the production costs.

For the process to be really competitive, innovative reactor design is required. Instead of a batch stirred tank reactor, a continuous reactor has to be designed in such a way that aggregation can be kept under control already during the reaction stage. This can be done either using high shear or additives that affect the surface charge of the particles.

As a suggestion for further research, kinetic parameters for silica particle growth, aggregation, and breakage of aggregates should be measured in laboratory experiments and combined with population balance and CFD models to test and simulate different reactor concepts. This data can then be used for scale-up to industrial scale.

## References

- Acker, E.G. and Winyall, M.E., Method of Preparing Loosely Aggregated 200-500 Millimicron Silica, *U.S. Pat. 4,049,781*, September 20, 1977.
- Alexander, G.B., Iler, R.K., and Wolter, F.J., Process for Producing Built-Up Silica Particles, *U.S. Pat. 2,601,235*, June 24, 1952.
- Anon., Prices & People, *Chemical Market Reporter* **267** (2005) no. 12 p. 16.
- Baker, C.L. and Frankle, J., Finely Divided Silica Product and its Method of Preparation, *U.S. Pat. 3,208,823*, September 28, 1965.
- Behälter KG Bremen, <http://www.behaelter-kg.com/>, 2007, visited July 30, 2007.
- Bergna, H.E. The Language of Colloid Science and Silica Chemistry. In *Colloid Silica*, edited by Bergna, H.E. and Roberts, W.O., CRC Press Taylor & Francis Group, Boca Raton FL, 2006, p. 5-7.
- Brekau, U., Block, H.-D., Moretto, H.-H., Schmidt, P., Schober, P., and Ludovici, W., Continuous Preparation of Silica Sols which Contain Large Particles, *U.S. Pat. 5,964,693*, October 12, 1999.
- Brinker, C.J. Sol-Gel Processing of Silica. In *The Colloid Chemistry of Silica*, edited by Bergna, H.E., American Chemical Society, Washington, DC, 1994, p. 361-402.
- Eka Chemicals, [www.colloidalsilica.com](http://www.colloidalsilica.com), 2002, visited May 3, 2007.
- Flörke, O.W., Graetsch, H., Brunk, F., Benda, L., Paschen, S., Bergna, H.E., Roberts, W.O., Welsch, W.A., Chapman, D.M., Ettlinger, M., Kerner, D., Maier, M., Meon, W., Schmoll, R., Gies, H., and Schiffmann, D. Silica. In *Ullmann's Encyclopedia of Industrial Chemistry*, Wiley-VCH Verlagsgesellschaft, Weinheim, 2005.
- Gellermann, C., Ballweg, T., and Wolter, H., Herstellung von funktionalisierten oxidischen Nano- und Mikropartikeln und deren Verwendung, *Chemie Ingenieur Technik* **79** (2007) 233-240.
- Ghosh, N.N. and Pramanik, P., Synthesis of Nano-Sized Ceramic Powders Using Precipitated Silica in Aqueous Sol-Gel method, *Nanostructured Materials* **8** (1997) 1041-1045.



Gradl, J., Schwarzer, H.-C., Schwertfirm, F., Manhart, M., and Peukert, W., Precipitation of nanoparticles in a T-mixer: Coupling the particle population dynamics with hydrodynamics through direct numerical simulation, *Chemical Engineering and Processing* **45** (2006) 908-916.

Hench, L.L. and West, J.K., The Sol-Gel Process, *Chemical Reviews* **90** (1990) 33-72.

Hüter, L. and Steenken, G., Verfahren zur Herstellung feinteiliger, aktiver Kieselsäure, *German Pat. 1,192,162*, February 21, 1962.

Iler, R.K., Solids Coated With Estersil, *U.S. Pat. 2,733,160*, January 31, 1956.

Iler, R.K., Microporous Membrane Process for Making Concentrated Silica Sols, *U.S. Pat. 3,969,266*, July 13, 1976.

Iler, R.K., *The Chemistry of Silica*, John Wiley & Sons, New York, 1979.

Jesionowski, T., Preparation of colloidal silica from sodium metasilicate solution and sulphuric acid in emulsion medium, *Colloids and Surfaces A: Physicochemical and Engineering Aspects* **190** (2001) 153-165.

Jesionowski, T., Characterization of silicas precipitated from solution of sodium metasilicate and hydrochloric acid in emulsion medium, *Powder Technology* **127** (2002a) 56-65.

Jesionowski, T., Effect of surfactants on the size and morphology of the silica particles prepared by an emulsion technique, *Journal of Materials Science* **37** (2002b) 5275-5281.

Judat, B., Racina, A., and Kind, M., Macro- and Micromixing in a Taylor-Couette Reactor with Axial Flow and their Influence on the Precipitation of Barium Sulfate, *Chemical Engineering & Technology* **27** (2004) 287-292.

Khan, S.A., Günther, A., Schmidt, M.A., and Jensen, K.F., Microfluidic Synthesis of Colloidal Silica, *Langmuir* **20** (2004) 8604-8611.

Klein, R.C., How to use immersion heaters in chemical process applications, *PlantServices.com*, 2006,

<http://www.plantservices.com/articles/2006/292.html?page=1>, visited July 10, 2007.

Koepenick, M., Paper innovation ramps up with nano-chemistry, *Pulp & Paper Canada* **102:1** (2001) III 17-21.

Kolb, G. and Scherer, G., *Superfine grinding in agitator mills*, Netzsch Feinmahltechnik GmbH, 2002.

Kwade, A. and Schwedes, J., Breaking characteristics of different materials and their effect on stress intensity and stress number in stirred media mills, *Powder Technology* **122** (2002) 109-121.

Lee, G.L., Kim, H.S., Park, S.S., Moon, B.Y., Kang, S.P., and Park, H.C., Synthesis of Nanosized Silica Powder by Ultrasonic Process, *Advanced Materials Research* **11-12** (2006) 669-672.

Lerner, I., Rhodia's Siloa Offers a Third Way for Silica, *Chemical Market Reporter* **265** (2004) no. 15 p. 10.

Machunsky, S. and Peuker, U.A., Designstudie eines kontinuierlichen Ultraschall-Fällungsreaktors, *Chemie Ingenieur Technik* **79** (2007) 251-256.

Maloney, T., Nanotechnology for a Mass Production Industry, presentation given at *FinNano annual seminar*, March 28, 2007.

Malvern Instruments, *Zetasizer Nano Series User Manual*, Malvern Instruments Ltd., Worcestershire, 2005.

Marchisio, D.L., Barresi, A.A., and Fox, R.O., Simulation of Turbulent Precipitation in a Semi-batch Taylor-Couette Reactor Using CFD, *AIChE Journal* **47** (2001) 664-676.

Matijević, E. Science and Art of the Formation of Uniform Solid Particles. In *Colloid Silica*, edited by Bergna, H.E. and Roberts, W.O., CRC Press Taylor & Francis Group, Boca Raton FL, 2006, p. 43-46.

McLaughlin, J.R., Bead Size and Mill Efficiency, *Ceramic Industry* **149** (1999) no. 13 34-40.

Mende, S., Stenger, F., Peukert, W., and Schwedes, J., Mechanical production and stabilization of submicron particles in stirred media mills, *Powder Technology* **132** (2003) 64-73.

Mende, S., Kolb, G., and Enderle, U., Nanoparticle Grinding and Dispersing, *Ceramic Industry* **156** (2006) no. 8 18-20.

Moyer, P.S., Process for Making Finely Divided Silica, *U.S. Pat. 2,386,337*, October 9, 1945.

Nalco Chemical Company, Continuous Method for Making Silica Sols (1963), *Brit. Pat. 1,071,060*, December 20, 1963.

National Nanotechnology Initiative, What is Nanotechnology?, <http://www.nano.gov/html/facts/whatIsNano.html>, visited August 3, 2007.

Netzsch-Feinmahltechnik GmbH, *Zeta RS marketing material*, 2005.

Netzsch-Feinmahltechnik GmbH, Netzsch Mahlen und Dispergieren, 2006, <http://www.netzsch-feinmahltechnik.de>, visited June 14, 2007.

Peters, M.S., Timmerhaus, K.D. and West, R.E., *Plant Design and Economics for Chemical Engineers*, 5<sup>th</sup> edition, McGraw-Hill, New York, 2003.

Pitt, M., Chemicals Cost Guide 2002, <http://ed.icheme.org/costchem.html>, visited July 12, 2007.

Pohl, M. and Schubert, H., Untersuchungen zum Dispergierverhalten nanoskaliger Pulver, *Chemie Ingenieur Technik* **75** (2003) 1111-1112.

Pohl, M., Hokekamp, S., Hofmann, N.Q., and Schuchmann, H.P., Dispergieren und Desagglomerieren von Nanopartikeln mit Ultraschall, *Chemie Ingenieur Technik* **76** (2004) 392-396.

Roberts, W.O. Manufacturing and Applications of Water-Borne Colloidal Silica. In *Colloid Silica*, edited by Bergna, H.E. and Roberts, W.O., CRC Press Taylor & Francis Group, Boca Raton FL, 2006, p. 131-175.

Rousseaux, J.-M., Falk, L., Muhr, H., and Plasari, E., Micromixing Efficiency of a Novel Sliding-Surface Mixing Device, *AIChE Journal* **45** (1999) 2203-2213.

Schaer, E., Ravetti, R., and Plasari, E., Study of silica particle aggregation in a batch agitated vessel, *Chemical Engineering and Processing* **40** (2001) 277-293.

Scherer, G.W. Sol-Gel Technology. In *The Colloid Chemistry of Silica*, edited by Bergna, H.E., American Chemical Society, Washington, DC, 1994, p. 51-66.



Schlomach, J. and Kind, M., Simulation der Aggregatstruktur bei der Fällung schwerlöslicher Substanzen, *Chemie Ingenieur Technik* **76** (2004a) 1695-1699.

Schlomach, J. and Kind, M., Investigations on the semi-batch precipitation of silica, *Journal of Colloid and Interface Science* **277** (2004b) 316-326.

Schlomach, J., Quarch, K., and Kind, M., Investigation of Precipitation of Calcium Carbonate at High Supersaturations, *Chemical Engineering & Technology* **29** (2006) 215-220.

Schwarzer, H.-C. and Peukert, W., Experimental Investigation into the Influence of Mixing on Nanoparticle Precipitation, *Chemical Engineering & Technology* **25** (2002) 657-661.

Schwarzer, H.-C. and Peukert, W., Combined Experimental/Numerical Study on the Precipitation of Nanoparticles, *AIChE Journal* **50** (2004) 3234-3247.

Schwarzer, H.-C. and Peukert, W., Prediction of aggregation kinetics based on surface properties of nanoparticles, *Chemical Engineering Science* **60** (2005) 11-25.

Schwarzer, H.-C., Schwertfirm, F., Manhart, M., Schmid, H.-J., and Peukert, W., Predictive simulation of nanoparticle precipitation based on the population balance equation, *Chemical Engineering Science* **61** (2006) 167-181.

Shelley, S., Taking High-Shear Mixing to the Next Level, *Chemical Engineering* **111** (2004) no. 4 24-26.

Shelley, S. (editor), High-Shear Mixing Don't Fall Victim to Common Misconceptions, *Chemical Engineering* **112** (2005) no. 4 46-51.

Siliconfareast.com, Properties of  $\text{SiO}_2$  and  $\text{Si}_3\text{N}_4$  at 300 K, 2004, <http://www.siliconfareast.com/sio2si3n4.htm>, visited March 22, 2007.

Silverson Machines, Inc., marketing information, <http://www.silverson.com>, visited June 29, 2007.

Silverson Machines, Inc. Application Report Chemicals, Preparation of Paper Coatings, 2003, available at <http://www.silverson.com/UK/Products/AppReports-Chemical.cfm#>.

Silverson Machines, Inc. Application Report Chemicals, Dispersion of Fumed Silica, 2005, available at <http://www.silverson.com/UK/Products/AppReports-Chemical.cfm#>.

Sinnott, R.K., *Coulson & Richardson's Chemical Engineering*, Volume 6, 3<sup>rd</sup> edition, Butterworth-Heinemann, Oxford, 1999.

Société Française des Silicates Spéciaux Sifrance, Production of Precipitated Silica, *Brit. Pat. 1,382,340*, April 28, 1972.

Sommer, K., 40 Jahre Darstellung von Partikelgrößenverteilungen – und immer noch falsch?, *Chemie Ingenieur Technik* **72** (2000) 809-812.

Smoluchowski, M., Versuch einer mathematischen Theorie der Koagulationskinetik kolloider Lösungen, *Zeitschrift für physikalische Chemie* **92** (1917) 129-168.

Tamenori, H., Hattori, A., and Yoshiyagawa, M., Process for Producing Silica in Fine Powder Form, *U.S. Pat. 4,678,652*, July 7, 1987.

Tavare, N.S. and Garside, J., Silica precipitation in a semi-batch crystallizer, *Chemical Engineering Science* **48** (1993) 475-488.

Thornhill, F.S. and Allen, E.M., Verfahren zur Herstellung feinteiliger Kieselsäure, *German Pat. 1,131,196*, March 1, 1955.

Tilton, J.N. Fluid and Particle Dynamics. In *Perry's Chemical Engineer's Handbook*, 7<sup>th</sup> edition, edited by Perry, R.H., Green, D.W. and Maloney, J.O., McGraw-Hill, Singapore, 1998.

Tsai, M.-S., The study of formation colloidal silica via sodium silicate, *Material Science and Engineering B* **106** (2004) 52-55.

Tsai, M.-S., Huang, P.-Y., and Wu, W.-C., The study of formation process of colloidal silica, *Materials Research Bulletin* **40** (2005a) 1609-1616.

Tsai, M.-S., Yang, C.-H., and Huang, P.-Y., Effects of seeds concentration on the formation of colloidal silica, *Material Science and Engineering B* **123** (2005b) 238-241.

Vogel, G.H. *Process Development*, Wiley-VCH Verlag GmbH & Co., Weinheim, 2005.

Walas, S.M. *Chemical Process Equipment – Selection and Design*, Butterworth-Heinemann, Newton, MA, 1990.

Way, H., Nanoparticles: Mild Dispersion, *Chemical Engineering* **114** (2007) no. 7 44-48.

Weldes, H.H., Boyle, F.A., and Bobb, J.S.S., Continuous Process for Making Silica Sols, *U.S. Pat. 3,440,175*, April 22, 1969.

Yoshida, A. Silica Nucleation, Polymerization, and Growth Preparation of Monodispersed Sols. In *The Colloid Chemistry of Silica*, edited by Bergna, H.E., American Chemical Society, Washington, DC, 1994, p. 51-66. Also in *Colloid Silica*, edited by Bergna, H.E. and Roberts, W.O., CRC Press Taylor & Francis Group, Boca Raton, FL, 2006, p. 47-56.

Zauner, R. and Jones, A.G., Scale-up of Continuous and Semibatch Precipitation Processes, *Industrial & Engineering Chemistry Research* **39** (2000a) 2392-2403.

Zauner, R. and Jones, A.G., Determination of nucleation, growth, agglomeration and disruption kinetics from experimental precipitation data: the calcium oxalate system, *Chemical Engineering Science* **55** (2000b) 4219-4232.



## Lists of experiments

Table A.1. Acid neutralization experiments

Experiment Number	Date (month/day/year)	Reactants / g		Acid addition time / min : sec	Temperature / °C	Stirrer speed / rpm	Result	Notes	Product pH
		Water	Water glass solution (28 wt-% SiO <sub>2</sub> )						
A1	4/30/2007	100.6	100.1	N/A	N/A	400	N/A	neutralization experiment	
A2	4/30/2007	1000.6	80.5	instantly	80	400	gel	fast acid addition	
A3	4/30/2007	1000.7	82.1	1:23	80	400	gel	fast acid addition	
A4	5/2/2007	999.6	80.8	1:05	82	400	stable sol		10.1
A5	5/2/2007	999.7	100.0	1:20	82	400	stable sol		10.0
A6	5/2/2007	1002.5	120.6	1:37	80-82	400	stable sol		10.0
A7	5/2/2007	998.6	145.9	1:56	82	400	rapid gelling		10.1
A8	5/4/2007	999.9	100.8	7:36	80-83	400	stable sol	slow feed	10.2
A9	5/4/2007	999.9	100.8	9:10	80-84	400	stable sol	slow feed	9.3

Table A.2. Precipitation experiments

Experiment set: Precipitation										
Number	Date (month/day /year)	Reactants / g		Sulfuric acid solution (20 wt-%)	Acid addition time / min : sec	Tempera- ture/ °C	Stirrer speed* / rpm	Result	Notes	Product pH
		Water	Water glass solution (28 wt-% SiO <sub>2</sub> )							
B1	5/11/2007	1000.1	141.0	80.5	12:37	80-85	400-650-800	gel-like precipitate		10.2
B2	5/15/2007	1000.1	142.7	79.9	12:40	80-85	400-1300	gel-like precipitate	total reaction time 25 min	9.8
B3	5/14/2007	1000.5	201.1	117.2	18:30	80-85	400-800	powder-like precipitate	total reaction time 30 min	9.5
B4	5/14/2007	699.6	301.7	160.0	25:30	80-85	400-1300	powder-like precipitate	total reaction time 30 min	9.9
B5	5/18/2007	501.0	285.6	159.7	30:00	80-85	400-1300	powder-like precipitate	total reaction time 35 min	9.4
B6	6/19/2007	501.1	298.9	170.5	46:22	80-85	400-1050	powder-like precipitate		8.9
B7	5/31/2007	401.7	406.9	230.0	42:23	80-85	400-1050	powder-like precipitate		8.7
B8	5/22/2007	702.1	285.7	120.0	N/A	80-85	1300	rigid gel		N/A
*Stirrer speed was increased when the gel point was approached										

\*Stirrer speed was increased when the gel point was approached

Table A.3. Coagulant experiments

Experiment set: Coagulation													
Number	Date (month/day /year)	Reactants / g						Temperature / °C	Stirrer speed / rpm	Result	Notes	Product pH	
		Water	Water glass solution	Sulfuric acid solution	Coagulant	Type	Add. Water*						
C1	5/21/2007	201.1	100.6	N/A	56.4	NaCl	65.5	room	N/A (mag- netic stirrer)	gel	solution gelled upon salt addition	N/A	
C2	5/21/2007	230.0	65.8	115.5	31.0	NaCl	79.8	room	N/A (mag- netic stirrer)	gel	solution gelled upon acid addition, 48 % acid	N/A	
C3	5/21/2007	700.7	69.7	N/A	32.1	NaCl	161.2	50	400	clear solution	instant acid addi- tion until pH about 1	1	
C4	5/21/2007	699.7	70.9	60.0	59.6	NaCl	376.6	50	1000	slightly turbid solution	instant acid addi- tion	1.6	
C5	5/23/2007	700.1	71.1	56.8	56.3	NaCl	193.3	45-55	1000	slightly turbid solution	instant acid addi- tion	1.8	
C6	5/22/2007	699.3	70.4	59.7	58.9	NaCl	225.9	45-50	1000	fine, powder- like precipitate	slow acid addition	1.5	
C7	5/25/2007	701.3	71.7	60.6	69.6	Na <sub>2</sub> SO <sub>4</sub>	212.6	50	1000	clear solution		2.6	
C8	5/25/2007	703.2	69.9	83.0	131.6	Na <sub>2</sub> SO <sub>4</sub>	409.7	45-50	1000	clear solution		N/A	

\*Water that the coagulant was dissolved in before adding to the water glass solution



Table A.4. Other experiments

Experiment set: Precipitation										
Number	Date (month/day /year)	Reactants / g			Acid addition time / min : sec	Tempera- ture/ °C	Stirrer speed* / rpm	Result	Notes	Product pH
		Water	Water glass solution	Sulfuric acid solution						
D1	5/30/2007	999.5	140.9	110.2	14:00	80	400-1300	smooth, paste-like gel	acid and water glass addition in two stages, in between dispersion with mixer	1.3
D2	5/30/2007	1000.4	139.9	79.1	14:56	80	400-1300	slightly turbid solution	after addition of 79.1 g acid slowly addition of 40 g of acid quickly	2
D3	6/1/2007	40.0	63.2	207.3	11	80	N/A (magnetic stirrer)	gel	rapid gelling (impurities)	N/A
D4	6/1/2007	40.9	59.8	200.2	6	70-80	N/A (magnetic stirrer)	gel	slow gelling	1.3

Table B.1. Details for experiments A4-A9

Experiment	A4	A5	A6	A7	A8	A9
<b>Batch</b>						
Water / g	996.6	999.7	1002.5	998.6	999.9	999.9
Water glass solution / g	80.8	100	120.6	145.9	100.8	100.8
SiO <sub>2</sub> / g	22.6	28.0	33.8	40.9	28.2	28.2
Na <sub>2</sub> O / g	7.1	8.8	10.6	12.8	8.8	8.8
Total SiO <sub>2</sub> (by mass)	2.1 %	2.5 %	3.0 %	3.6 %	2.6 %	2.6 %
Total Na <sub>2</sub> O (by mass)	0.7 %	0.8 %	0.9 %	1.1 %	0.8 %	0.8 %
SiO <sub>2</sub> / mol	0.376	0.466	0.562	0.680	0.470	0.470
Na <sub>2</sub> O / mol	0.114	0.141	0.170	0.206	0.142	0.142
<b>Sulfuric acid addition</b>						
Solution / g	39.9	49.9	60	71.6	49.9	60.2
H <sub>2</sub> SO <sub>4</sub> / g	7.98	9.98	12	14.32	9.98	12.04
H <sub>2</sub> SO <sub>4</sub> / mol	0.081	0.102	0.122	0.146	0.102	0.123
reaction time/s	65	80	97	116	456	550
H <sub>2</sub> SO <sub>4</sub> addition rate / g/s	0.12	0.12	0.12	0.12	0.02	0.02
Proportion neutralized	71 %	72 %	72 %	71 %	72 %	86 %
<b>Measurements</b>						
Number peak	6.82	8.62	11.9	N/A	7.29	12.2
Intensity peak	14.2	33.1	70.8	N/A	16.3	40.7
Final pH	10.1	10.0	10.0	10.1	10.2	9.3
<b>Calculated</b>						
Free SiO <sub>2</sub> / mol	0.27	0.34	0.40	0.48	0.34	0.41
Free SiO <sub>2</sub> / g	16.14	20.18	24.27	28.96	20.18	24.35
Free SiO <sub>2</sub> concentration (by mass)	1.4 %	1.8 %	2.1 %	2.4 %	1.8 %	2.1 %
Na <sub>2</sub> SO <sub>4</sub> / mol	0.08	0.10	0.12	0.15	0.10	0.12
Na <sub>2</sub> SO <sub>4</sub> / g	11.56	14.45	17.38	20.74	14.45	17.44
Na <sub>2</sub> SO <sub>4</sub> concentration (by mass)	1.0 %	1.3 %	1.5 %	1.7 %	1.3 %	1.5 %
approx. batch volume / ml	1197	1223	1249	1272	1224	1233
total SiO <sub>2</sub> / g/ml	0.02	0.02	0.03	0.03	0.02	0.02
total SiO <sub>2</sub> / g/100 ml	1.89	2.29	2.70	3.21	2.31	2.29
free SiO <sub>2</sub> / g/ml	0.01	0.02	0.02	0.02	0.02	0.02
free SiO <sub>2</sub> / g/100 ml	1.35	1.65	1.94	2.28	1.65	1.97
Na-norm/total	0.19	0.23	0.27	0.32	0.23	0.23
Na-norm/free	0.13	0.17	0.19	0.23	0.16	0.20
Critical Na-normality from Iler's formula	0.18	0.18	0.18	0.18	0.18	0.18

Table C.1. Details for experiments B2-B7

Experiment	B2	B3	B4	B5	B6	B7
<b>Batch</b>						
Water / g	1000.1	1000.5	699.6	501.0	501.1	401.7
Water glass solution / g	142.7	201.1	301.7	285.6	298.9	406.9
SiO <sub>2</sub> / g	40.0	56.3	84.5	80.0	83.7	112.0
SiO <sub>2</sub> / mol	0.665	0.937	1.41	1.33	1.39	1.86
Na <sub>2</sub> O / mol	0.201	0.284	0.426	0.403	0.422	0.565
Na <sub>2</sub> O / g	12.5	17.6	26.4	25.0	26.2	35.0
SiO <sub>2</sub> conc. (by mass)	3.3 %	4.3 %	7.3 %	8.5 %	8.6 %	10.9 %
<b>Sulfuric acid addition</b>						
Solution / g	79.9	117.2	160.0	159.7	170.5	230.0
H <sub>2</sub> SO <sub>4</sub> / g	16.0	23.4	32.0	31.9	34.1	46.0
H <sub>2</sub> SO <sub>4</sub> / mol	0.16	0.24	0.33	0.33	0.35	0.47
reaction time / s	760	1110	1530	1800	2782	2543
H <sub>2</sub> SO <sub>4</sub> addition rate / g/s	0.02	0.02	0.02	0.02	0.01	0.02
Proportion neutralized	80.9 %	84.2 %	76.6 %	80.8 %	82.4 %	83.1 %
<b>Calculations</b>						
free silica / g	32.3	47.4	64.7	64.6	69.0	93.0
Na <sub>2</sub> SO <sub>4</sub> / mol	0.163	0.239	0.326	0.326	0.348	0.469
Na <sub>2</sub> SO <sub>4</sub> / g	23.1	33.9	46.3	46.3	49.4	66.6
Na <sub>2</sub> SO <sub>4</sub> / wt-%	1.9 %	2.6 %	4.0 %	4.9 %	5.09 %	6.5 %
Approx. batch volume / ml	1223	1319	1161	946	971	1030
<b>Measurements</b>						
Stirrer speed/rpm	1300	800	1300	1300	1050	1050
Final pH	9.8	9.5	9.9	9.4	8.9	8.7
Characterization	gel-like precipitate	white, powder-like precipitate	white, powder-like precipitate	white, powder-like precipitate	white, powder-like precipitate	white, powder-like precipitate
Primary particle size / nm	10.5	18.4	32.5	N/A	34.5	50
Free silica conc. (by mass)	2.6 %	3.6 %	5.6 %	6.8 %	7.1 %	9.0 %



## Appendix D

Table D.1. Details for experiments C1-C6 with NaCl as coagulant

Experiment	C1	C2	C3	C4	C5	C6
Water / g	201.1	230.0	700.7	699.7	700.1	699.3
Water glass / g	100.6	65.8	69.7	70.9	71.1	70.4
SiO <sub>2</sub> / g	28.2	18.4	19.5	19.9	19.9	19.7
NaCl / g	56.4	31.0	32.1	59.6	56.3	58.9
Additional water / g	65.5	79.8	161.2	376.6	193.3	225.9
NaCl conc. (by mass)	13.3 %	7.6 %	3.3 %	4.9 %	5.5 %	5.6%
SiO <sub>2</sub> conc. (by mass)	6.7%	4.5 %	2.0 %	1.7%	2.0	1.9%
Characterization	wax-like precipitate upon salt addition	rigid gel	clear liquid	slightly turbid liquid	slightly turbid liquid	white precipitate
Temperature	20	20	50	50	50	50
Approx. batch vol. / l	0.35	0.36	0.92	1.13	0.95	0.98
NaCl conc. / g/l	162	86	35	53	59	60

Table D.2. Details for experiments C7 and C8 with Na<sub>2</sub>SO<sub>4</sub> as coagulant

Experiment	C7	C8
Water / g	701.3	703.2
Water glass / g	71.7	69.9
SiO <sub>2</sub> / g	20.076	19.572
Na <sub>2</sub> SO <sub>4</sub> / g	69.6	131.6
Additional water / g	212.6	409.7
Na <sub>2</sub> SO <sub>4</sub>	6.6 %	10.0 %
SiO <sub>2</sub> conc. (by mass)	1.9 %	1.5%
Characterization	clear liquid	clear liquid
Temperature	50	50
Approx. batch vol. / l	0.97	1.17
Na <sub>2</sub> SO <sub>4</sub> conc. / g/l	72	113

Table E.1. Details for experiment D1

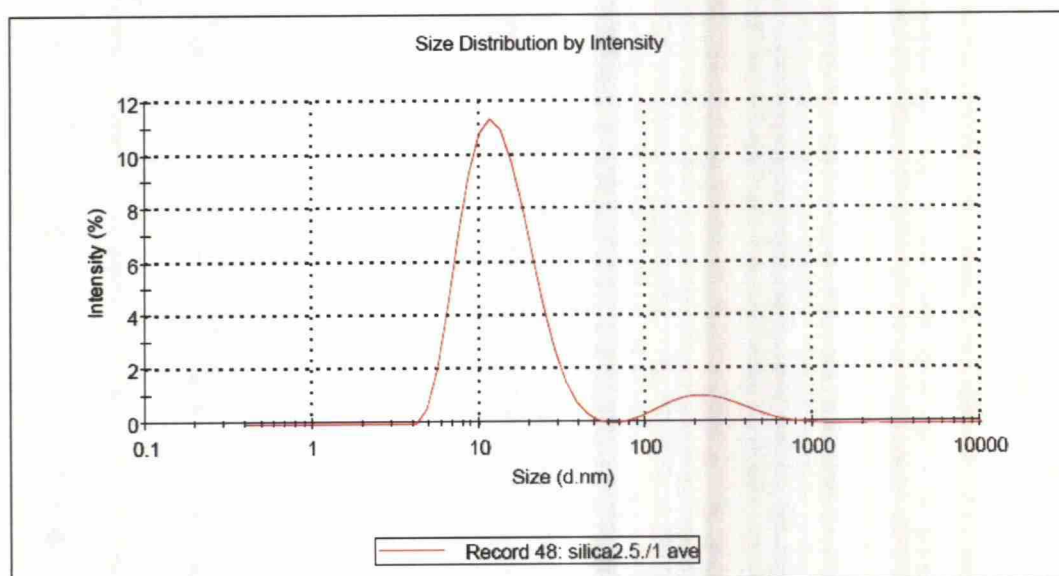
Experiment	D1
<b>Initial batch</b>	
Water / g	995.5
Water glass solution / g	140.9
SiO <sub>2</sub> / g	39.5
SiO <sub>2</sub> / mol	0.656
Na <sub>2</sub> O / mol	0.199
Na <sub>2</sub> O / g	12.3
SiO <sub>2</sub> conc. (by mass)	3.5 %
<b>Sulfuric acid addition (first stage)</b>	
Solution / g	80.2
H <sub>2</sub> SO <sub>4</sub> / g	16.04
H <sub>2</sub> SO <sub>4</sub> / mol	0.164
Proportion neutralized	82 %
<b>Water glass addition</b>	
Additional water glass solution / g	54.8
Additional SiO <sub>2</sub> / g	15.3
Additional SiO <sub>2</sub> / mol	0.255
Additional Na <sub>2</sub> O / mol	0.077
Additional Na <sub>2</sub> O / g	4.8
Total SiO <sub>2</sub> conc. (by mass)	4.6 %
<b>Sulfuric acid addition (second stage)</b>	
Solution / g	30
H <sub>2</sub> SO <sub>4</sub> / g	6
H <sub>2</sub> SO <sub>4</sub> / mol	0.061
Total proportion neutralized	81 %

The initial batch was heated to a reaction temperature of about 80 °C and then the first stage of sulfuric acid addition was performed. Then, the reaction mixture was stirred with a high-speed kitchen mixer and additional water glass was added to the batch. The second stage of acid addition was performed using the regular stirrer. The result was a smooth, paste-like gel completely different from the gels obtained in other experiments.

## Sample A4

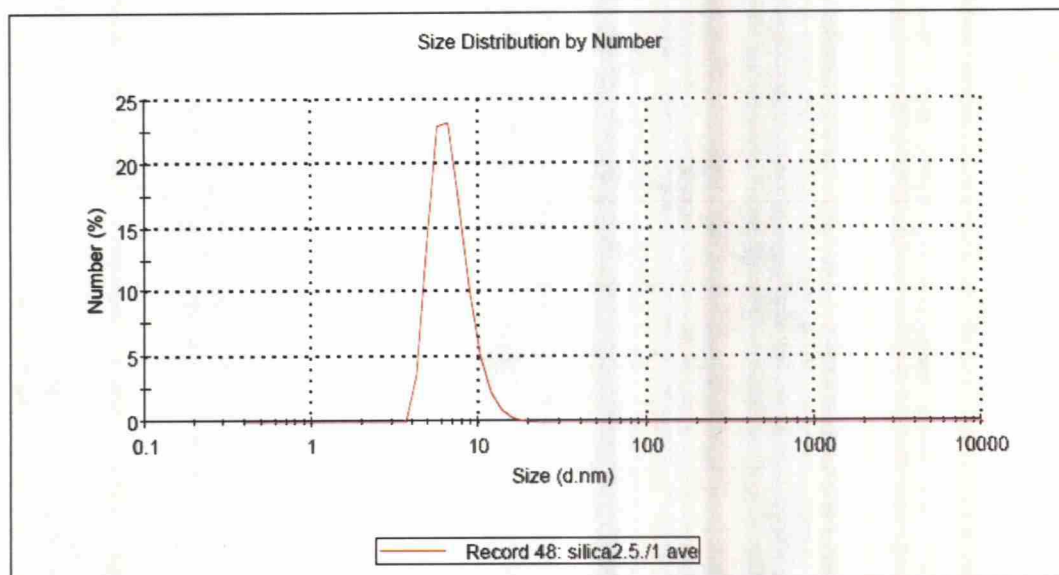
## Results

	Diam. (nm)	% Intensity	Width (nm)
<b>Z-Average (d.nm):</b> 13.1	<b>Peak 1:</b> 14.2	90.4	6.89
<b>Pdl:</b> 0.266	<b>Peak 2:</b> 258	9.6	144
<b>Intercept:</b> 0.947	<b>Peak 3:</b> 0.00	0.0	0.00



## Results

	Diam. (nm)	% Number	Width (nm)
<b>Z-Average (d.nm):</b> 13.1	<b>Peak 1:</b> 6.82	100.0	1.94
<b>Pdl:</b> 0.266	<b>Peak 2:</b> 0.00	0.0	0.00
<b>Intercept:</b> 0.947	<b>Peak 3:</b> 0.00	0.0	0.00

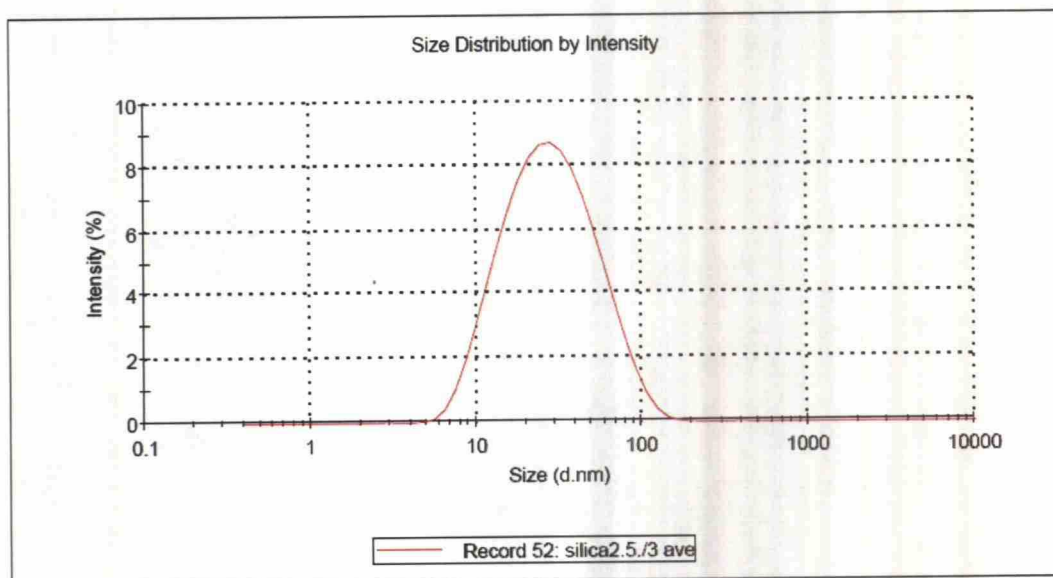




## Sample A5

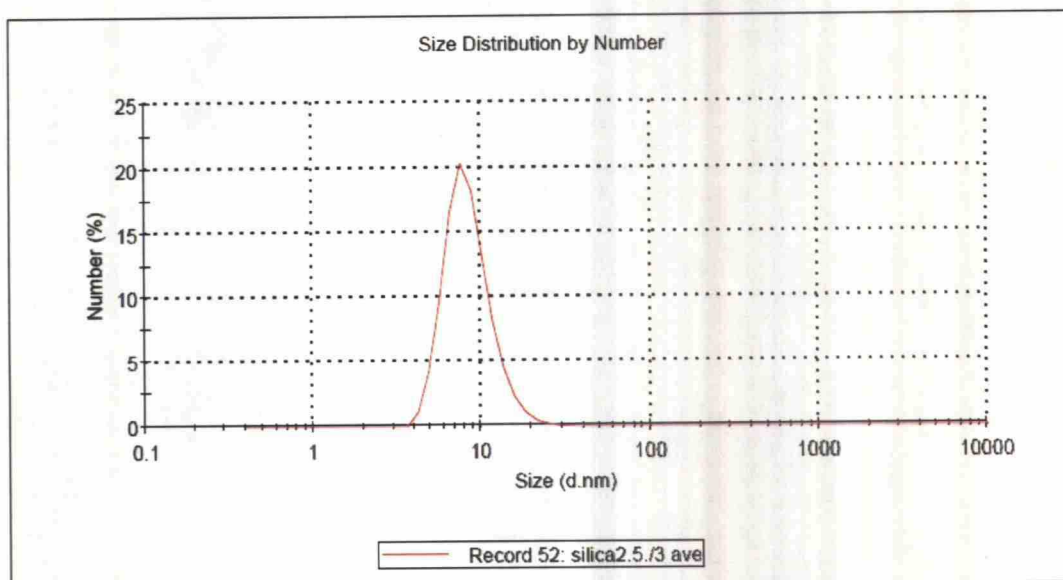
## Results

	Diam. (nm)	% Intensity	Width (nm)
<b>Z-Average (d.nm): 23.6</b>	<b>Peak 1: 33.1</b>	100.0	21.4
<b>Pdl: 0.239</b>	<b>Peak 2: 0.00</b>	0.0	0.00
<b>Intercept: 0.953</b>	<b>Peak 3: 0.00</b>	0.0	0.00



## Results

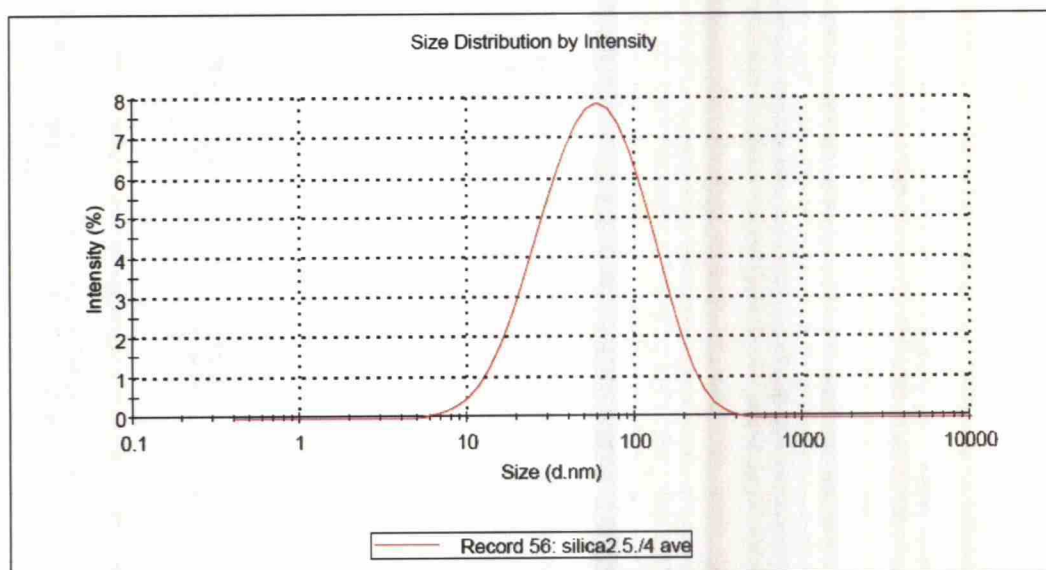
	Diam. (nm)	% Number	Width (nm)
<b>Z-Average (d.nm): 23.6</b>	<b>Peak 1: 8.62</b>	100.0	3.02
<b>Pdl: 0.239</b>	<b>Peak 2: 0.00</b>	0.0	0.00
<b>Intercept: 0.953</b>	<b>Peak 3: 0.00</b>	0.0	0.00



## Sample A6

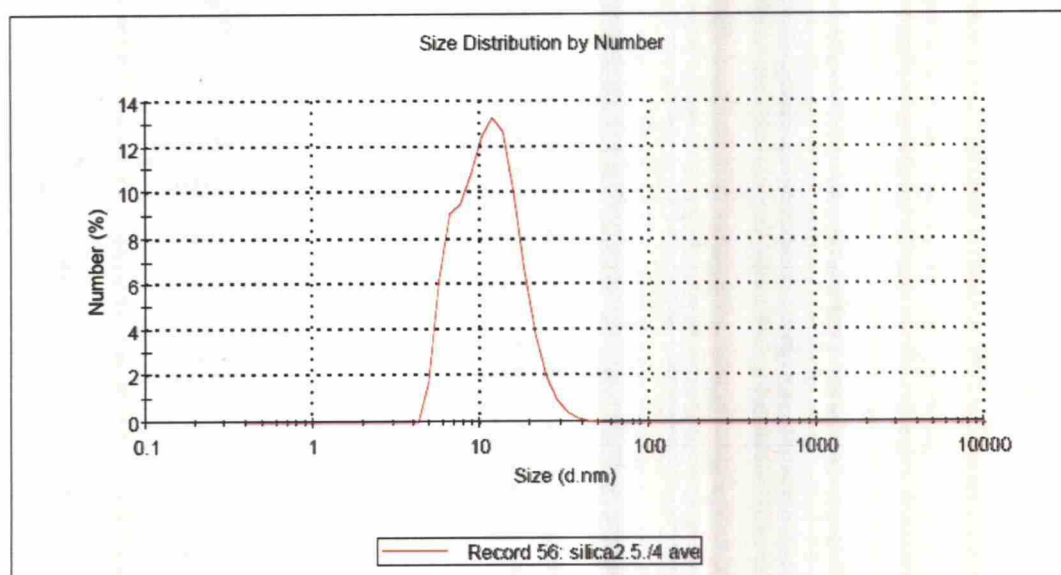
## Results

	Diam. (nm)	% Intensity	Width (nm)
<b>Z-Average (d.nm): 46.2</b>	<b>Peak 1: 70.8</b>	100.0	51.8
<b>Pdl: 0.311</b>	<b>Peak 2: 0.00</b>	0.0	0.00
<b>Intercept: 0.951</b>	<b>Peak 3: 0.00</b>	0.0	0.00



## Results

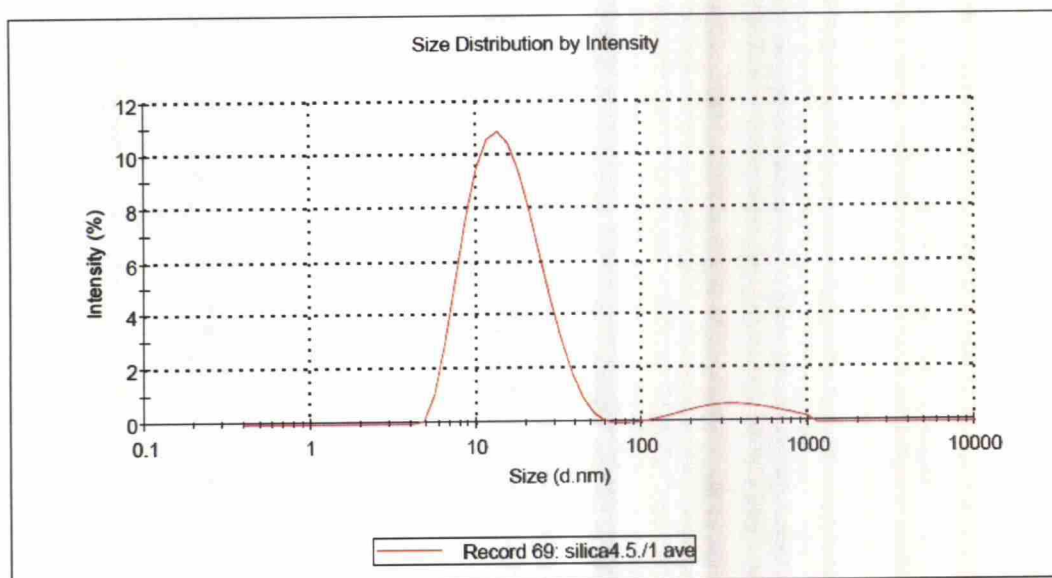
	Diam. (nm)	% Number	Width (nm)
<b>Z-Average (d.nm): 46.2</b>	<b>Peak 1: 11.9</b>	100.0	5.37
<b>Pdl: 0.311</b>	<b>Peak 2: 0.00</b>	0.0	0.00
<b>Intercept: 0.951</b>	<b>Peak 3: 0.00</b>	0.0	0.00



## Sample A8

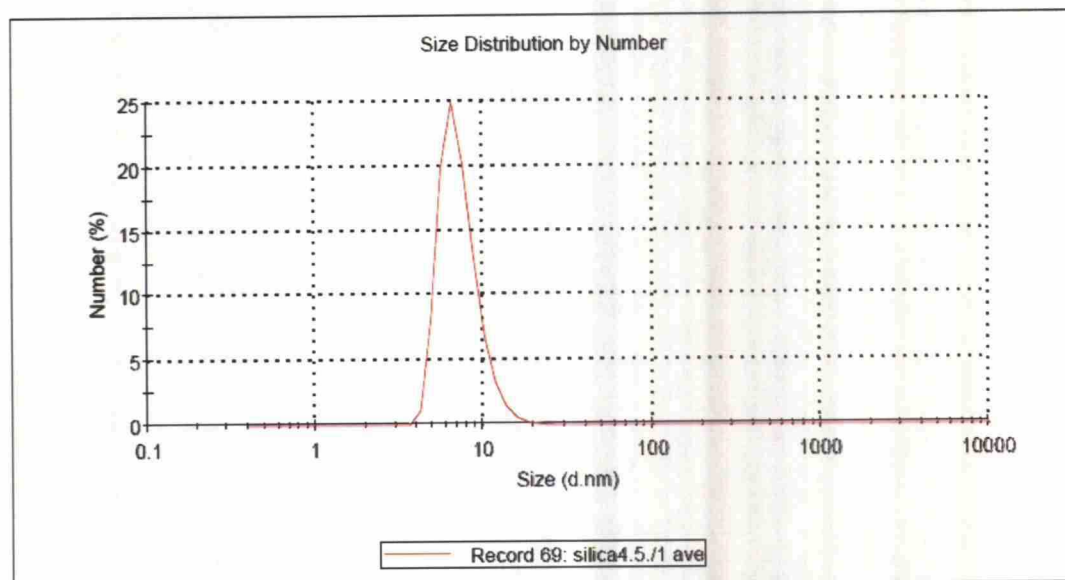
## Results

	Diam. (nm)	% Intensity	Width (nm)
<b>Z-Average (d.nm): 14.4</b>	<b>Peak 1: 16.3</b>	<b>92.7</b>	<b>8.17</b>
<b>Pdl: 0.242</b>	<b>Peak 2: 399</b>	<b>7.3</b>	<b>213</b>
<b>Intercept: 0.937</b>	<b>Peak 3: 0.00</b>	<b>0.0</b>	<b>0.00</b>



## Results

	Diam. (nm)	% Number	Width (nm)
<b>Z-Average (d.nm): 14.4</b>	<b>Peak 1: 7.29</b>	<b>100.0</b>	<b>2.09</b>
<b>Pdl: 0.242</b>	<b>Peak 2: 0.00</b>	<b>0.0</b>	<b>0.00</b>
<b>Intercept: 0.937</b>	<b>Peak 3: 0.00</b>	<b>0.0</b>	<b>0.00</b>

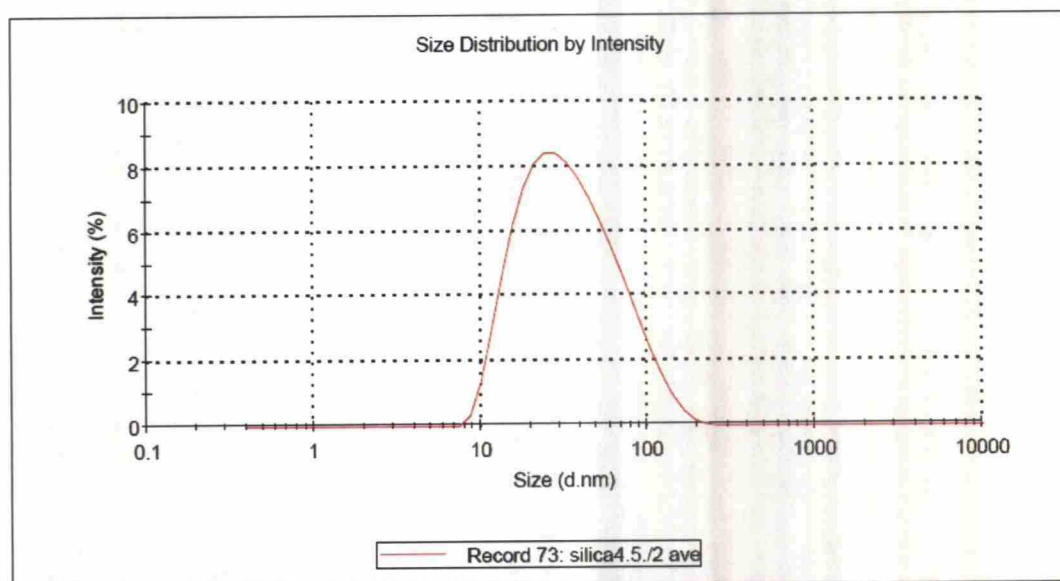




## Sample A9

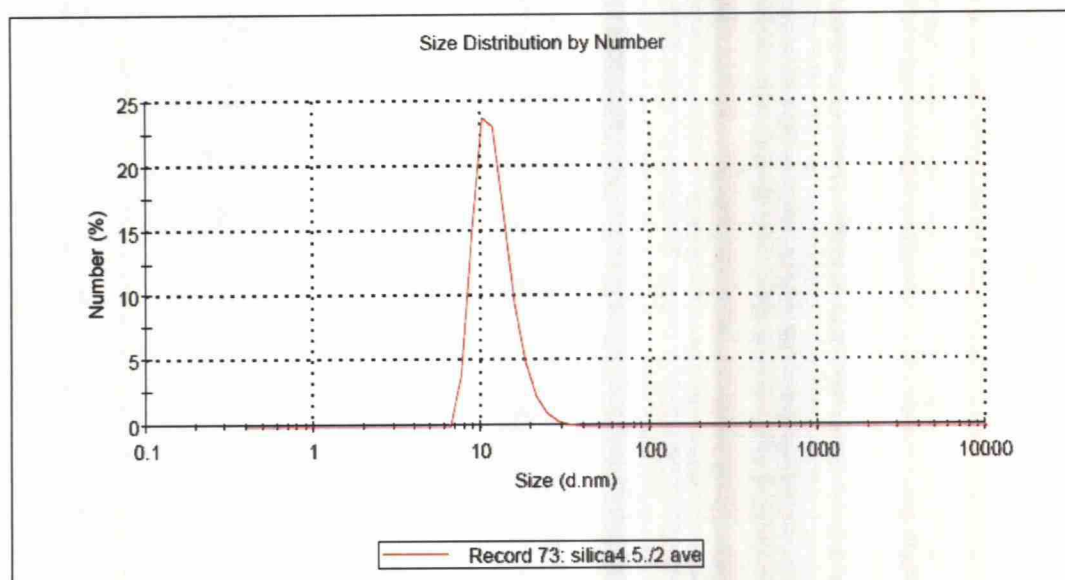
## Results

	Diam. (nm)	% Intensity	Width (nm)
<b>Z-Average (d.nm): 28.2</b>	<b>Peak 1: 40.7</b>	100.0	28.9
<b>Pdl: 0.241</b>	<b>Peak 2: 0.00</b>	0.0	0.00
<b>Intercept: 0.963</b>	<b>Peak 3: 0.00</b>	0.0	0.00



## Results

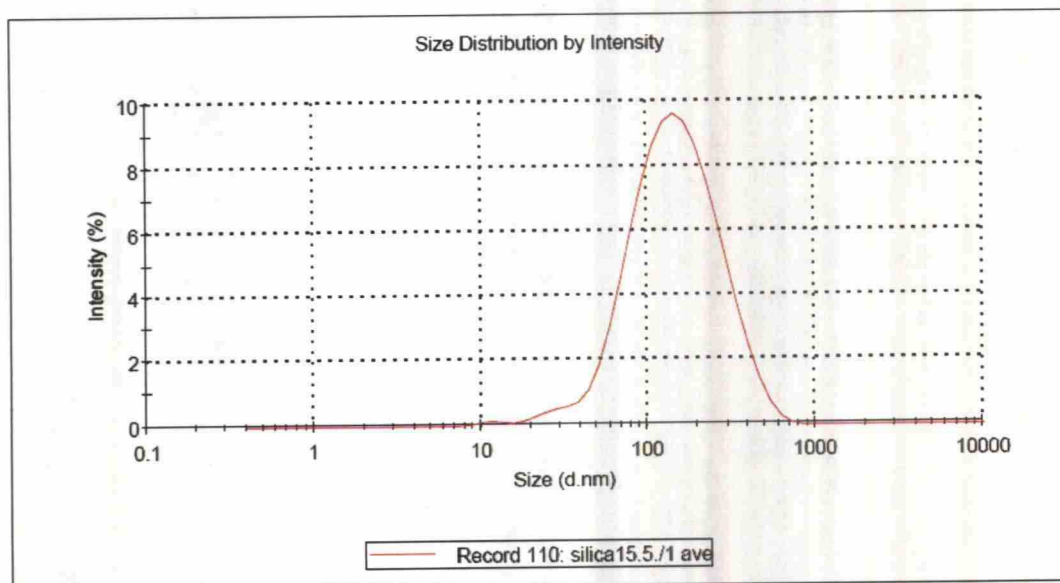
	Diam. (nm)	% Number	Width (nm)
<b>Z-Average (d.nm): 28.2</b>	<b>Peak 1: 12.2</b>	100.0	3.62
<b>Pdl: 0.241</b>	<b>Peak 2: 0.00</b>	0.0	0.00
<b>Intercept: 0.963</b>	<b>Peak 3: 0.00</b>	0.0	0.00



## Sample B2

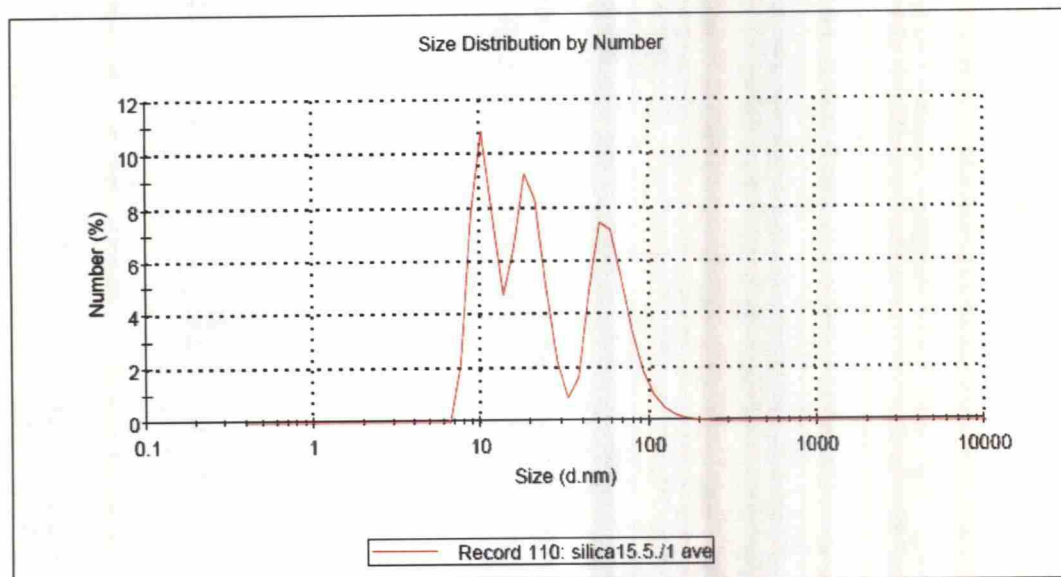
## Results

	Diam. (nm)	% Intensity	Width (nm)
<b>Z-Average (d.nm): 122</b>	<b>Peak 1: 168</b>	99.5	101
<b>Pdl: 0.312</b>	<b>Peak 2: 12.3</b>	0.5	2.09
<b>Intercept: 0.936</b>	<b>Peak 3: 0.00</b>	0.0	0.00



## Results

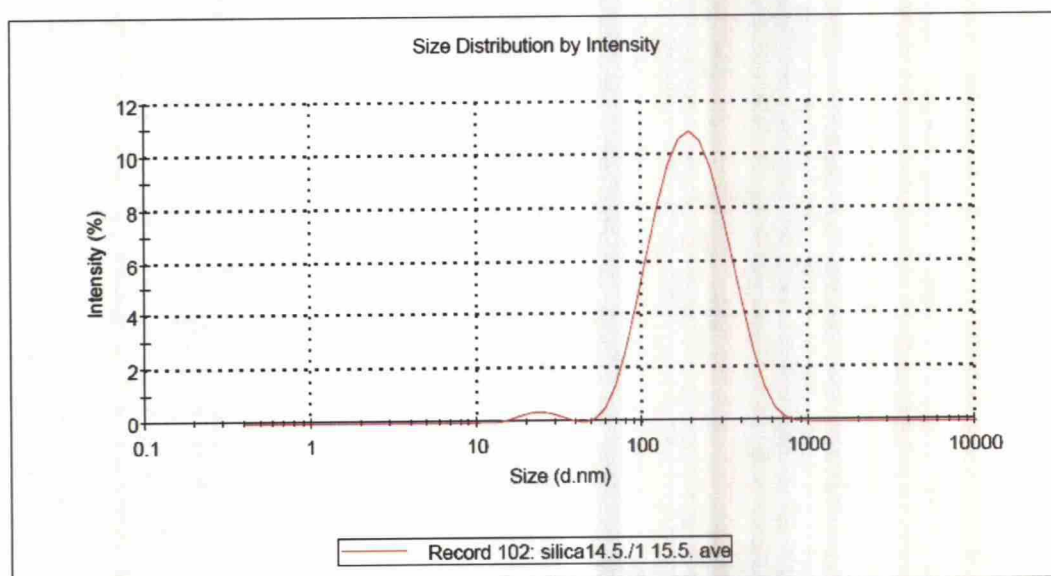
	Diam. (nm)	% Number	Width (nm)
<b>Z-Average (d.nm): 122</b>	<b>Peak 1: 10.5</b>	31.7	1.74
<b>Pdl: 0.312</b>	<b>Peak 2: 19.6</b>	35.1	4.50
<b>Intercept: 0.936</b>	<b>Peak 3: 62.7</b>	33.2	23.6



## Sample B3

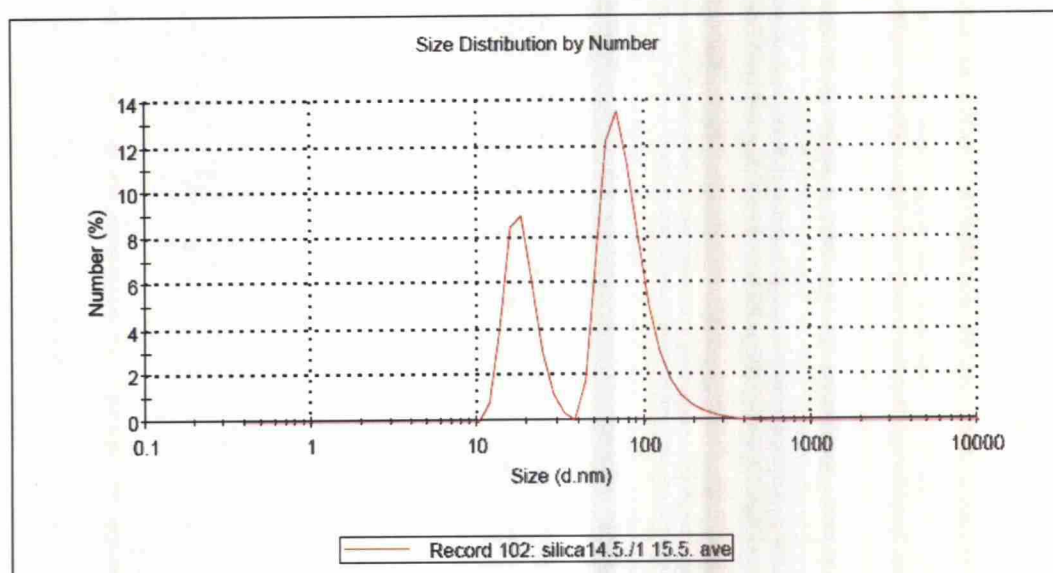
## Results

	Diam. (nm)	% Intensity	Width (nm)
<b>Z-Average (d.nm): 149</b>	<b>Peak 1: 213</b>	<b>98.2</b>	<b>108</b>
<b>Pdl: 0.288</b>	<b>Peak 2: 24.5</b>	<b>1.8</b>	<b>5.83</b>
<b>Intercept: 0.929</b>	<b>Peak 3: 0.00</b>	<b>0.0</b>	<b>0.00</b>



## Results

	Diam. (nm)	% Number	Width (nm)
<b>Z-Average (d.nm): 149</b>	<b>Peak 1: 82.6</b>	<b>66.7</b>	<b>39.2</b>
<b>Pdl: 0.288</b>	<b>Peak 2: 18.4</b>	<b>33.3</b>	<b>4.14</b>
<b>Intercept: 0.929</b>	<b>Peak 3: 0.00</b>	<b>0.0</b>	<b>0.00</b>

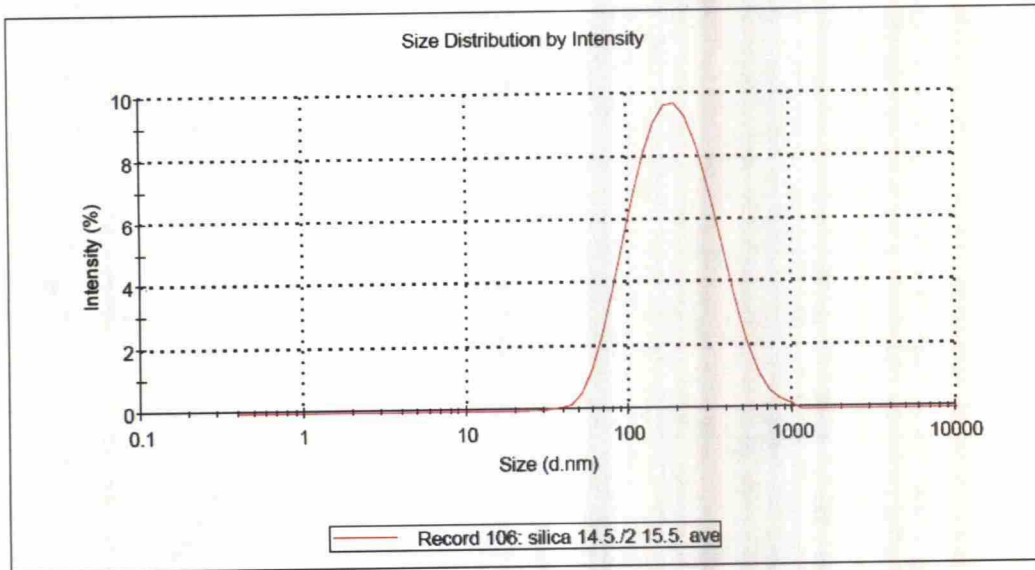




## Sample B4

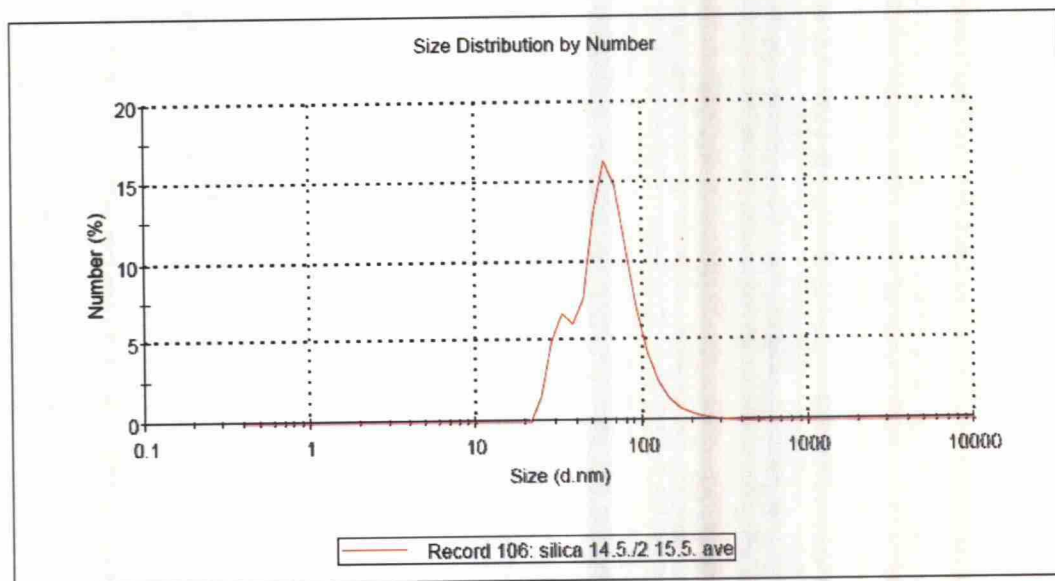
## Results

	Diam. (nm)	% Intensity	Width (nm)
<b>Z-Average (d.nm): 168</b>	<b>Peak 1: 218</b>	<b>100.0</b>	<b>132</b>
<b>Pdl: 0.284</b>	<b>Peak 2: 0.00</b>	<b>0.0</b>	<b>0.00</b>
<b>Intercept: 0.864</b>	<b>Peak 3: 0.00</b>	<b>0.0</b>	<b>0.00</b>



## Results

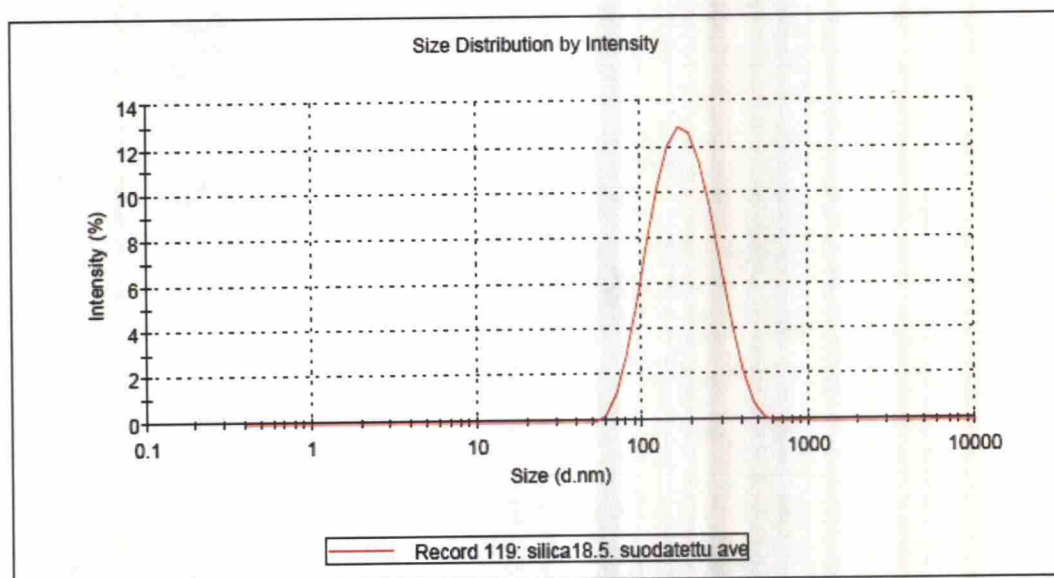
	Diam. (nm)	% Number	Width (nm)
<b>Z-Average (d.nm): 168</b>	<b>Peak 1: 32.5</b>	<b>18.4</b>	<b>4.37</b>
<b>Pdl: 0.284</b>	<b>Peak 2: 71.5</b>	<b>81.6</b>	<b>35.4</b>
<b>Intercept: 0.864</b>	<b>Peak 3: 0.00</b>	<b>0.0</b>	<b>0.00</b>



## Sample B5

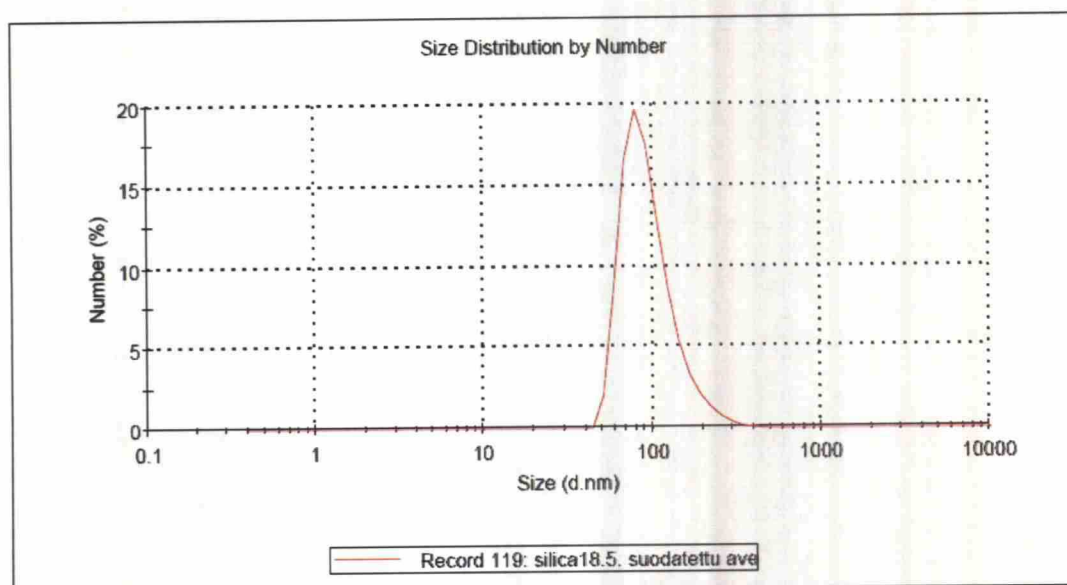
## Results

	Diam. (nm)	% Intensity	Width (nm)
<b>Z-Average (d.nm): 157</b>	<b>Peak 1: 187</b>	<b>100.0</b>	<b>80.3</b>
<b>Pdl: 0.162</b>	<b>Peak 2: 0.00</b>	<b>0.0</b>	<b>0.00</b>
<b>Intercept: 0.935</b>	<b>Peak 3: 0.00</b>	<b>0.0</b>	<b>0.00</b>



## Results

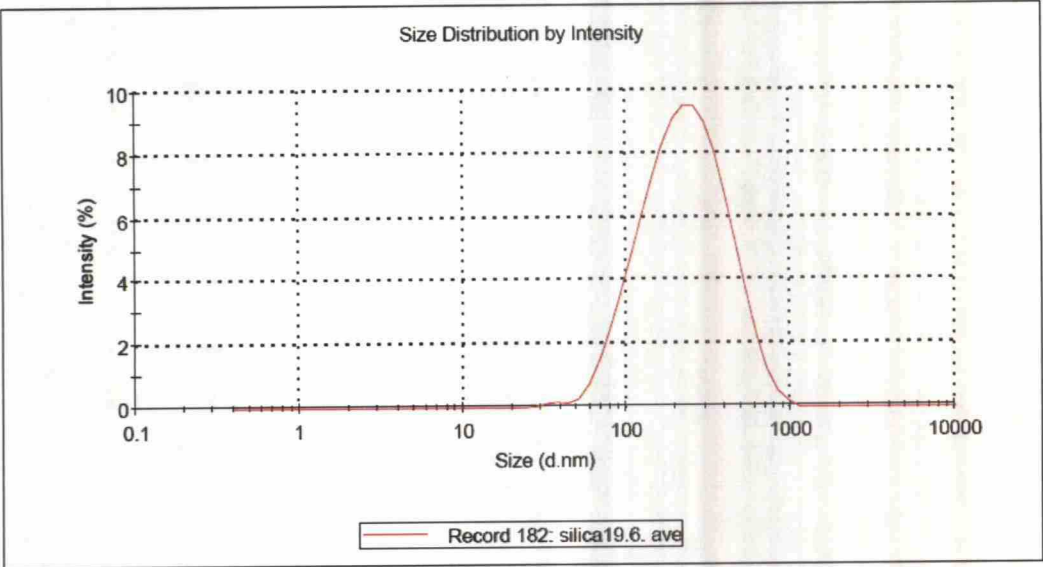
	Diam. (nm)	% Number	Width (nm)
<b>Z-Average (d.nm): 157</b>	<b>Peak 1: 98.1</b>	<b>100.0</b>	<b>41.1</b>
<b>Pdl: 0.162</b>	<b>Peak 2: 0.00</b>	<b>0.0</b>	<b>0.00</b>
<b>Intercept: 0.935</b>	<b>Peak 3: 0.00</b>	<b>0.0</b>	<b>0.00</b>



Sample B6

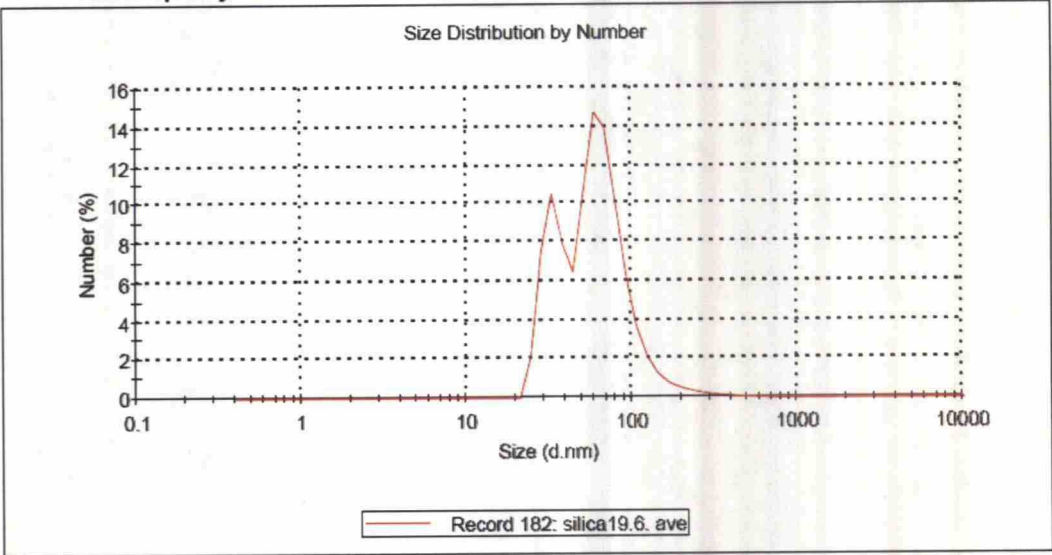
Results

	Diam. (nm)	% Intensity	Width (nm)
<b>Z-Average (d.nm):</b> 192.1	<b>Peak 1:</b> 258.0	99.5	148.5
<b>Pdl:</b> 0.241	<b>Peak 2:</b> 37.63	0.5	4.953
<b>Intercept:</b> 0.876	<b>Peak 3:</b> 0.000	0.0	0.000
<b>Result quality :</b> Good			



Results

	Diam. (nm)	% Number	Width (nm)
<b>Z-Average (d.nm):</b> 192.1	<b>Peak 1:</b> 75.87	67.5	41.18
<b>Pdl:</b> 0.241	<b>Peak 2:</b> 34.46	32.5	5.903
<b>Intercept:</b> 0.876	<b>Peak 3:</b> 0.000	0.0	0.000
<b>Result quality :</b> Good			

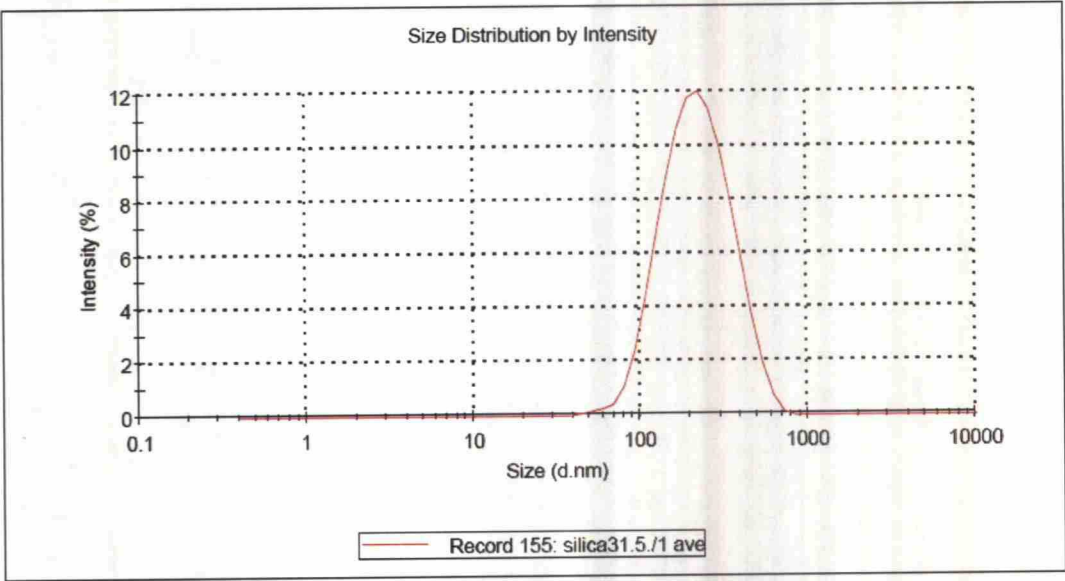




Sample B7

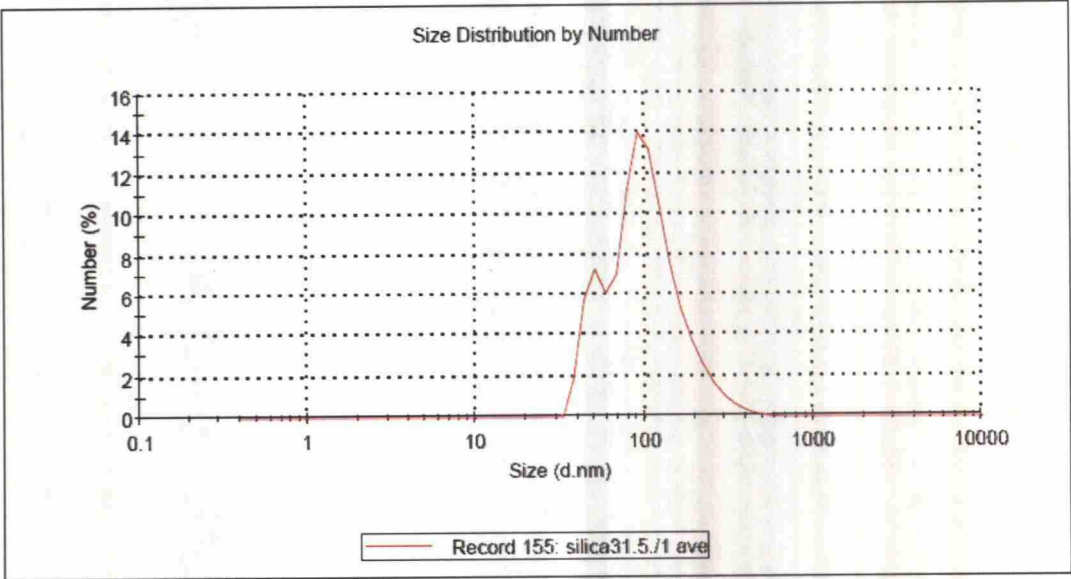
Results

	Diam. (nm)	% Intensity	Width (nm)
<b>Z-Average (d.nm):</b> 197	<b>Peak 1:</b> 237	100.0	109
<b>Pdl:</b> 0.219	<b>Peak 2:</b> 0.00	0.0	0.00
<b>Intercept:</b> 0.907	<b>Peak 3:</b> 0.00	0.0	0.00



Results

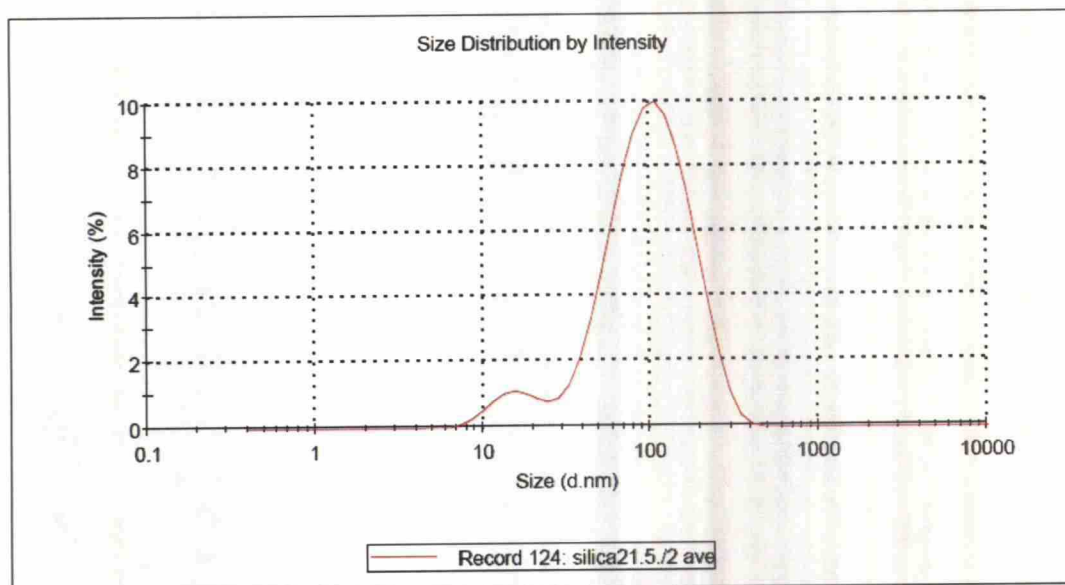
	Diam. (nm)	% Number	Width (nm)
<b>Z-Average (d.nm):</b> 197	<b>Peak 1:</b> 50.0	19.8	6.80
<b>Pdl:</b> 0.219	<b>Peak 2:</b> 119	80.2	59.1
<b>Intercept:</b> 0.907	<b>Peak 3:</b> 0.00	0.0	0.00



## Sample C4

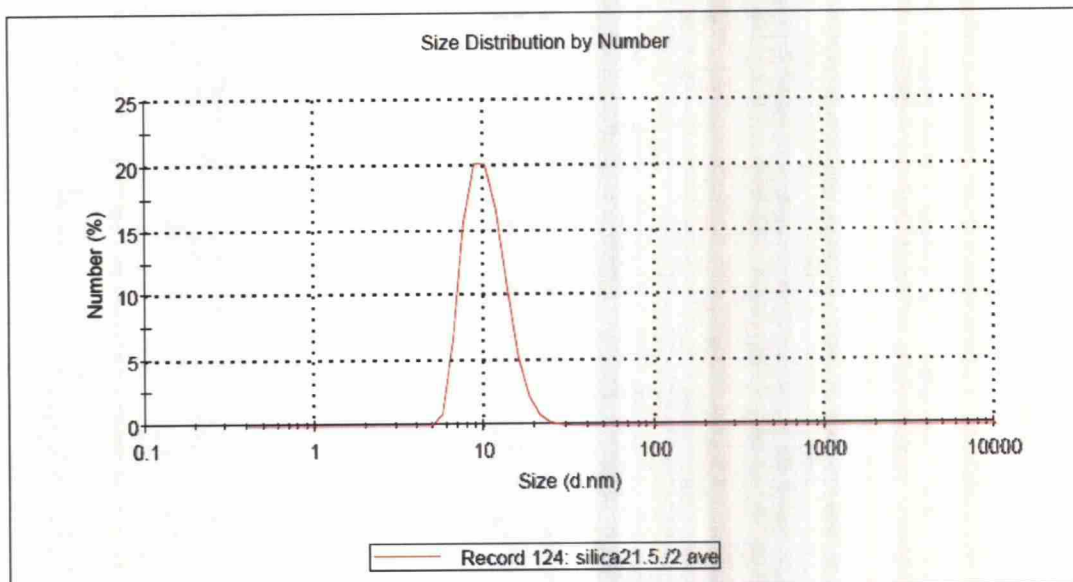
## Results

	Diam. (nm)	% Intensity	Width (nm)
<b>Z-Average (d.nm): 74.6</b>	<b>Peak 1: 112</b>	<b>93.4</b>	<b>58.9</b>
<b>Pdl: 0.320</b>	<b>Peak 2: 16.1</b>	<b>6.6</b>	<b>4.71</b>
<b>Intercept: 0.956</b>	<b>Peak 3: 0.00</b>	<b>0.0</b>	<b>0.00</b>



## Results

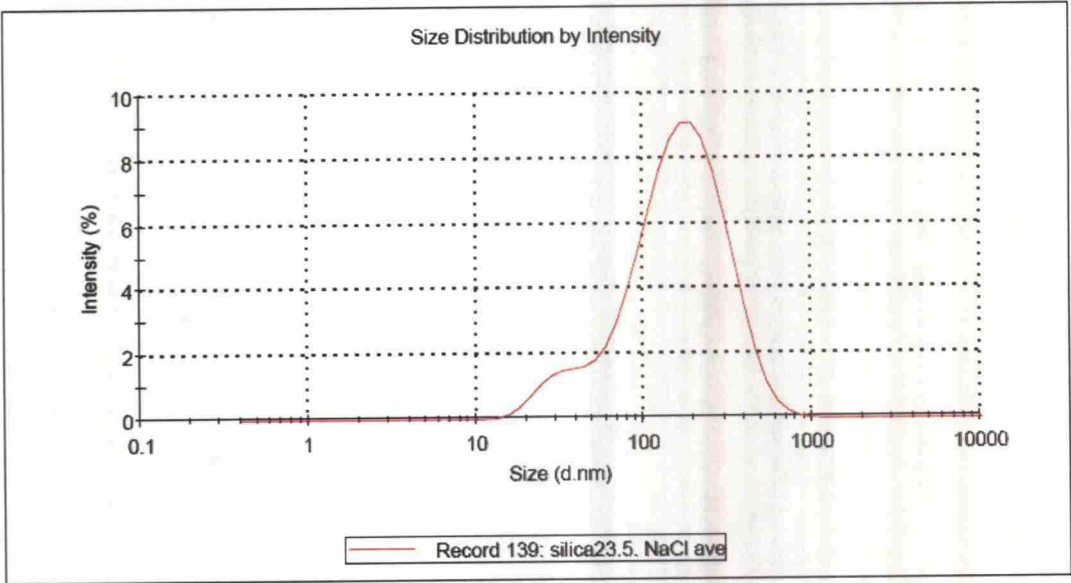
	Diam. (nm)	% Number	Width (nm)
<b>Z-Average (d.nm): 74.6</b>	<b>Peak 1: 10.4</b>	<b>100.0</b>	<b>3.27</b>
<b>Pdl: 0.320</b>	<b>Peak 2: 0.00</b>	<b>0.0</b>	<b>0.00</b>
<b>Intercept: 0.956</b>	<b>Peak 3: 0.00</b>	<b>0.0</b>	<b>0.00</b>



Sample C5

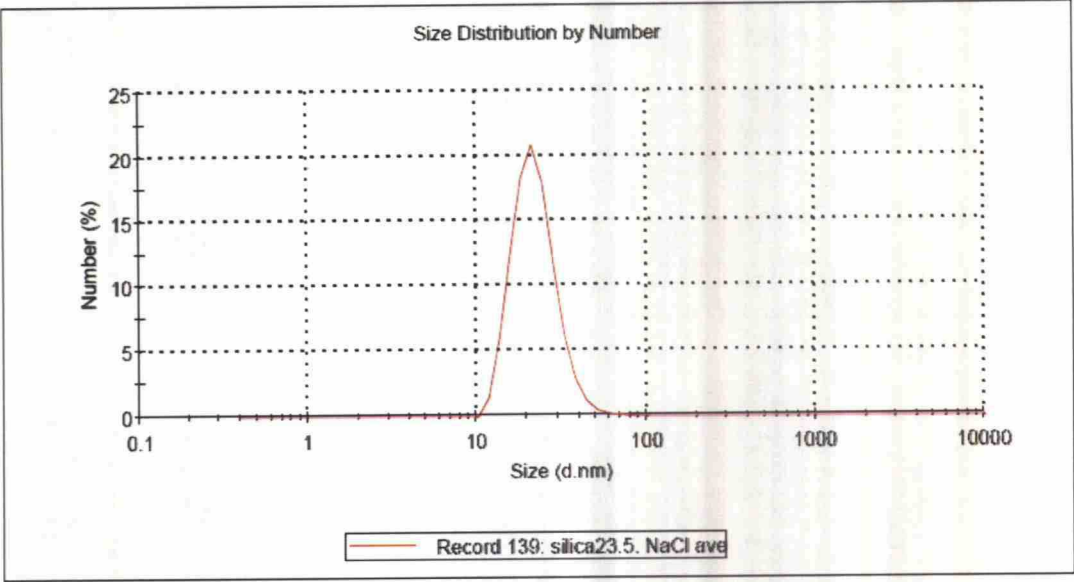
Results

	Diam. (nm)	% Intensity	Width (nm)
<b>Z-Average (d.nm): 120</b>	<b>Peak 1: 183</b>	<b>100.0</b>	<b>117</b>
<b>Pdl: 0.356</b>	<b>Peak 2: 0.00</b>	<b>0.0</b>	<b>0.00</b>
<b>Intercept: 0.952</b>	<b>Peak 3: 0.00</b>	<b>0.0</b>	<b>0.00</b>



Results

	Diam. (nm)	% Number	Width (nm)
<b>Z-Average (d.nm): 120</b>	<b>Peak 1: 22.6</b>	<b>100.0</b>	<b>8.02</b>
<b>Pdl: 0.356</b>	<b>Peak 2: 0.00</b>	<b>0.0</b>	<b>0.00</b>
<b>Intercept: 0.952</b>	<b>Peak 3: 0.00</b>	<b>0.0</b>	<b>0.00</b>



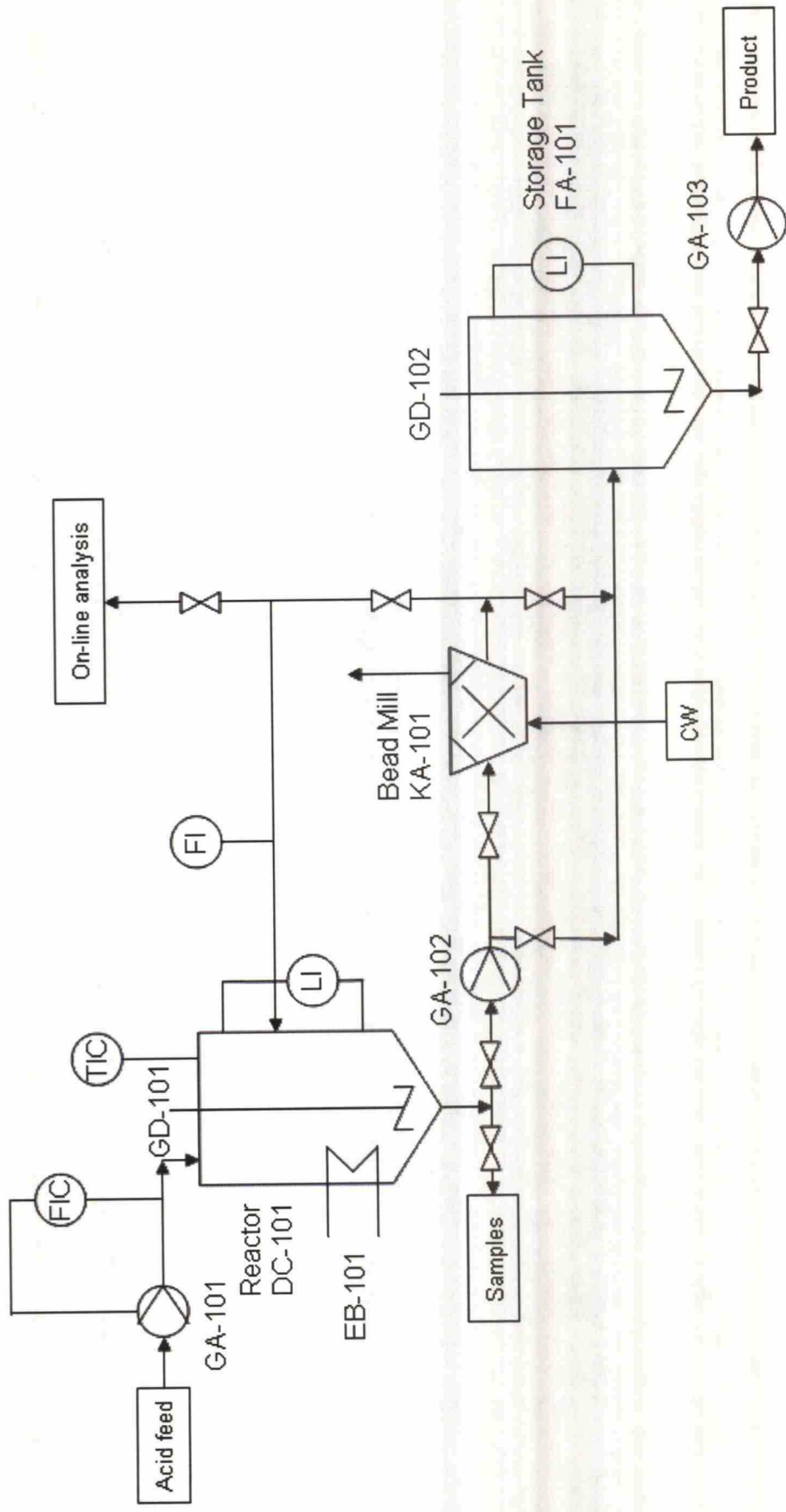


## Appendix I

SEM images of sample B6 (taken by Eero Haimi at TKK Laboratory of Materials Science)



Pilot Process Flow Sheet



TKK Kem. Koperasi  
Kemiskinan 02150 ESPOO  
no. 434 2516